Response to Referee #1

Please see our responses to each referee comment (in blue):

Anonymous referee #1: This paper investigates post-wildfire erosion using multitemporal lidar over time. I think some of the methods used by the authors are quite unique as compared to similar post-wildfire lidar studies (e.g. Pelletier and Orem, 2014 and Orem and Pelletier, 2015). In particular, I like their approach for removing DEM pixels that were determined to be disturbed by the canopy. That technique is novel, and I think it will provide a robust new method that will be embraced by the community. I also applaud the authors for their use of radar estimated rainfall and the approach used to correct it based on local rain gauge data. That allowed the authors to analyze spatially continuous rainfall data, which was useful for their overall analysis. I think that the general thrust of the paper is unique and I think that this manuscript is close to being ready for publication. However, there are a few general suggestions that I will make, in addition to many specific suggestions below.

We thank the referee for reviewing and provided general and specific suggestions. We have responded to each of your suggestions below. In most cases we agree to the suggested changes, and the following documents each of our responses and the changes that we have made to the manuscript.

Consider re-writing section 4.2. Section 4.2 is a long chronological narrative, I understand the temptation to write it this way, because that is the way it unfolded in time. But it is really boring to read and fails to convey the salient points well. Consider organizing it in terms of drivers and response. This will help to generalize the paper beyond a case study.

We appreciate this comment, and we (the three authors) had discussed how to best organize the paper. We understand the potential value of organizing the paper by processes ("drivers and response"), but this proved unwieldy and even more difficult to follow given the diverse responses over time, space, and between watersheds, and the different drivers in terms of convective storms, snowmelt, the large mesoscale flood, and the reduction in post-fire effects over time. We have extensively revised Section 4.2 by deleting a number of the more specific details, combining some of the paragraphs, and emphasizing the key points and processes as suggested by the reviewer.

Section 5.2 also needs some attention. The way that you break up the paragraphs is a little strange. I suggest abandoning the enumeration that you use "First, second, third." For example, on P17 line 19, why does that paragraph start with "third", and contain the "forth" point, but the next paragraph doesn't start with "Fifth"? I think the same points can be conveyed without this type of enumeration, and then paragraphs can be grouped by similar ideas.

We appreciate the comment, and have revised this section to make the enumeration more consistent. We do feel that numbering the points makes it easier for the reader to keep track of the larger organization and the progression of the extended series of points that we are making based on our experience with sequential differencing of ALS datasets.

I was also confused by your use of the term “sediment availability” in the discussion. At present, I don’t see how your data speak to the sediment availability at all, and yet it is invoked as an explanation. I would consider either adding in data that relates to sediment availability, or rephrasing the sentences in which you point to sediment availability.

Our interpretation of “sediment availability” is based on: a) visual observation of sediment deposition in the valley bottoms and channels; and b) the estimates of deposition based on the lidar differencing. The underlying concept is that the amount of erosion depends on the amount of available sediment, with the post-fire sediment being more readily erodible than the older sediment that is protected by vegetation. We have revised the manuscript to more clearly define “sediment availability” and show how sediment availability seems to be an important control on the amount of erosion in the channels and valley bottoms.

Lastly, I think it would be really helpful to synthesize these really unique results that moves beyond the case study. This could just be a paragraph in the discussion, but consider helping readers to see how the erosion/deposition sequence could be converted into something that might lead to more insight at different sites in the future.

Thanks for the suggestion. We have tried to streamline the last parts of the discussion to better emphasize how our results can have implications for predicting sediment deposition and erosion following disturbances.

This paper is really interesting, and despite my detailed comments, I enjoyed the approach, and I think that this manuscript will be a nice addition to the literature.

Thank you for this very positive overall summary of your evaluation of our manuscript. We have recently presented this story at several conferences, and have received a very positive response from the audience as this article does break some new ground in terms of comparing fires and floods, and also focusing on larger scale effects.

Specific Comments:
P2. L14: Rengers et al. modeled basin scale post-wildfire runoff. doi: 10.1002/2015WR018176

Thanks, we have modified the text and included this citation.

P3 L7-8: remove “very”

We have deleted “very” as suggested by the reviewer.

P3 L21: replace “small- to moderate-sized watersheds” to “stream channels” because it seems like all of your analysis is in the channels, not in the larger watershed.

We agree, and have revised the manuscript to read “in the valley bottoms of small- to moderate-sized watersheds”.

P3 L28: I didn’t see any hypsometric curves

We did not include the hypsometric curves as we are only trying to indicate that the watersheds are very similar. The hypsometric curves are not critical to interpreting or understanding the results, and so we provided this fact. However, since the paper already has 12 figures we did not want to add yet another figure when this is not critical to our study. When describing a study area it is common to provide these kinds of descriptive statements without providing all the underlying data, and we believe that providing a statement about the hypsometric curves without providing the data is consistent with standard practices.

P3 L30: Use a more specific term than “evergreen”

We have added a sentence to provide more details on the forest cover.

P4 L3: Say how straw and wood mulch were applied

We have added “from helicopters” to clarify this. Wood chips were spread manually to a very small area (less than one hectare) that was mostly on a ridgetop and accessible by road.

P4 L6: add “channels” after the word combined

We presume that the reviewer means “confined” rather than “combined”, and we have added the word “channels” to make this more explicit.

P5 L4: Are you going to post the python scripts anywhere?

The scripts referenced here piggyback off the FluvialCorridor ArcGIS add-on, and they were written specifically for our analysis so they would not be immediately useful to others. If a reader is interested they can contact us at the email address listed in the manuscript, and we will be happy to provide them with the scripts and any additional information, but they will have to make some modifications.

P5 L18: Can you explain why you used the 50 m sections? You could have just analyzed the lidar on a pixel-by-pixel basis, so why create short reaches to analyze? This would benefit from some more explanation.

The two main objectives of our paper were to: 1) characterize the spatially-explicit changes in sediment deposition, erosion, and net change over time throughout the channel network; and 2) relate these changes to both the morphometric characteristics and the characteristics of the contributing area (e.g., precipitation and burn severity). We therefore needed to do the analyses on larger segments rather than at the pixel scale as suggested. The segment length of 50 m is somewhat arbitrary, but we chose 50 m because: 1) this is an appropriate length to characterize the local morphometrics (i.e., channel slope and valley width) as well as the rate of change in these morphometrics given our valley bottom widths (i.e., long enough to minimize local noise but short enough to be relatively homogeneous); 2) the 50-m segment length matches up with the 50-m long longitudinal profiles that we were surveying at each cross-section; and 3) a rough rule of thumb is that longitudinal profiles should be about 10 times the channel width, and after the

2013 flood our channels ranged from about 2-10 m wide, so a 50-m long segment is "about right".

Given this comment and a similar comment from the second reviewer, we have added two sentences to explain and justify why we divided the channel network into 50-m segments.

P5L28-29: area-maximum maximum? Is that just a typo or does the second maximum go with the 30-min. rainfall intensity? Maybe rephrase so easier to understand.

This is not a typo, as we took the maximum value from the maximum values for all of the pixels. We have revised the wording to make this less confusing.

P5 L30: Did you generate the burn severity map, if so mention that, if not say where it came from.

At the end of the sentence we provide the reference for the burn severity map (Stone, 2015).

P6L5 is that 7am on one day and 7am the next day? Maybe make that more clear

On line 2 we state that the radar data were corrected with daily rain gage data, and on line 5 we state that the radar precipitation were summed from 0700 to 0700 to match the daily rain gage data. It also is standard observing practice that daily rainfall is measured from 0700 on one day to 0700 the following day, so we don't think that this needs any additional clarification.

P6L17: for the Moody 2013 ref, you should also ref. Kean et al. 2011 doi:10.1029/2011JF002005 See their figure 8 and reconcile that with your current statement.

It appears that Kean et al.'s (2011) Figure 8 indicates that I15 is most closely in phase with peak stage, but the lag between I30 and peak stage is only a few minutes. We have added a reference to Kean et al.'s paper here.

P6L26: state goodness of fit for correlation

We presume that by "goodness of fit values" the reviewer wants us to provide either the correlation coefficient (r) or the coefficient of determination (r^2). First, this would be a result, not in methods. Second, we cannot provide goodness of fit values in the text because of the very large number of correlations that we compute for our results. We explicitly state on lines 25-26 that we collected a number of morphometric measurements (valley bottom, channel, contributing area), and on lines 26-27 we state that these data were correlated to the calculated volume changes. Figure 10 displays the correlations graphically for each of the nine independent variables and three dependent variables for each of the four time periods for each of the two watersheds (n=9 x 3 x 4 x 2, or a total of 216 correlations).

P6L31 ref a figure after "intervals"

This section provides an explanation of how we calculated the channel slopes and changes in slope ("curvature"). We have revised the text to better clarify how we calculated the slope and curvature, but a figure would be largely superfluous as the methodology is relatively simple.

P6 L31: I had (have) a really hard time visualizing exactly what you trying to say here in the sentence that begins "Topographic curvature" Can you add a figure that is a schematic of what you are doing? A lot hinges on understanding this process, so I think it will be important that people don't miss what you are saying here.

As indicated in the previous comment, we are revising the text to make the methodology for calculating curvature more explicit. Curvature did not turn out to be a very important variable, so we would respectfully disagree that "A lot hinges on understanding this process."

P7L32: Why not just extract a line across the DoD at your X-S location?

That may be another approach to checking the validity of the lidar differencing. However, because the analyses in this paper focus on volume changes in the 50-m segments, we felt it was appropriate to compare the segment volumes to the volumes calculated from an extrapolation of the field data.

P8L11: Cool approach!

Thank you!

P9L23: do you mean "The lowest TOTAL amount..."

We have revised this sentence to clarify that total precipitation was lowest during the T1 period.

P9L29: Does mesoscale refer to the 2013 flood? Make sure that is clear

We have defined the September 2013 flood as the "mesoscale flood" as this is consistent with other published accounts of this flood, and we have not used this term to refer to any other flood event. Inserting "2013" before "mesoscale flood" would imply that there was more than one mesoscale flood. We have closely checked the manuscript to ensure that we are consistent in how we reference the 2013 mesoscale flood, and that we explicitly note that there was only one mesoscale storm and corresponding long-duration flood.

P9L32: Add this rainfall to table 2

We have added a short table to summarize the total rainfall and the maximum 30-minute intensities for each watershed and each time period.

P10L4: Do you have a way to estimate the size of the footprint of each laser point on the ground?

We do not have any information on the size of each laser footprint on the ground. Table 2 provides the point densities and the mean absolute error for each ALS dataset in each watershed, and we believe that this is sufficient to document the data quality and that the data quality generally improved over time.

P10L9: I don't think it is accurate to say that "the ALS data ... generally fall along a 1:1 line". There seems to be a lot of deviation.

We agree that this wording was a bit strong, and we have revised this to note that the data generally plot close to the 1:1 line and then note the exceptions for the first time period in Hill Gulch and one cross section for the second period in Skin Gulch. We also have adding text to explain that we would not expect a perfect match because the cross sectional changes are extrapolated out to 50 m to obtain a volume.

P10L15: reference tables after the word "ratios"

We don't understand this comment, as the tables do not provide any data on the similarity in channel slopes, valley widths, or confinement ratios. Similar to our earlier response, the purpose of this paragraph is to summarize these data to: 1) provide a more detailed description of these characteristics in the two watersheds; and 2) show that the two watersheds are relatively comparable with respect to their physiographic characteristics.

P10L18: Did you observe step pools?

Our field observations would suggest that there were a limited number of step-pool channels prior to the 2013 mesoscale flood, but these were generally smoothed out during the 2013 mesoscale flood. Since we have quantitative data on channel slope but only qualitative observations on channel type, we focus on channel slope. We also would argue that channel type is not an important control given the very large magnitude changes induced by the post-fire thunderstorms, snowmelt, and mesoscale flood.

P10L20: add "reaches" after channels

We have added "segments" to address the concern of the reviewer, as this terminology is consistent with our study.

P10L31: add "within our LoD" after "deposition"

By "LoD" we assume the reviewer is referring to our limits of detection. Since this caveat would apply to nearly every result pertaining to our DoD methodology, mentioning it here would imply that we should add it everywhere else. Since we are very explicit in noting that we can only evaluate elevation differences and hence volume changes in the channel and valley bottoms, we think it is best not to mention this caveat here to avoid the potential for confusion when reporting all our other DoD results.

P11L10 :is the net deposition number (19000) from the ALS or your cross-sections? There is so much missing data that it is hard to believe this is a complete number. I am more interested in the longitudinal patterns than the specific volume estimates because of the missing data.

Given the limited number of cross sections and our extended explanation of how we analysed the ALS data, we are confused that the reviewer could think that this volume was somehow derived from our cross section data. Nevertheless, we have revised the text to clarify how we estimated the changes in sediment volumes. We assume by "so much missing data" the reviewer is referring to a net deposition calculation using field cross-sections; however, this number reflects ALS differencing, so we do not believe missing data is an issue here. Altogether our study does include 83% of the total channel length in Skin Gulch and 87% of the total channel length in Hill Gulch as stated in Section 4.1.

Figures 6 and 7 present the complete data in space for each watershed and each time period, and the reader can use these to draw their own conclusions, and Figures 8 and 9 also show the longitudinal distribution of erosion and deposition for each time period in each watershed.

P12L26: There is so much missing data that it is hard to feel confident in the total volumes of erosion/deposition values in SG or HG. Consider focusing more on the patterns.

As noted in our previous comment, it is not clear to us what data are "missing". There are clear limitations on the minimum elevation change that we can detect, and we are very explicit about this (e.g., Table 1). Figures 6 and 7 present the longitudinal data, and a close inspection of these figures show that the longitudinal patterns are very complex. Our correlation analyses also show that the volume changes cannot be explained to a high degree of certainty or resolution. We worked hard to try and identify clear and strong patterns, but our efforts had only limited success. Hence we see no way to focus more on the "patterns" as they are not nearly as clear as implied by the reviewer.

P13L5: "this plus other data..." what other data are you referring to?

We agree that this is ambiguous, and the inference was that "other data" was referring back to the list of previously published work on erosion and deposition after the High Park Fire (p. 3, lines 15-21 of our original manuscript). We have revised the text to make it more explicit that we are referring to other published studies on the High Park Fire.

P13L6: you mention hillslope scale, but I didn't think you had data on the hillslopes

A paper on the hillslope-scale erosion results has already been published, and we have revised the text to more clearly indicate the source of the hillslope erosion data. We also have provided the reference for the deposition in the lower portions of HG and SG as measured from cross-sections and longitudinal profiles (Brogan et al., *Geomorphology*, 2019).

P13L9: not quite a mass balance here, but I understand why

These are all net volume changes, and per normal convention positive values indicate net deposition and negative values indicate net erosion.

P13L16: "highly correlated" with what?

We appreciate the reviewer noting that this statement is ambiguous, and have added wording to explain that we are first looking at the cross correlations among the different independent variables.

P13L33: "erosion occurred in the lower gradient" hmm that doesn't seem intuitive if slope is a major component of the driving shear stress. Can you help to explain why this makes sense somewhere?

Yes, this initially appears counterintuitive. The reason is that there was more post-fire deposition in the lower gradient downstream segments, and because there was much more available sediment then there was more erosion. We have revised the text to explain that the greater erosion was associated with greater amounts of post-fire deposition and that there was more sediment that could be readily eroded by snowmelt and lower intensity rainstorms.

P14L6: Is BS_m already defined? On page 5 BS is burn severity

We appreciate this comment. BS_h and BS_m refer to the proportion of the contributing area that was burned at high and moderate severity, respectively, and we have now defined these terms in methods.

P14L8: reference a figure after the word "scatterplots"

As noted above, the amount of deposition, erosion, and net volume change was correlated with each of the independent variables for each time period. Hence this result is a more general result, and in the interest of brevity we did not present any of the 200+ scatterplots in the paper. Figure 10 does graphically present the correlation results, and a table of the overall correlations is included in the supplemental material.

P16L1: What field data shows grain size?

We will include a reference here to Brogan et al. (2019), where field grain size data are presented.

P16L7: Add a ref like Passalaqua 2015 doi:10.1016/j.earscirev.2015.05.012 I also am not sure I agree with the word "recent" We're going on >20 years of lidar differencing

Thank you for this, and we have extensively revised the text so that the section with "recent" is no longer present. The revisions also obviate the need for a reference.

P16L11: "the predominant post-fire effect is deposition in the channels and valley bottoms" This is a more general statement than I think you are intending. For example, I don't think you would argue that this is necessarily true for the Poudre River. That is a channel/valley bottom, but it sounds like there was not extensive deposition there. So I suggest just refining the language to focus on the spatial scale at which you think it is representative.

We appreciate this comment, but we do not say that deposition is universal, only that it is the predominant post-fire effect and we have provided extensive references and support for this statement in the introduction and results. We acknowledge appreciate the importance of spatial scale as suggested by the reviewer, and we therefore inserted the word "downstream" because incision is the predominant post-fire response at the hillslope scale. In confined valleys with large amounts of stream power there may not be widespread post-fire deposition until the channels and valley bottoms widen out. In the confined reaches of the Cache la Poudre River large amounts of coarse sediment were occasionally delivered into the river, and these did create relatively persistent alluvial fans. Hence the statement is more generally true, and we provide the material to support this statement.

P16L15 what fraction of the channel network does your ALS capture?

The point we were making is that the measured cross sections and longitudinal profiles represent only a small fraction of the channel network, so the DoD of repeated ALS surveys is needed in order to assess erosion and deposition over the entire channel network. This section has been rewritten to better contrast the higher temporal resolution field data with the ALS data, where the latter has lower temporal resolution but can evaluate nearly the entire channel network.

P16L28: Seems like you should mention the coarse substrate and depth to water table before this

We have deleted this sentence on the riparian vegetation as it was not crucial to the points we are making.

P16L28: What exactly do you mean by stripping and coarsening of the channels?

This statement is in reference to the changes induced by the mesoscale flood. As noted in the previous response, we will provide more description of the extensive channel erosion (stripping) and coarsening that occurred as a result of the mesoscale flood.

P17L2: string "large" and add "documented" after "debris flows"

We have deleted this sentence as it was not critical to our paper.

P17L15: I don't think you actually mean "allow researchers to be repeated" consider clarifying

Good catch, and we have revised this sentence.

P17L25: you qualitatively describe lidar here, why not just suggest a point density (pt/m^2) that you think would be good to shoot for.

Good suggestion; we will change the text to note that the highest mean point density we had from our data was 3.8 pts m^{-2}. We have added text recommending a minimum point density of 4 pts m^{-2}, noting that higher point densities would allow for a more detailed and accurate analysis.

P18L15: What proportion of the area was reduced from this approach?

Vegetation removal reduced the analyzed areas in both valleys by about 2%. We will point this out in the text, as it shows how vegetation artifacts in just a small area can have a very large effect on the calculated differences in volumes.

P18L18: Your 7th point seems pretty obvious, but I guess the people at NEON didn't think about that. I thought it was typically standard practice.

Yes, it should be obvious for volume differencing studies, although researchers with other interests (e.g., vegetation succession) may prefer data collection at different times of year.

P18L24: ref a figure at end of this sentence

We have added a reference to Fig. 10.

P18L25: ref a figure at end of this sentence

Since we reference Figure 10 at the end of the previous sentence, we do not think it is necessary to repeat this reference here.

P19L2: As far as I can tell, sediment availability is not something you measured (is it measureable?). Your results may allow you to make some inferences about sediment availability, but I don't think that the way things are presented right now allow you to say that the geomorphic changes were largely controlled by sediment availability.

Please see the response to the general comment above related to this topic. Again, we are evaluating sediment availability on the basis of our field observations, field measurements at the cross sections and longitudinal profiles, and our DoD differencing. We present a number of lines of evidence to support our argument that sediment availability is a key control on the amount of subsequent erosion (e.g., Figure 11).

P19L12-14: Maybe they aren't correlated because you calculated them across 50 m averages.

This may be the case, but we think that 50 m is an appropriate window for computing valley widths, and should be a reasonable approximation of local slope in the absence of a sub-segment-scale knickpoint or other local discontinuity.

P19L16: What data do you have on sediment supply?

This sentence refers to sediment availability – we will change "supply" to "availability."

P19L21: Am I missing something? How do you know that sediment availability increased? What data are you pointing to for this statement?

This and other comments about sediment availability make it clear that the reviewer had a problem with our description of sediment availability. We have substantially revised the text to define sediment availability, describe how we assess sediment availability, and how sediment availability is related to the volume of subsequent erosion.

P19L29-30: Spatially explicit models are being used: McGuire et al 2016 doi: 10.1002/2016JF003867; McGuire et al. 2017 doi: 10.1002/2017GL074243

Good point, we have cited these studies here.

P20L27: What makes sediment "available"?

Please see our previous comments relating to the issue of sediment availability.

Figure 1: Mark the location of Laramie with a dot. What determines the thickness of the blue lines?

"Laramie" in the figure refers to Laramie County – county names are one of the layers on this map. The caption has been updated to reflect this. The caption already designates the thickness of the blue lines.

Figure 2: How did you calculate the maximum intensity?

This is described in section 3.3 in the methods.

Figure 10: Make sure to say these are "Pearson" correlation coefficients. They are averaged for each time period, right?

We have modified the caption to state that these are Pearson correlation coefficients. They represent the overall relationship between the change in volume for each time period versus the independent variable. So there is no "averaging", and we are confused by this comment.

Figure 11: Consider using equal axes in A and D.

We prefer this figure as presented. Erosion and deposition rates in SG and HG differed enough that showing the plots at the same scale would compress the HG results and make the data more difficult to visualize.

Response to Referee #2

Please see our responses to each referee comment below (in blue):

Anonymous referee #2: This manuscript reports on quantitative changes in erosion & deposition along 50–meter length channel sections of two stream networks that experienced wildfire and flooding in a mountainous region of Colorado. Using DEMs of difference calculations from 4 time intervals spanning a total of 3 years, they show that significant volume changes in the 50-meter valley segments from erosion or deposition were correlated to contributing area, channel width, burn severity, channel slope, and rainfall intensity. The value of the manuscript is two-fold, because they develop thoughtful methods for analyzing the spatial and temporal pattern of sediment storage from repeat DEM data (including a canopy interference correction), and their conclusions about the landscape and meteorological controls on valley response can be used to predict downstream risks in fire-prone landscapes. This is a very powerful paper with a nice dataset and is pretty close to being ready for publication.

We greatly appreciate the referee's positive comments about the two-fold value of our paper, and that it is "pretty close to being ready for publication". ☺

While the authors were transparent in how they approached the study, there are some aspects that could be clarified simply to help the reader follow the rich dataset and somewhat involved analytical approach. Here are some suggestions that may help the presentation of the work:

-How did the authors land on 50-meter channel sections? Clearly this is a balance of resolving power and obtaining analytical units with meaningful change, but a few lines explaining the rationale of this length scale would be helpful

As noted in our response to a similar comment from Reviewer 1, we have inserted two sentences in the text to explain why we divided the channel network into 50-m segments.

-Skin Gulch and Hill Gulch received significantly different volumes and intensities of precipitation over the study period: the magnitude of this difference should be generalized perhaps in a table (a row or two could be tacked on to Table 1) with maximum 30-minute rainfall rates measured over the time period or something that generalizes the total rainfall or intensity difference that the watersheds had. I appreciate the images in Figure 3 that show precipitation data in grids but I'm still left unclear on the magnitude of differences between the watersheds with regards to precipitation.

This again is something that Reviewer 1 noted, so we will add a short table to summarize the total rainfall and the maximum 30-minute intensities for each watershed and each time period.

-I'm interested in the relationship between fire intensity and erosion/deposition measured in the channel sections. Fire intensity appeared to be one of the more significant predictors of net volume change in the channel, yet I'm unclear as to how and over what scale Burn Severity was calculated.

We first note that fire intensity is heat lost per unit time per unit flame length, while severity is the effect on the vegetation ("vegetation burn severity") and soils ("soil burn severity"). We presume that the reviewer is concerned with burn severity, as there are no data on fire intensity. In the methods we specify that we did have a burn severity map and provide a reference for this. We also state in Section 3.2 that for each segment we determined the percent of the contributing area that was burned at high and moderate severity, respectively (p. 5, lines 29-31 in the original manuscript). In response to this comment we are altering the wording in this sentence to make it more explicit: "Percent area burned at both high and moderate severity were determined **for the contributing area** of each segment using **the** burn severity (BS) map …(Stone, 2015)." (changes in bold).

Brogan et al. find here that %burned at moderate to high intensity may be a good predictor of erosion/deposition measured in the channel; these results are consistent with the recent findings of Abrahams et al. 2018 (DOI:10.1002/esp.4348) showing that burn severity was the biggest predictor of hillslope erosion in Fourmile Canyon, central Colorado.

The fact is that researchers have long recognized the importance of burn severity for predicting hillslope runoff and erosion, and we have already referenced some of the most directly relevant papers (e.g., Benavides-Solorio and MacDonald, 2001; Wagenbrenner et al., 2006). The problem is that burn severity is a categorical variable, so it is generally better to relate erosion rates to percent bare soil, as percent bare soil is a continuous variable that can be plotted directly against erosion rates, which is another continuous variable. We appreciate this new reference, and now refer to it in the discussion.

Minor Comments:
The paragraph structure in several parts of the paper is weak, especially on pages 10-14: lots of small (2-4 sentence) paragraphs starting with the same word or phrase. Combine some of these short paragraph fragments into larger paragraphs that flow into one another.

Yes, there are a lot of short paragraphs. We separated the paragraphs in order to make it more clear that we were switching topics or locations. We have extensively revised Section 4.2 in response to the first reviewer, and as we delete some of the details and focus on the broader story we have consolidated many of the short paragraphs that were a concern for the reviewer.

On Figures 8 and 9, the general shape of the canyons is given in the upper pane (A. longitudinal profile, slope, valley width, etc.)- which DEM sources was used for these initial data? Because so many DEMS are used here, just be clear about which one is used for various visuals.

We have added a sentence to the captions to make it clear that the data in the first panel are derived from the October 2013 DEM developed by the USGS.

Figure 12: the x-axis title should be "channel slope".

We appreciate this comment, and have changed both the x-axis labels and the caption so that slope is now explicitly labeled as "channel slope".

Spatial and temporal patterns of sediment storage and erosion following a wildfire and extreme flood

Daniel J. Brogan[1], Peter A. Nelson[1], and Lee H. MacDonald[2]

[1]Department of Civil and Environmental Engineering, Colorado State University, Fort Collins, Colorado 80523-1372, USA
[2]Department of Ecosystem Science and Sustainability, Colorado State University, Fort Collins, Colorado 80523-1476, USA

Correspondence: Peter A. Nelson (peter.nelson@colostate.edu)

Abstract. Post-wildfire landscapes are highly susceptible to rapid geomorphic changes at both the hillslope and watershed scales due to increases in hillslope runoff and erosion, and the resulting downstream effects. Numerous studies have documented these changes at the hillslope scale, but relatively few studies have documented larger-scale post-fire geomorphic changes over time. In this study we used five airborne laser scanning (ALS) datasets collected over four years to quantify ~~valley bottom changes~~ erosion and deposition throughout the channel network in two $\sim$15 km^2 watersheds, Skin Gulch and Hill Gulch, ~~after the June 2012 High Park fire~~ in northern Colorado ~~and a~~ after a wildfire followed by a large, long-duration large ~~mesoscale~~ flood 15 months later. The objectives were to: 1) quantify ~~spatial and temporal patterns~~ the volumes, spatial patterns, and temporal changes over time of erosion and deposition ~~throughout the channel network following the wildfire and including the mesoscale flood~~over a nearly four-year period; and 2) evaluate ~~whether these~~ the extent to which these spatially and temporally explicit changes are correlated to precipitation metrics, burn severity, ~~or~~ and morphologic variables. ~~Geomorphic~~ The volumetric changes were calculated ~~using a DEMs of difference (DoD) approach for~~ from a differencing of DEMs for 50-m long segments of the channel network ~~segmented into 50-m lengths~~and associated valley bottoms. The results showed net sediment accumulation after the wildfire in the valley bottoms of both watersheds, with ~~the greatest~~ greater accumulations in the ~~first two years after burning in~~ wider and flatter valley bottoms in the first two years after burning. In contrast, the mesoscale flood caused large ~~net~~ amounts of erosion, with ~~the greatest erosion in the areas with the greatest~~ higher erosion in those areas with more post-fire deposition. Only minor changes occurred over the two years following the mesoscale flood. Volume changes for the different time periods were weakly but significantly correlated to, in order of decreasing correlation, contributing area, channel width, percent burned at high and/or moderate severity, channel slope, confinement ratio, maximum 30-minute ~~rainfall~~precipitation, and total ~~rainfall~~precipitation. These results suggest that morphometric characteristics, when combined with burn severity and a specified storm, can indicate the relative likelihood and locations for post-fire erosion and deposition. This information can help assess downstream risks and prioritize areas for post-fire hillslope rehabilitation treatments.

1 Introduction

Wildfires alter hydrologic response by creating conditions that can lead to greatly increased runoff and erosion rates. At plot to hillslope scales increased rates of runoff have been attributed to a decrease in canopy cover, ground cover and surface roughness, and an increase in soil sealing and soil water repellency (e.g., Benavides-Solorio and MacDonald, 2001; Huffman et al., 2001; Larsen and MacDonald, 2007; Onda et al., 2008; Larsen et al., 2009; Ebel et al., 2012; Stoof et al., 2012; Schmeer et al., 2018). At the hillslope scale these fire-induced changes increase a variety of erosional processes, including rainsplash, sheetflow, rilling, gullying, landslides, and debris flows (e.g., Benda and Dunne, 1997; Inbar et al., 1998; Cannon et al., 2001; Gabet and Dunne, 2003; Roering and Gerber, 2005; Wagenbrenner and Robichaud, 2014; Rengers et al., 2016b). As spatial scale increases channel erosion can become important (e.g., Meyer et al., 1992; Legleiter et al., 2003; Wagenbrenner and Robichaud, 2014), but ~~the literature predominantly reports~~ at larger scales the predominant post-fire response is deposition, including alluvial fans, channel infilling, floodplain accretion, reservoir filling, and a sediment superslug (e.g., Moody and Martin, 2001; Reneau et al., 2007; Santi et al., 2008; Orem and Pelletier, 2015; Moody, 2017).

Considerable advances have been made in understanding post-wildfire runoff, erosion, and mass wasting at hillslope and small watershed scales (see Shakesby and Doerr, 2006; Moody et al., 2013, and references within); however, the larger-scale effects of fires on flooding, water quality, and sedimentation are often the most significant due to their adverse human and resource impacts (Hamilton et al., 1954; Doehring, 1968; Moody and Martin, 2001, 2004; Rhoades et al., 2011; Writer et al., 2014). ~~Most~~ Despite recent advances in modeling basin-scale post-wildfire runoff (Rengers et al., 2016a), most efforts to model post-fire runoff and erosion have focused at the hillslope scale, and include WEPP (e.g., Elliot, 2004; Miller et al., 2011), RUSLE (Renard et al., 1997), AGWA (Goodrich et al., 2005), and ERMiT (Robichaud et al., 2007). The first two models have been used as the basic building blocks for predicting changes at scales larger than a few hundred hectares (e.g., GeoWEPP; Miller et al., 2011; Elliot et al., 2016), but downstream post-fire flooding, erosion, and sedimentation are not a simple sum of hillslope-scale processes. Accurate predictions and upscaling from hillslopes require a more explicit consideration of sediment storage and erosion, and a failure to do so will result in unreliable estimates of watershed-scale peak flows, sediment production, sediment deposition, and sediment delivery (e.g., Moody and Kinner, 2006; Stoof et al., 2012). ~~Larger-scale studies also have generally quantified sediment delivery rather than explicitly evaluating the magnitude and controls on the spatially-varying geomorphic changes over the channel network (e.g., Pelletier and Orem, 2014; Orem and Pelletier, 2015).~~ Efforts to measure and better understand ~~these~~ larger-scale geomorphic changes have been hampered by the lack of high spatial- and temporal-resolution data at the watershed scale (Moody et al., 2013). The lack of quantitative data have precluded a spatially-explicit evaluation of the controls on the volumetric changes in erosion and deposition throughout a channel network (e.g., Pelletier and Orem, 2014; Orem and Pelletier, 2015).

To some extent the larger-scale effects of fires should be analogous to the observed patterns of erosion and deposition following large floods (e.g., Wolman and Eiler, 1958). More specifically, stream power—or gradients in stream power—and lateral confinement have ~~generally~~ typically been the best predictors of the spatial patterns of erosion and deposition (e.g., Miller, 1995; Fuller, 2008; Thompson and Croke, 2013; Gartner et al., 2015; Stoffel et al., 2016; Surian et al., 2016; Yochum et al., 2017), although strong correlations are not always apparent (e.g., Nardi and Rinaldi, 2015). Total energy expenditure during floods (Costa and O'Connor, 1995) can be equally important as stream power and lateral confinement in estimating total sediment transport (e.g., Wicherski et al., 2017). In contrast to fire studies, studies on the geomorphic impacts of extreme floods have usually focused on the erosional changes, even though short-duration, high-energy floods may cause substantial ~~and long-lasting~~ sediment deposition (e.g., Magilligan et al., 2015; Brogan et al., 2017).

New technologies, such as repeat airborne laser scanning (ALS), offer the potential to greatly improve our ability to quantify and analyse post-fire sediment storage and erosion over time and space (sensu Passalacqua et al., 2015). However, the decimeter-scale uncertainty in detecting elevation change means that ALS differencing is most useful in stream channels and valley bottoms where ~~there is a greater likelihood of detectable elevation changes . As suggested in Moody et al. (2013), the goal is to relate the measured volumetric changes to key controls such as rainfall amounts and intensity, burn severity, and geomorphic characteristics, and use these to help predict the type and likelihood of downstream effects~~the elevation changes are more likely to exceed the measurement uncertainty.

In June 2012 the High Park Fire (HPF) burned 350 km^2 of primarily montane forest just west of Fort Collins, Colorado, U.S.A. Within the HPF burn area we began intensively monitoring two similar $\sim$15 km^2 watersheds to quantify post-wildfire geomorphic changes (viz., Brogan et al., 2019). Subsequent ~~rainfall-runoff floods~~ convective storms created a unique comparison between the two watersheds, as ~~one watershed was subjected to a very~~ a high intensity summer thunderstorm just one week after ~~the fire was contained, and this~~ burning caused very extensive downstream deposition that was not replicated in the other watershed. Fifteen months after burning an exceptionally large and long-duration mesoscale flood caused sustained high flows and channel erosion in both watersheds, and this severely altered the expected post-fire trajectory of persistent and progressively declining deposition. We were fortunate to have two ALS datasets to evaluate the post-fire changes prior to the mesoscale flood, and three more ALS datasets to document the flood and ~~subsequent~~ two more years of post-fire ~~effects over the following two years~~effects. This unique collection of sequential ALS data allows us to both quantify and compare the geomorphic changes due to the fire and the flood over time and space. We also can ~~evaluate how the differences in the initial post-fire storms affected~~ infer how the different amounts of deposition in the two watersheds may have altered the relative effects of the mesoscale flood. The validity and our understanding of the ALS differences were greatly enhanced by ~~other~~ several closely-related studies, including the intensive monitoring of 21 channel cross sections and longitudinal profiles in the two study watersheds (Brogan et al., 2019), estimated peak flows due to the large convective storm one week after the fire was contained (Brogan et al., 2017, 2019), the identification of ~~rainfall~~ precipitation thresholds for runoff and sediment delivery (Wilson et al., 2018), measured hillslope-scale erosion rates (Schmeer et al., 2018), and a more limited study of the hillslope erosion rates and channel changes in summer 2013 (Kampf et al., 2016). Together these data allow us to answer two key questions: 1) what are the spatial and temporal patterns of erosion and deposition following a wildfire and a large flood in the valley bottoms of small- to moderate-sized watersheds (0.1–15 km^2)? and 2) to what extent can these patterns be related to precipitation depths and intensities, burn severity, and valley and basin morphology? The results should help predict the likelihood and potential magnitude of downstream erosion and deposition after large high-severity wildfires and large floods, and hence the potential for adverse downstream effects.

2 Site Description

Two proximate and very similar watersheds, Skin Gulch (SG) and Hill Gulch (HG), were selected to investigate post-wildfire geomorphic changes (Figure 1). Both watersheds burned in the High Park fire, both drain north into the Cache la Poudre River, and they are similar in size at 15.3 and 14.2 km^2, respectively. ~~Elevations~~ In SG elevations range from 1890 to 2580 m~~in SG and HG is slightly farther east and~~ , while HG is about 8 km to the east and therefore slightly lower at 1740 to 2380 m (Table 1). Average terrain slopes and drainage density for SG and HG are very similar at 23% and 24%, and 2.5 and 2.3 km km^{-2}, respectively. The two watersheds have nearly identical hypsometric curves with ~~the bulk of the elevations falling within~~ much of the area at mid-elevations, ~~with~~ although there are some flatter areas in the upper portions of each watershed. ~~Land cover is primarily uninhabited wildland with~~ About 81% of SG and 89% ~~evergreen forest in SG and HG, respectively~~ of HG is largely unmanaged coniferous forest that is predominantly ponderosa pine with some increasing amounts of douglas fir and lodgepole pine on north-facing slopes and at higher elevations (Jin et al., 2013). SG is predominantly National Forest land, while HG is primarily privately owned. In each watershed there are several very small reservoirs that were presumably established as stock ponds. ~~No~~ A control watershed could not be identified due to the lack of sequential ALS data outside of the High Park fire.

Approximately 65% of each watershed was burned at moderate to high severity. In SG most of the area burned at moderate to high severity was in the upper headwaters, while in HG most of the moderate to high severity burned areas were in the lower portion of the watershed (Figure 1). Straw and wood mulch were applied from helicopters in 2012 and 2013 to approximately 6% and 18% of the hillslopes in SG and HG, respectively. The underlying geology is primarily schist with scattered rock outcrops (Abbott, 1970, 1976; Braddock et al., 1988), and the soils are predominantly Redfeather sandy loams (HPF BAER Report, 2012; Soil Survey Staff, 2018). Headwater reaches range from wide shallow swales to steep and confined channels; the middle reaches generally are steep and confined with scattered floodplain pockets; and the downstream reaches are wider with mostly continuous floodplains. Sediment is stored predominantly in the channel bed and on the floodplains. The area is characterized as semiarid with mean annual precipitation of 450-550 mm (PRISM Climate Group, Oregon State University, http://prism.oregonstate.edu). Summer precipitation is usually derived from convective thunderstorms, while spring and fall storms tend to be lower intensity frontal storms. Approximately one-third of the annual precipitation falls as snow.

Streamflow in both watersheds was seasonal prior to burning, and the downstream mainstem channels were only about 1-2 m wide. After the fire streamflow noticeably increased and became perennial. One week after the fire had been contained a convective storm in SG generated large amounts of hillslope and upstream channel erosion ~~,~~ and extensive downstream deposition (Brogan et al., 2017). Two-dimensional hydraulic modeling yielded an estimated peak ~~flow of~~ flow–without accounting for sediment bulking–of nearly 30 m^3 s^{-1} km^{-2}, and ~~extensive downstream deposition (Brogan et al., 2017);~~ this event is henceforth referred to as the ~~'convective flood' throughout the paper. No comparable storm occurred~~ "convective flood". There was no comparable storm in HG, but both watersheds were subjected to a series of smaller convective storms during each of the summers. The other major event was a spatially large and long-duration mesoscale storm in September ~~2013 a large mesoscale storm caused~~ 2013 that caused extensive destruction throughout the Colorado Front Range as well as widespread and prolonged high flows in both ~~watersheds~~SG and HG. Peak flows were estimated to be 2.3~~–5.7~~ -5.7 m^3 s^{-1} km^{-2} in SG and 0.9~~–1.4~~ -1.4 m^3

s^{-1} km^{-2} in HG, with the range of values depending primarily on whether the peak flow ~~is estimated using~~ was modeled with pre- or post-flood topography (Brogan et al., 2017, 2019).

3 Methods

3.1 ALS preparation

In each of the four years after the fire an ALS dataset was collected over the entire burn area by the National Ecological Observatory Network (NEON) Airborne Observatory Platform. Each ALS dataset is referred to in this paper by the year and month of collection using the format of yyyymm, so the four NEON datasets are 201210, 201307, 201409, and 201506. A fifth ALS dataset, 201310, was collected by the U.S. Geological Survey (USGS) and Federal Emergency Management Agency (FEMA) in fall 2013 to help assess the damage caused by the September 2013 mesoscale flood. The four time periods between the five ALS datasets are referred to in this paper as T1, T2, T3 and T4. The 201307 ALS data in SG had substantial alignment issues, so we used OPALS (Orientation and Processing of Airborne Laser Scanning software Mandlburger et al., 2009) to improve the flightline alignment. ~~Aerial photographs from~~ We attempted to estimate the volume changes in the channels and valley bottoms for the first summer after burning by constructing point clouds from 2008 ~~were used to construct point clouds covering our study watersheds~~ aerial photographs using structure-from-motion ~~photogrammetry~~ [unpublished data from S. Filippelli, Colorado State University, 2015]. Unfortunately ~~these data did not allow for accurate volumetric differencing with respect to the first ALS dataset because~~ the extensive vegetation cover ~~hampered the measurement~~ prevented the accurate delineation of bare-earth elevations over most of the study area~~.~~, and this meant that we were not able to quantify the post-fire deposition that occurred prior to the first ALS dataset in October 2012.

For each ALS dataset the raw point clouds were merged, ground classified, and clipped to our two study watersheds using LAStools (Isenburg, 2015). Ground classification parameters included: a buffer of 50 m; a step size of 5 m; and an extra fine search for initial ground points. From these processed point clouds we created digital elevation models (DEMs) with 1 x 1 m pixels (Isenburg, 2015). Care was taken to align all ALS DEMs as closely as possible using a Python script to calculate the differences in slopes and aspects between each NEON DEM and the 201310 USGS/FEMA DEM ~~(following the co-registration methodology f~~ (following Nuth and Kääb, 2011). The resulting estimate of the XYZ translation required to rectify the location of each NEON DEM was repeated until translation changes in X, Y, and Z were less than 1 cm, or the required shift for that iteration was less than 2% of the overall required shift. Each point cloud was shifted by the computed translation, and DEM rasters were recreated from the translated point clouds. Finally, the rectified point clouds were compared to total station and RTK-GNSS survey points to calculate the mean absolute error (MAE) as an indication of the accuracy of each ALS dataset.

3.2 ~~Valley bottom~~ Delineating and characterizing the valley bottoms and contributing ~~area delineation~~areas

We used FluvialCorridor, an ArcGIS Toolbox that extracts a number of riverscape features (Roux et al., 2015), to delineate the valley bottoms in each watershed from the 201310 DEM. Defining a channel network is the first step, and for this we set a contributing area threshold of 0.1 km^2 based on local field surveys (Henkle et al., 2011). The valley bottom was then computed and adjusted using a number of user-controlled input parameters, such as elevation threshold aggregation and disaggregation distances, buffer sizes, and smoothing tolerance. We adjusted these parameters until the valley bottom delineation satisfactorily matched aerial photographs and 2-m contour lines derived from the 201310 DEM.

Valley bottom polygons were segmented into 50-m long sections oriented in the downstream direction, yielding 595 segments in SG and 559 segments in HG. ~~FluvialCorridor had~~ A segment length of 50 m was selected because this length is sufficiently long to characterize the local morphometrics while also allowing for a relatively high resolution assessment of the rate of change in slopes, valley bottom widths and other characteristics. Fifty meter segments also match the typical length of the longitudinal profiles that we surveyed to obtain higher temporal resolution data on channel geomorphic changes (Brogan et al., 2019). FluvialCorridor did have difficulty characterizing valley bottoms for the headwaters of several tributaries with gently sloping topography; ~~unrealistically wide delineated valleys~~ the resulting unrealistically wide valley bottoms caused us to remove 89 and 56 segments in the headwaters of SG and HG, respectively. Another eight segments near the outlet of SG were excluded because the deposited sediment was repeatedly excavated by the state highway department (for example see Figure 10C in Kampf et al., 2016). Seven more segments in lower SG were excluded during T4 due to channel realignment and rehabilitation efforts, and one segment was excluded in lower HG during T4 due to the reconstruction of a house. A few other segments were removed from each watershed due to small reservoirs and unreliable ground classification. Ultimately 490 segments in SG and 484 segments in HG were used for summarizing morphometrics (see section 3.4) and for statistical analysis (see section 3.7), and these represent 83% of the total channel length in SG and 87% of the total channel length in HG.

Contributing area polygons were delineated for each segment using a looped Python script that uses the ‘Hydrology’ toolset and ‘Raster to Polygon’ tool in ArcGIS. The resulting polygons were used to determine ~~mean total rainfall and area-maximum~~ the total precipitation and maximum 30-minute ~~rainfall intensity~~ precipitation intensities for each segment for each of the four time periods (see section 3.3 for more detail). Percent ~~contributing~~ area burned at both high severity (BS_h) and moderate severity (BS_m) were determined for the contributing area of each segment using ~~a~~ the burn severity (BS) map derived from RapidEye imagery and a multistage decision tree (Stone, 2015).

3.3 Precipitation

The amount and intensity of precipitation over the two study watersheds was determined from the National Weather Service WSR-88D Doppler radar in Cheyenne, WY, corrected with local daily rain gage data. We began by converting the dual-polarized one-hour precipitation accumulation (DAA) radar products into gridded precipitation estimates using a 0.5-km grid. The precipitation was summed for each grid cell from 0700 to 0700 local time to match the daily rain gage data. These radar estimates were then compared to the rain gage estimates to come up with a daily mean field bias (Wright et al., 2014):

$$B_i = \frac{\sum G_{ij}}{\sum R_{ij}} \tag{1}$$

where B_{i} is the bias for day i, G_{ij} is the daily ~~rainfall~~ precipitation for day i and gage j, and R_{ij} is the summed 24-hour ~~rainfall~~ precipitation for day i and radar pixel containing j. Sources of gage data include four-inch diameter rain gages monitored by members of the Community Collaborative Rain, Hail & Snow (CoCoRaHS) Network (url: www.cocorahs.org), and tipping-bucket gages monitored by researchers at Colorado State University, the National Center for Atmospheric Research, and the U. S. Geological Survey. The number of rain gages used to compute the bias ranged from 36 to 97 depending on how many of the tipping-bucket gages were active and how many manual observations were recorded for a given day. These gages were located in and around our study watersheds, with the farthest gage being 40 km away.

Daily total ~~rainfall~~ precipitation and maximum 30-minute precipitation intensity (MI_{30}) were calculated from the bias-corrected DAA radar data for every 0.5-km grid cell across the HPF from October 2012 to November 2015. MI_{30} was chosen over other intensity intervals (e.g., MI_{5}, MI_{15}, etc.) because it correlates best with peak flood discharge (Moody et al., 2013), and also is closely correlated with peak stage (Kean et al., 2011) and with hillslope erosion rates from the HPF (Schmeer et al., 2018). Since volume changes over the intervals between ALS datasets represent cumulative geomorphologic effects, daily ~~rainfall~~ precipitation was summed for each of the four time periods. In contrast, the maximum MI_{30} value between each ALS dataset was determined for each cell in each watershed. Finally, the mean total ~~rainfall~~ precipitation and the maximum MI_{30} was computed for the upstream area of each channel segment for each DoD. This meant that the maximum MI_{30} values for different cells within a given contributing area did not always originate from the same storm as the different summer thunderstorms were often very localized.

3.4 Topographic and hydraulic controls

A series of valley bottom, channel, and contributing area metrics, called morphometrics in this paper, were estimated for each 50-m segment. These data were correlated to the calculated volume changes to help determine possible controls on the volumes of erosion, deposition, and net change. A series of Python scripts were written to clip, extract and compute morphometrics directly from the DEMs and/or a combination of outputs from FluvialCorridor (e.g., stream network, segment polygons, valley widths). ~~Stream~~ Streamline networks for each ALS dataset were created for each watershed, and the mean channel slope (S) for each segment was ~~calculated using~~ determined by the slope of a linear regression on streamline elevations extracted from each ALS dataset at one-meter intervals. Topographic curvature (ΔS) was quantified for each segment by calculating the slope of ~~a linear regression where the channel slope of the~~ the linear regression between the channel slopes of a given segment and the two upstream segments ~~were plotted against the~~ versus distance upstream. A positive ~~curvature indicates a decrease in slope~~ slope indicates an increasing slope and negative curvature, while a negative ~~curvature indicates an increase in slope~~ slope indicates a decreasing slope and a positive curvature. Valley width (w_v) was computed at one-meter intervals along the valley centerline and an average width was calculated for each 50-m segment. Valley constriction and expansion (Δw_v) was computed in the same way as ΔS. Since the resolutions of the DEMs and aerial imagery were too coarse to accurately delineate the channels, channel width (w_c) was estimated from a regional downstream hydraulic geometry equation (Bieger et al., 2015):

$$w_c = 1.24A^{0.435} \tag{2}$$

where A is the drainage area in km^2 and channel width is in m.

We defined channel confinement as the ratio of valley width to channel width (C_r). Unit stream power, a hydraulic control, is often a good predictor of erosion and deposition (e.g., Baker and Costa, 1987). Unit stream power ω is equal to:

$$\omega = \frac{\gamma Q S_f}{w_c} \tag{3}$$

where γ is the specific weight of water (N m^{-3}), Q is discharge (m^3 s^{-1}), and S_f is the friction slope (m m^{-1}). Because continuous stage or flow data were not available, and given the potential uncertainty in the regression equation for w_c, we used the ratio of channel slope to valley width ($\frac{S}{w_v}$) as a proxy for stream power. Downstream changes in the slope-width ratio ($\Delta\frac{S}{w_v}$) were computed in the same way as ΔS and Δw_v.

3.5 Valley change

DEMs of difference (DoDs) were computed using the geomorphic change detection (GCD) tool add-in for ArcGIS (gcd.joewheaton.org, version 6; Wheaton et al., 2010). GCD uses a fuzzy inference system (FIS) to propagate spatially explicit DEM uncertainties, and consequently the uncertainties in the DoD. Spatially ~~propagated~~ explicit errors are much more accurate than assuming a uniform uncertainty, as the latter can lead to large errors in the calculated volumes of erosion and deposition (e.g., Wheaton et al., 2010; Milan et al., 2011).

Point quality, point density, and slope were included as membership functions in our FIS procedure. We assumed uniform point quality based on the accuracy of the ALS after adjustment (i.e., the MAE for each dataset). Point density was computed for each DEM pixel based on the point cloud, and slopes were derived directly from the DEM. After differencing the DEMs, pixels with elevation changes smaller than the spatially propagated errors were ignored, and the remaining values constitute the thresholded DoD. The GCD tool also calculates total volumes of erosion, deposition, and net change, along with the uncertainty for each volume estimate. The uncertainties in the total volumes of erosion and deposition were computed by multiplying individual error heights times the pixel area and summing these. Uncertainty in each net volume difference was propagated from the corresponding uncertainties in erosion and deposition. Using the thresholded DoDs and our own Python script we computed the volumes of erosion, deposition, and net change for each 50-m segment for each time period.

The sign and overall magnitude of ALS-derived volumetric changes for the 50-m segments were compared to the ~~surveyed changes at~~ measured changes for the 10 cross sections in SG and 11 cross sections in HG ~~(see Brogan et al., 2019, for more information on t~~ (Brogan et al., 2019). The measured changes in cross-sectional area were multiplied by 50 m to obtain volumes that were then compared to the calculated ALS volume ~~change for a given segment~~changes for the 21 channel segments where there was a cross section.

3.6 Removal of spurious vegetation artifacts

A visual check of the DoD results revealed the calculated volume changes were being affected by seasonal changes in leaf cover. For example, some locations had up to 3 m of deposition calculated from fall to summer (i.e., ~~201210—201307 (~~201210-201307, or T1~~), 201409—201506 (~~, 201409-201506 or T4)~~)~~, and nearly identical amounts of erosion from summer to fall (i.e., ~~201307—201310 (~~201307-201310, or T2). Vegetation issues were not immediately obvious in the ~~201310—201409~~

~~(~~201310-201409 or T3 ~~)~~DoD, as both ALS datasets were collected in the fall. A raster-based algorithm was written to identify possible spurious changes due to changes in the deciduous leaf cover on a pixel-by-pixel basis for the DoDs that covered different seasons (i.e., T1, T2, and T4). An example of the algorithm's logic is as follows: If for a given pixel the change in both fall-to-summer differences (T1 and T4) were small, but the change from summer-to-fall (T2) was large compared to the T1 and T4 changes, it would indicate that vegetation was contaminating the signal at that location. This logic applies for other combinations of DoD differences, and takes the form of Algorithm 1.

Algorithm 1 Vegetation removal algorithm

if $DoD_{T1} - DoD_{T4} \leq \theta$ **and** $DoD_{T4} + DoD_{T2} \leq \theta$ **and** $DoD_{T2} + DoD_{T1} \leq \theta$ **then**
  pixel value = 0
else if $DoD_{T1} - DoD_{T4} \leq \theta$ **and** $DoD_{T4} + DoD_{T2} \leq \theta$ **then**
  pixel value = 0
else if $DoD_{T1} - DoD_{T4} \leq \theta$ **and** $DoD_{T2} + DoD_{T1} \leq \theta$ **then**
  pixel value = 0
else if $DoD_{T4} + DoD_{T2} \leq \theta$ **and** $DoD_{T2} + DoD_{T1} \leq \theta$ **then**
  pixel value = 0
else
  pixel value = 1
end if

In Algorithm 1, $DoD_{T\#}$ refers to the DoD for a given time period (i.e., T1, T2, or T4), and θ is a threshold in meters. We used this algorithm to classify each pixel as a 0 or 1, with 0 indicating a seasonal vegetation artifact when at least two of the three DoDs showed a difference in elevation change that was less than or equal to 1m (θ). This raster of 1's and 0's was multiplied on a cell-by-cell basis for each DEM to exclude those pixels with a seasonal vegetation artifact for that DOD, and the GCD tool was rerun to more accurately estimate the volume and uncertainty of geomorphic changes. Figure 2 shows an example of this vegetation filtering for a location in Skin Gulch that showed around ~~1 to 3~~ 1-3 m of deposition from fall 2012 to summer 2013 (Figure 2A) and around ~~1 to 3~~ 1-3 m of erosion from summer 2013 to fall 2013 before filtering out the seasonal artifacts (Figure 2B). A site visit in September 2016 verified the lack of such large vertical geomorphic change and confirmed a predominantly deciduous cover of narrowleaf cottonwood, Rocky Mountain maple, alders, chokecherry, and wild raspberries (Figure 2C).

3.7 Statistical analysis of controls on erosion and deposition

Pearson correlation coefficients were calculated between the different site factors and the erosion, deposition and net volume changes in the 50-m segments for each of the four time periods and each watershed. The different site factors were total ~~rainfall~~precipitation, MI_{30}, percent of contributing area burned at high and/or moderate severity, and drainage network morphometrics ~~(~~as explained in section 3.4~~)~~. Since some of the morphometric variables changed from the beginning to the end of a given time period (i.e., S, ΔS, $\frac{S}{w_v}$, and $\Delta\frac{S}{w_v}$), we calculated the correlations for each time period using both the ~~before and the after~~ beginning and end values. We found negligible differences in the strength of the correlations depending on whether we used the ~~before or after~~ beginning or end values, so we only present the results for the ~~before values~~ values at the beginning of each time period. Normalizing the net volume changes by contributing area generally did not improve the correlations, so these results also are not presented here. Correlations were also calculated after stratifying the data by channel slope ($<$ or $\geq$ 4%) and contributing area ($<$ or $\geq$ 4 km^2), but these results are not presented as these did not greatly improve the correlations or lead to clear insights about the underlying processes. We did not stratify the data by physiographic unit or lateral confinement as suggested by Rinaldi et al. (2013) and Nardi and Rinaldi (2015) because the stream ~~type~~ types in our two study watersheds ~~is predominantly classified as cascade~~ were predominantly cascade channels (Montgomery and Buffington, 1997). It should be noted that a positive correlation indicates increasing deposition or decreasing erosion with an increasing independent variable, while a negative correlation indicates decreasing deposition or increasing erosion. We recognize that each stream segment is not necessarily spatially independent because upstream erosion or deposition can affect downstream segments or reaches, but auto-correlations of the dependent variables generally ~~fall~~ fell below r = 0.5 ~~within~~ for five segments upstream or downstream. This ~~initial~~ correlation analysis provides a useful~~way to explore~~, initial assessment of how morphologic and site characteristics are generally related to the magnitudes of erosion, deposition, and net volumetric change. In the results we primarily focus on correlation coefficients that are either greater than 0.32 and less than -0.32 (i.e., $R^2 > 0.10$).

4 Results

Precipitation

Total ~~rainfall~~ precipitation and maximum 30-minute intensities varied considerably between each DoD time period, but the values were relatively similar within and between the two watersheds (Figure 3). ~~The lowest amount of precipitation was in~~ Total precipitation was lowest during T1 with a mean in SG of only 174 mm ~~for SG and~~ and and 185 mm ~~for HG (~~in HG (Table 2 and Figure 3A). ~~This~~ The T1 period also generally had the lowest ~~MI30~~ MI_{30} values other than a few very localized high-intensity storms (Table 2) (Figure 3B). ~~The second period included the large mesoscale storm and the rainfall from this storm was distributed relatively evenly across both watersheds (Kampf et al., 2016). Total rainfall over this three-month period ranged from 276 to 439 mm (Figure 3C), and this period tended to have the highest MI_{30} values of 32-73 mm hr^{-1}~~ Mean total precipitation over the short second period was much larger than in T1 with 366 mm in SG and ~~36-106 mm hr^{-1}~~ 327 mm in HG (~~Figure 3D). These higher values were due to convective summer thunderstorms as rainfall~~ Table 2), with most of this rainfall due to the mesoscale storm. Total precipitation was relatively evenly distributed over the two watersheds (Kampf et al., 2016) . Precipitation intensities during the mesoscale flood generally did not exceed 40 mm hr^{-1} (Kampf et al., 2016), but intense localized thunderstorms prior to the mesoscale flood generated some of the highest MI_{30} values recorded over the period covered by the ALS datasets (Table 2) (Figure 3D).

The third period was nearly a year so it had relatively high total ~~rainfall~~ precipitation values but low MI_{30} values (Table 2) (Figure 3F). As in T1 and T2, the relative variation in maximum MI_{30} values was much greater than the variation in total

~~rainfall~~ precipitation due to the high spatial variability of the summer thunderstorms. ~~The total rainfall of about 260-450 mm during the fourth time period was less than T2 and~~ Mean total precipitation in T4 was lower than in T3 (~~Figure 3G). Mean~~ Table 2), and the mean MI_{30} values ~~also were lower at~~ of around 30 mm hr^{-1} for SG and 38 mm hr^{-1} for HG (Figure 3H) were both lower than in T2 and T3, indicating less potential for hillslope erosion and downstream channel ~~changes~~change.

4.1 ALS data accuracy and valley morphometrics

Point density increased with each ALS dataset from a minimum of just under 1.2 pts/m^2 in the first ALS dataset to over 3.5 pts/m^2 for the last dataset in Skin Gulch and the next to last dataset in Hill Gulch ~~. Mean~~ (Table 3). After alignment the mean absolute errors (MAE) of the ~~final~~ ALS point clouds ~~in each watershed~~ were only 9-13 cm ~~,~~ except for the ~~MAEs of 23 and 15 cm for the~~ first and second ALS datasets in HG, ~~respectively~~which had MAEs of 23 and 15 cm, respectively (Table **??**).

The volume changes estimated from cross section data and the calculated volume changes from the ALS data for the corresponding segments generally ~~fall along a~~ plot close to the 1:1 line except for ~~one cross section for the second period in Skin Gulch and several cross sections for the~~ the first time period in ~~Hill~~ Hill Gulch and one cross section in the second period in Skin Gulch (Fig. 4). ~~The~~ Some differences between these two datasets should ~~not be too surprising~~ be expected given that the measured cross-section change was extrapolated to the entire 50-m segment. The ~~main~~ key point is that the ALS differencing results appear to be valid given the general agreement in the sign and magnitude of the ALS differencing and measured cross-section changes~~indicate that our ALS differencing is producing reasonable results~~.

The ~~inherent~~ overall comparability of SG and HG is further confirmed by the generally similar spatial distributions and trends in channel slopes, valley widths, and confinement ratios. For the 490 segments in SG and 484 segments in HG used in our analyses 86% and 73% had channel slopes greater than 0.065 m m^{-1}, respectively, and were classified as cascade according to Montgomery and Buffington (1997). ~~In SG and HG, respectively, 13% and~~ Thirteen percent of the channel segments in SG and 22% of the segments in HG had channel slopes of 0.03 to 0.065 m m^{-1}, which would be classified as step-pool~~, and less~~ . Less than 2% of the segments in SG and 5% of the segments in HG had channel slopes less than 0.03 m m^{-1}~~, and would be classified as either pool-riffle or plane bed (Montgomery and Buffington, 1997)~~. The few ~~channels~~ channel segments with slopes less than 0.03 m/m are primarily in a few headwater areas, near tributaries, and towards the outlet of each watershed.

Valley widths tended to increase downstream, with the exception of certain headwater locations where FluvialCorridor had difficulty characterizing the valley bottoms. Approximately 80% of the valley widths in each watershed were between 10 and 40 m. As might be expected, confinement ratios tended to decrease downstream and were relatively similar in the two watersheds with about 75% of the valley bottoms having values between 10 and 35, about 20% ~~were~~ having values greater than 35, and no segments had ~~confinement ratios less than~~ a confinement ratio below 5.

4.2 Spatial and temporal erosion and deposition volumes

The T1 ~~(201210–201307) included both~~ period (201210-201307) only began after the first summer of thunderstorm-driven runoff and erosion, so the two main periods of geomorphic change were spring snowmelt and ~~some summer thunderstorms, and the DoD data show considerable variability in the~~ the first summer thunderstorms. Snowmelt runoff was almost entirely erosional while the summer thunderstorms were primarily depositional but highly variable in space, and these different processes are reflected in the high variability and complex spatial patterns of deposition and erosion within and between the two watersheds (Figures 5~~–~~-9; see also Figures A1~~–~~-A4). ~~In SG there was more deposition than erosion, which resulted in a net volume increase in the valley bottoms of nearly 8000 m^3 (Figure 5A). In the headwaters there was relatively little~~ Many of the headwater reaches in SG had little or no erosion or deposition, ~~especially in the westward flowing channels in the easternmost part of the watershed (Figure 6A). In the~~ while in the middle portions of SG ~~deposition was predominant~~ there was more extensive deposition (Figure 6A), ~~and this was particularly evident~~ particularly along the main stem about 4-5 km above the outlet (Figure 8B). Lower in the watershed there ~~was net erosion and only limited deposition~~were areas with substantial amounts of net erosion with some deposition, particularly in the eastern tributary (Figures 6A and 8B). ~~This erosion in the lower watershed was due primarily to snowmelt incising through the large amounts of sediment that had been deposited during the first summer after burning but before~~ The total net volume change was nearly 8000 m^3 of deposition (Figure 5A), but our extensive field observations indicate that the total post-fire deposition was actually much larger as the first lidar ~~dataset of October 2012. The~~ data were collected only after the summer thunderstorms. It is of interest that the greatest erosion of 130 m^3 in one 50-m segment was just downstream of a confluence about 2 km above the outlet (Figure 8B), which is where ~~we observed showed tremendous deposition resulting from a large convective flood~~ our field observations showed tremendous sediment deposition from the exceptionally large convective rainstorm and flood that occurred just one week after the fire (see reference to confluence and XS6 in Brogan et al., 2017, 2019). ~~At this location there is a very sharp~~ This confluence marks a very large decrease in channel slope ~~and~~ for the west branch of Skin Gulch and a tremendous widening of the ~~main valley~~ valley bottom (Figure 8A), which largely explains ~~why there had been so much deposition. In general, however, the amounts of erosion or depositionwere not obviously related to the morphometric characteristics in SG because the first ALS dataset in fall 2012 was only collected after the extensive hillslope erosion and downstream deposition in summer 2012.~~

the large amount of deposition. In HG there was much more net deposition during T1, and the calculated volume of 19,000 m^3 ~~of net deposition during T1, mostly in the main channels about 2-4 km above the watershed outlet~~ was spread throughout much of the channel network (Figures 5B, 7A, and 9B). Much of this deposition was in the middle reaches where the channel slopes decreased to less than ∼0.10 and valley widths increased to more than ∼30 m (Figure 9). ~~Peak deposition of nearly 300 m^3 was in a segment about 2.5 km from the outlet, which is where the valley width abruptly increases to nearly 75 m and the slope drops below 0.05 (Figure 9).~~ Similar to SG, ~~the headwaters in HG~~ a number of the headwater reaches had only minor erosion or deposition ~~and there was a distinct lack of geomorphic changes in the westward-flowing channels in the easternmost portion of the watershed~~ (Figure 7A). Aerial imagery and soils data (Soil Survey Staff, 2018) indicate that these areas are ~~steeper with a greater~~ steep with a high density of exposed rock outcrops, suggesting ~~shallower soils. These characteristics, combined with the steep narrow channels, limit the sediment supply as well as the capacity for~~ a limited capacity for both channel incision and deposition.

In September 2013 ~~, which was 15 months after the fire and during T2, the~~ the mesoscale flood caused widespread and often dramatic erosion in SG (Brogan et al., 2017, 2019)~~, with a total net erosion of~~ . While there was some deposition in the downstream channels due to the summer thunderstorms (Brogan et al., 2019) (Figure 8C), the total net change in SG was

39,000 m^3 ~~. In SG erosionin the headwaters was minimal compared to the extensive channel changes~~ of erosion, with the vast majority of this occurring in the middle and downstream reaches (Figures 6B, and 8C). In the middle ~~reaches~~ portion of the watershed channel incision was ~~common, especially~~ particularly prevalent in the narrower valley bottoms (see Figures 4.13D, 4.13E, and 4.13F in Brogan, 2018). ~~Downstream channel widening and a few avulsions occurred where the valley was wide enough to contain a more continuous floodplain (see Figures 4.13B and 4.13C in Brogan, 2018). Many of the~~ Often the segments with the greatest ~~erosion were in areas where there was simply more sediment to be eroded. These locations included floodplain pockets (e.g., ∼2.5 km, ∼2.9 km and ∼3.5 km from the outlet), tributary junctions (e.g., ∼1.4, ∼2.0 km and ∼3.7 km from the outlet), colluvial deposits from hollows (e.g., ∼1.8 km from the outlet), and deposition from a combination of processes (e.g., ∼0.6 km and ∼1.0 km from the outlet). The available sediment is believed to be a combination of~~ eroded volumes were where we had observed larger amounts of deposited sediment from summer 2012 that could be easily eroded. From a more process-based perspective, the sediment available for erosion consisted of of pre-fire deposits accumulated over centuries to millennia (Cotrufo et al., 2016) that would have been somewhat protected from erosion by the vegetative cover, while the ~~extensive hillslope erosion in summers 2012 and 2013 added considerably more sediment that was readily accessible to the high flows during the mesoscale flood (Brogan et al., 2017, 2019).~~

~~During T2 the greatest erosion in SG was at ∼1.8 km from the outlet where over 1,800 m^3 of sediment was removed (see Figures 4.13B and 4.13C in Brogan, 2018); the four segments upstream of this location also experienced substantial erosion, and similar to T1 the large amounts of erosion can be attributed to the very large amounts of deposition from the large convective flood that occurred just after the fire (Figures 6B and 8C; see also reference to confluence and XS6 in Brogan et al., 2017, 2019). There also was up to 4.4 m of incision near a confluence in the middle of the SG.~~ post-fire sediment was more readily accessible because it usually was at lower elevations within the valley bottom and unprotected by any vegetative cover. Overall the total erosion in SG during T2 was 3.6 times larger than the total deposition during T1, and this large discrepancy can be largely attributed to the fact that most of the post-fire sediment ~~was~~ had been deposited in summer 2012 ~~before~~ prior to the first ALS survey ~~. Similar to T1, there were little to no geomorphic changes in the westward-flowing channels in the easternmost part of each watershed (Figure 6B).~~ (Brogan et al., 2017, 2019).

~~During T2~~ HG also experienced widespread erosion during T2 (Figures 6B and 7B; Brogan et al., 2017, 2019), but the net volume change was only two-thirds of the ~~net volume change in~~ value calculated for SG (Figure 5). ~~Similar to SG,~~ Some of the greatest erosion ~~in HG~~ occurred where there was more pre-fire sediment storage, including floodplain pockets (e.g., ∼2.4 km, ∼3.7 km and ∼4.7 km), tributary junctions (e.g., ∼2.2 km and ∼3.3 km), and colluvial deposits from hollows (e.g., ∼4.4 km; Figure 9). Substantial erosion also occurred where the hillsides constricted the valley width to less than 20 m; for example, there was over 800 m^3 and 1300 m^3 of erosion around 3.4-3.5 km and 3.8-4.0 km from the outlet (Figure 9C). ~~Similar to T1, there were minimal geomorphic changes in the westward-flowing channels in the easternmost part of the watershed (Figure 7B).~~

The pattern of erosion during T2 closely mirrored the depositional patterns from T1 (Figures 8 and 9), and this was particularly true for HG because there was ~~much more deposition during T1 and~~ qualitatively less deposition in summer 2012 prior to the first lidar dataset and proportionally more deposition during T1. For example, ~~there was~~ during T1 there was an estimated 2,300 m^3 of deposition in the valley bottom ~~in HG~~ between 2 and 3 km upstream of the outlet~~during T1~~, and this large amount of deposition was ~~where the slope decreases~~ associated with a slope decrease to around 0.04 m m^{-1} and ~~the valley width increases~~ an increase in valley width to 55 m. During T2 this same reach experienced 2,700 m^3 of erosion, or just slightly more than the amount of deposition during T1.

During T3 the patterns of erosion, deposition, and net change in both watersheds were similar in direction and location to T1 but smaller in magnitude (Figure 5)~~. The~~ , with the decline in magnitude is attributed to the reduced upslope erosion due to vegetative regrowth (**?**). SG and HG had more similar magnitudes of change ~~were more similar between the two watersheds~~ in T3 than in T1 because there were no undocumented periods of erosion or deposition. In SG erosion ~~in the southeastern headwaters resulted in small alluvial fan deposits (Figure 6C), and again there also~~ there again was substantial deposition about 4-5 km ~~from the outlet on the mainstem~~ upstream of the outlet (Figure 8D)~~. Farther downstream~~ , while goingdownstream there was a more even balance between erosion and deposition (Figure 6C). ~~The greatest erosion in SG occurred at a confluence around 3.7 km from the outlet where there was bank sloughing, which was largely a result of the channel incision and bank oversteepening that took place during the mesoscale flood in the previous time period (Figure 8D).~~

~~The T3 period in HG had~~ In HG there tended to be more consistent deposition from the headwaters to the outlet than in SG (Figure 7). The total volumes of erosion and deposition were slightly greater in HG than in SG, but this difference was much smaller than the 2-3-fold difference ~~measured~~ in T1 (Figure 5). The largest ~~depositional volumes of~~ volumes of sediment deposition were in the headwaters and the lowest portion of the watershed where the ~~post-flood sediment was~~ sediment left by the mesoscale flood could be reworked and transported by spring snowmelt and the runoff from summer thunderstorms (Figure 7C).

The ~~magnitude of total net volume change in~~ T4 ~~was less~~ period had smaller volume changes than any of the other time periods (Figure 5). ~~The overall pattern in both watersheds—like in~~ Like T1 and ~~T3—was deposition with very little erosion and a net volume change~~ T3, the overall pattern was deposition with net volume increase of just over 5,000 m^3 ~~. The similarity in total erosion, total~~ in both SG and HG. Most of the net erosion was focused in the lowest portions of the watersheds, especially in lower HG where there had been more deposition in T3 and therefore more sediment to be eroded in T4 (Figures 6D, 7D, 8E, and 9E). The similarities between the two watersheds in the amounts and patterns of erosion, deposition, and net volume changes ~~between the two watersheds~~ indicate a similarity in the primary driving processes of summer thunderstorms, hillslope erosion, downstream deposition, and erosion due to snowmelt. The lower absolute magnitude of these changes ~~were the lowest~~ in T4 ~~as this was the third year after burning and the hillslopes were recovering (Figure 5). As with the other time periods there generally were minimal changes in the headwaters of each watershed (Figures 6-9), and most of the larger volumetric changes were in the middle and lower portions of each watershed~~is consistent with the overall trend of vegetative recovery leading to less runoff and erosion as observed in other fires in the Colorado Front Range (e.g., **?**).

To summarize, the calculated volume changes for SG and HG were similar in their direction over the four time periods, and they also generally had roughly similar trends in magnitude (Figure 5). ~~Net volume changes~~ There was a positive net volume change in T1, T3, and T4 for both ~~channel networks were positive, and this plus other data show~~ watersheds, and other studies have documented that the primary effect of the ~~fire and subsequent rainstorms~~ High Park fire and the summer thunderstorms was erosion at the hillslope scale ~~and deposition at scales larger than a few km^2. Over these three time periods both watersheds showed a decrease in the~~ (?) and deposition in the lower portions of both SG and HG (?). The data presented here show that this post-fire deposition occurred nearly throughout the entire channel network, and that amount of geomorphic change decreased sharply over time, particularly in HG ~~, as~~ where the estimated net volume change dropped from nearly 20,000 m^3 in ~~the first period~~ T1 to just over 7,000 m^3 and 5,000 m^3 in ~~the third and fourth periods~~T3 and T4, respectively (Figure 5B). In SG the net volumes over these same time periods also decreased from nearly 8,000 m^3 in T1 to over 6,000 m^3 and then 5,000 m^3 in T3 and T4, respectively (Figure 5A). ~~Total deposition over all~~ This overall pattern of deposition was counterbalanced by the large volumes of erosion during T2 as a result of the mesoscale flood. Hence in SG the total deposition over the four time periods was just over 38,000 m^3~~in SG and just over 46, 000 m^3 in HG, while total erosion~~ , while the total erosion was nearly 50% larger because the mesoscale flood eroded virtually all of the sediment that had been deposited in summer 2012 but was not captured by the first lidar dataset. In HG the total deposition over all four time periods was ~~similar with nearly 58~~just over 46,000 m^3~~in SG and~~ , and this was very similar to the total erosion over the study period of nearly 41,000 m^3~~in HG. Seventy-eight percent and 72~~. The importance of the mesoscale flood is indicated by the fact that 78% of the total erosion in SG and ~~HG, respectively,~~ 72% of the total erosion in HG took place during T2~~as a result of the September 2013 mesoscale flood~~. This means that, in the absence of the highly unusual mesoscale flood, the HPF would ultimately have caused extensive net deposition ~~at scales greater than a few km^2~~throughout nearly all of the channel network.

4.3 Statistical analysis of controls on erosion and deposition

Pearson correlation coefficients indicate that several of the independent variables were ~~highly correlated~~ closely correlated with one or more of the other independent variables (Figure 10; see also Tables A1 and A2). ~~These included: the~~ The strongest correlations between the independent variables included: percent area burned at high severity and percent area burned at moderate and high severity ($r = 0.99$ for both watersheds); slope-width ratio vs. channel width ($r = -0.59$ in SG and $r = -0.51$ in HG)~~,~~ ; and contributing area versus channel width ($r = 0.94$ in SG and $r = 0.96$ in HG). ~~As a result we removed~~ These relationships led us to remove percent area burned at high severity, slope-width ratio, and channel width from further analyses. ~~We also removed the~~ The removal of these three independent variables also necessitated the removal of the change in slope-width ratio and ~~confinement ratio because of their dependency on other removed metrics~~the change in confinement ratio as these also were based on one of the independent variables that was removed from the analysis.

~~Correlation~~ There was considerable variability in the correlation coefficients (r) between the various independent variables and the net volume change in each segment~~varied greatly between metrics and across~~ , and in the value of the correlations and across the four time periods (Figure 10). ~~The~~ Given the differences in the direction and magnitudes of geomorphic changes among the different time periods, the following sections summarize the key results for each ~~time period in chronological order~~successive time period, and we report correlations ~~are to indicate~~ rather than coefficients of determination in order to indicate both the direction and the ~~direction as well as the~~ magnitude of the ~~relationship. Positive correlations indicate that increasing values of~~ different relationships. By definition a positive correlation indicates that an increase in the independent variable ~~were~~ is associated with either ~~decreasing erosion or increasing~~ a decrease in erosion or an increase in deposition, while ~~negative correlations indicate either increasing erosion or decreasing~~ a negative correlation indicates that an increase in the independent variable is associated with either an increase in erosion or a decrease in deposition.

In SG the absolute correlations ($|r|$) for net volume change during T1 never exceeded 0.17 (Figure 10), and this was primarily a result of the generally limited geomorphic change ~~during this period~~ detected between the first and second ALS datasets (Figures 6A and 8B). ~~The ALS data for~~ Since the T1 ~~did not include~~ period did not capture the large amounts of deposition that ~~we~~ were qualitatively observed in SG in the first three months after burning, ~~but it did include the erosion of some of these deposits by subsequent spring runoff (Brogan et al., 2017, 2019). Hence, the~~ the correlations were substantially ~~greater when~~ stronger for segment-scale erosion volumes ~~were the dependent variable rather than deposition or net volume change~~ because the primary causal process was spring snowmelt rather than thunderstorm-driven deposition (Figure 10). ~~Segment-scale erosion was~~ The independent variables that were most strongly correlated with segment-scale erosion volumes were contributing area (r = -0.56), MI_{30} (r = -0.42), and channel slope (r = 0.33). These results indicate that ~~much of the~~ more erosion occurred in the lower gradient, wider downstream reaches with larger contributing areas, and this is because these reaches were where we qualitatively observed the greatest amounts of post-fire deposition and therefore had more sediment that could be readily eroded by snowmelt and lower intensity rainstorms. We posit that the correlations for deposition and net volume change in SG would have been much greater had the ~~first ALS dataset captured~~ T1 period recorded the extensive post-fire deposition that ~~we observed~~ was so apparent in the first summer after burning (Brogan et al., 2017, 2019).

Overall the correlations ~~in HG~~ for T1 were slightly stronger in HG than in SG (Figure 10). In contrast to SG, deposition was more strongly correlated with the independent variables than either net volume change or total erosion. This difference is likely due to the greater magnitudes of deposition in the middle and lower reaches in HG relative to SG (Figure 7)~~; the highest correlations with deposition were for~~ . As in SG, two of the independent variables that were most strongly correlated with the volume of deposition were contributing area (r = 0.35) ~~,~~ and MI_{30} (r = 0.34), and ~~BS_m and BS_{m+h} (r = 0.33 and -0.42, respectively)~~ these are consistent with our understanding of the underlying causal processes of post-fire erosion and downstream deposition.

Further investigation of the scatterplots indicate ~~deposition~~ that–particularly in SG–deposition predominated when contributing areas were less than about ~~4–5~~ 4-5 km^2, while erosion ~~dominated at~~ tended to dominate when contributing areas greater than about ~~4–5~~ 4-5 km^2. Since the T1 period only included spring snowmelt and smaller convective storms in the first part of summer 2013, this indicates that the smaller convective thunderstorms had limited impact at larger scales, while elevated baseflow could cause significant channel changes if there was sufficient readily erodible sediment in the channels and valley bottoms.

Correlations for T2 were generally stronger than for any of the other three time periods in both SG and HG, and this was primarily due to the substantial and consistent erosion resulting from the large mesoscale flood (Figure 10; Brogan et al., 2017, 2019). In SG three metrics had r values $>$ 0.32 or $<$ -0.32 with net volume change, and ~~these included channel slope (r = 0.35),~~ again these were contributing area (r = -0.63), ~~and~~ MI_{30} (r = -0.36), and channel slope (r = 0.35). These results indicate increasing erosion in the downstream direction and that nearly 40% of the variance in the amount of net change can be explained ~~by A alone~~solely by the increase in contributing area. The correlations with erosion were generally stronger than the correlations with net volume change, and the ~~highest correlation for any variable for any time period was~~ r value of -0.71 between contributing area and erosion for T2 in SG was the strongest correlation for any variable for any time period (~~r = -0.71). Overall, the correlations with deposition as the dependent variable were weaker than the volumes of either net change or erosion (Figure 10).~~

~~As in SG, the correlations during T2 in HG were generally higher than for the other three time periods (~~Figure 10). The correlations for HG were not as high as for SG, and this can be largely attributed to the lower volume changes in HG compared to SG (Figure 5). In HG ~~two metrics had $r > 0.32$ or < -0.32~~ the two variables most strongly correlated with net volume change ~~, and these included~~ were again channel slope (r = 0.35) and MI_{30} (r = -0.33). ~~Similar to SG, the correlations in HG generally improved when~~ As in SG, correlations were generally stronger when the volume of erosion was the dependent variable ~~and decreased when deposition was the dependent variable~~ as compared to deposition (Figure 10).

Overall the volume changes in T2 were similar in magnitude but opposite in sign to the volume changes in T1 (Figures 8 and 9). ~~Plots~~ Scatterplots of the segment-scale net volume changes for T2 against the net volume changes for T1 show that ~~much~~ the bulk of the data plots along a line with a slope of -1 for SG and -0.8 for HG (Figure 11). This indicates that ~~for many segments~~ the volumes eroded primarily by the mesoscale flood ~~were very similar~~ tended to be similar or proportional to the volumes deposited in T1. However, ~~the overall R^2 value was near zero in SG because a number of segments~~ in both watersheds there about 30 segments of the several hundred segments that had far more erosion in T2 than was deposited in T1; these points plot well below the regression line and are shown in red in Figure 11A~~. A closer examination show that~~ ,B. In the case of SG these segments are almost exclusively ~~in the areas where there was tremendous~~ along the channels where we observed massive deposition by the July 2012 convective storm ~~and lesser deposition by other~~ along with some additional deposition by subsequent summer thunderstorms (Figure 11B) (Brogan et al., 2017). Since this deposition was prior to the first ALS dataset~~. The shift in~~ , it should not be surprising that these points had much more erosion in T2 than deposition in T1. The sign changes in the correlations from negative to positive, or vice versa, between T1 and T2 are particularly notable for channel slope (r = -0.14 in T1 and 0.35 in T2) and valley width (r = 0.13 in T1 and -0.17 in T2; Figure 10), and these are consistent with the expected controls on post-fire deposition and flood-induced erosion, respectively.

In HG the volumes of deposition in T1 and erosion in T2 were more ~~similar~~ closely matched (Figure 9) as indicated by the stronger R^2 value of 0.40, but ~~again there is~~ there is again a cluster of about 30 points below the 1:-1 line (Figure 11C). The number and absolute magnitude of the differences between these points and the 1:-1 line is smaller than in SG, and this can be attributed to the smaller ~~storms and associated deposition prior to the first ALS data set in October 2012. The segments~~ amounts of qualitatively observed deposition during the first summer after burning and the measured deposition during the T1 period, and hence the smaller volumes of sediment readily available for erosion by the mesoscale flood. A closer evaluation of the points below the 1:-1 line ~~are almost exclusively in~~ show that they come almost exclusively from a major tributary draining an area burned at high severity (Figure 11D), and our field ~~obserations~~ observations indicate that this area ~~also~~ was subjected to extensive deposition prior to the first ALS dataset (see Figure 3.9 in Brogan, 2018). ~~Excluding these points~~ If the points in red are excluded from the regression ~~increases the R^2~~ the r^2 increases to 0.64, and this confirms the relative importance of the initial post-fire storms ~~and the overall close relationship between the volumes of segment-scale deposition in T1 and the eroded~~

~~volumes during T2~~in providing large amounts of sediment that was then eroded by the mesoscale flood. As in SG, many of the correlations ~~in HG~~ between the independent variables and the volume changes shifted from negative to positive, or vice versa, between T1 and T2, including channel slope (r = -0.25 in T1 and 0.35 in T2), contributing area (r = 0.28 in T1 and -0.24 in T2), and MI_{30} (r = 0.29 in T1 and -0.33 in T2; Figure 10).

In T3 and T4 the correlations between the independent variables and the segment-scale volume changes were generally low in both watersheds (Figure 10). The lower correlations can be attributed in part to the much lower amounts of erosion and deposition (Figure 5). The correlations in T3 and T4 generally had the same direction as in ~~T3 and T4 as~~ T1 ~~, as~~ because each of these periods was primarily depositional. In SG the only correlations with ~~net change with~~ $r > 0.32$ or < -0.32 (~~R^2 > 0.10) were~~ $r^2 > 0.10$) were between net volume change and the percent area burned at moderate severity (r = -0.35) in T3 and ~~total rainfall~~ the total precipitation (r = -0.33) in T4 (Figure 10). In HG none of the independent variables explained much more than 8% of the variation in net volume change, and the volumes of erosion and deposition ~~again~~ also were only weakly correlated with the independent variables. ~~For~~ In HG there were only three correlations with an $r > 0.32$ or < -0.32, and these were for increasing segment-scale erosion in T4 with increasing contributing area (r = -0.49) and valley width (r = -0.38), and decreasing deposition in T3 with increasing percent area burned at moderate and high severity (r = -0.38). The results for both watersheds indicate that the spring high flows continued to erode the relatively raw and enlarged channel created by the mesoscale flood.

5 Discussion

5.1 Mechanisms of watershed-scale post-fire erosion~~and~~, deposition, and recovery

~~As~~ When post-fire rainfall intensities exceed the sharply diminished infiltration rates (e.g., Cammeraat, 2004; Kampf et al., 2016)~~the greatly enhanced hillslope runoff causes rapid~~ , hillslope runoff is greatly enhanced and this causes a dramatic expansion and incision of the headwater channels (Wohl, 2013). The increased ~~runoff and increased connectivity~~ hillslope-channel connectivity and increased runoff transports the eroded sediment ~~from the hillslopes~~ down into the channel network (e.g., Prosser and Williams, 1998; Schmeer et al., 2018), with the finer particles being readily transported much further downstream as suspended load. In contrast, ~~coarse sand~~ the coarser sands and gravel are usually transported much shorter distances as bedload (e.g., Moody and Martin, 2001; Reneau et al., 2007), and are usually deposited in the wider, lower gradient reaches (e.g., Doehring, 1968; Anderson, 1976; Meyer et al., 1995; Moody and Martin, 2009).

The ash and sediment transported into the Cache la Poudre River after the High Park Fire greatly increased turbidities and suspended sediment concentrations (Writer et al., 2014), but our observations indicated that these sediment inputs generally did not alter the channel morphology of the mainstem other than at a few tributary confluences, ~~at~~ immediately behind a diversion dam, and much further downstream where the river ~~emerged~~ suddenly emerges from the foothills into a ~~wide~~ unconfined valley bottom. ~~Field data and observations both showed~~ Our qualitative observations indicate that fine sands, silts and clays did not comprise much of the post-fire deposits in either in the valley bottom of our two study watersheds or the mainstem of the Cache la Poudre River. Particle-size data collected in both watersheds before the mesoscale flood show that only five of our

21 cross-sections had a D_{16} smaller than 2 mm, and this dropped to only one cross section after the flood (?). This means that the ~~topographic changes~~ volume changes in our two study watersheds as quantified by the ALS differencing ~~primarily reflect the hillslope delivery, deposition , and some~~ is primarily the deposition and subsequent movement of the coarser bedload particles~~within our two study watersheds~~.

~~The detailed, spatially-explicit calculations of erosion and deposition in our two study watersheds were only possible because of the relatively recent technology for differencing high-resolution topographic datasets.~~ Our study was unique in terms of being able to compare five ~~post-fire and post-flood ALS datasets , and the~~ ALS datasets taken over a three-year period following the June 2012 High Park Fire and then the September 2013 mesoscale flood. These allowed us to quantify erosion and deposition volumes throughout the channels and valley bottoms in our two study watersheds on a spatially explicit basis. More specifically we could calculate the combined effects of snowmelt and thunderstorms in the second summer after burning, evaluate the changes due to the mesoscale flood, and then quantify the changing volumes of erosion and deposition over the next nearly two years as the watersheds recovered from the fire and the flood. The resulting maps of valley bottom changes ~~show considerable~~ allow a far more detailed assessment of the spatial and temporal complexity ~~that would not~~ of geomorphic changes than would be possible from manual measurements (sensu Schumm, 1973). ~~Although complex, the DoDs clearly documented net overall~~ While the ALS data do not allow us to fully separate the effects of snowmelt runoff versus summer thunderstorms, the results clearly show net deposition in both study watersheds during ~~T1, T3, and T4, and~~ three of the four time periods, with net erosion in ~~T2~~the second time period. This illustrates that–other than the mesoscale flood–the predominant post-fire effect is deposition in the downstream channels and valley bottoms (Figure 5; see also Figure 3.21 in Brogan, 2018), and ~~this~~ that deposition from the summer thunderstorms substantially exceeds the erosion from snowmelt and low intensity rainstorms. This preponderance of deposition over erosion is a typical post-fire response (e.g., Swanson, 1981; Morris and Moses, 1987; Moody and Martin, 2001; Wagenbrenner et al., 2006). Our ~~surveyed~~ more intensive field surveys of the cross sections and longitudinal profiles in each watershed do provide a more ~~sensitive evaluation~~ detailed assessment of post-fire changes within the larger time periods delineated by the ALS datasets (Brogan et al., 2019), but ~~these only represent a~~ our field measurements necessarily represent only a relatively small fraction of the channel network. In contrast, the ~~ALS differencing covered~~ DoD results cover the entire channel network, but the ~~DoDs had much higher~~ trade-off is that the ALS differencing has a lower temporal resolution and higher measurement uncertainties due to alignment issues, horizontal displacement errors, interpolation errors, and errors ~~associated with vegetation~~due to leaf on and leaf off. Hence both types of data are needed to ~~accurately and fully~~ more accurately and completely characterize the effects of the ~~fire and subsequent~~ High Park Fire and subsequent mesoscale flood, and together they highlight the ~~need to collect data~~ importance of collecting data using different techniques at different spatial and temporal scales with ~~different techniques and their associated levels of~~ their accompanying differences in spatial extent, temporal resolution, and measurement accuracy.

The smaller geomorphic changes in T3 and T4 relative to T1 are due to several factors. ~~These include~~ Of primary importance is the ongoing hillslope vegetation recovery, reduction in headwater channel length (Wohl and Scott, 2017), and the relative paucity of large convective storms. Together these factors have resulted in a sharp decline in hillslope runoff, erosion, and connectivity as documented in the High Park and other Front Range fires (Benavides-Solorio and MacDonald, 2005; ?; Schmeer et al., 2018

, and these declines directly cause much smaller amounts of downstream deposition. In this study we also have to add another factor, which is the stripping and coarsening of the channel and valley bottoms due to the mesoscale flood ~~. The poor accuracy of the first two ALS datasets in HG also means that~~ (?). The resulting reduction in available sediment in the channels and valley bottoms, when combined with the coarsening of the bed material in the active channel, limits the amount of erosion that can take place as a result of increased baseflows, runoff from convective thunderstorms, and spring snowmelt (e.g., Brunsden and Thornes, 1979; Thomas, 2001; Phillips and Van Dyke, 2016; Rathburn et al., 2017; Fryirs, 2017; Brogan et al., 2019) . We should believe that the difference in the amount of deposition and net change between T1 and T3/T4 is ~~almost certainly~~ much larger than what we ~~calculated. These factors have resulted in a sharp decline in hillslope runoff, erosion, and connectivity (Schmeer et al., 2018), and downstream channel geomorphic changes since September 2013. The presence and regrowth of riparian vegetation is another factor that can affect the amounts of erosion and deposition after fires and floods (e.g., ?), and in SG there has been minimal riparian growth following the mesoscale flood due to the very coarse substrate and depth to the water table. We argue that the stripping and coarsening of~~ have shown here (e.g., Figure 5) primarily because the first ALS data were collected after the first summer when there were very large amounts of post-fire sediment deposited in the channels and valley bottoms ~~has resulted in a greatly reduced sensitivity to convective thunderstorms, increased baseflows, and spring snowmelt (e.g., Brunsden and Thornes, 1979; Thomas, 2001; Phillips and Van Dyke, 2016; Rathburn et al., 2017; Fryirs, 2017; Brogan et al., 2019)~~ of both watersheds (?), and also because of the poorer accuracy of the first ALS dataset.

~~Given that the uncertainty of~~ The uncertainty in our ALS differencing ~~was usually~~ also affects the extent to which we can fully understand the underlying geomorphic processes during our study. With average uncertainties of 10-15 cm~~with a maximum of 23 cm, the ALS differencing was most able to~~ , we generally could only detect elevation changes at tributary junctions and in larger channels and valley bottoms rather than on the hillslopes or in the ~~smaller tributaries.~~ headwater channels. Hence it was difficult to tell exactly where the break was between upslope incision versus downstream deposition. Most of the largest volume changes were in downstream locations where channel slopes were generally less than ∼10% and valley widths were greater than ∼30 m. The ~~general trend of deposition at and near confluences corroborates previous research (e.g., ?Nardi and Rinaldi, 2015), but in our case these changes were due to primarily to “standard” fluvial processes as there were few large debris flows after the High Park Fire and September 2013 mesoscale storm (?). The~~ limited accuracy of the ALS differencing also leads us to posit that we underestimated deposition more than erosion because deposition tended to be more widespread and shallower compared to the more localized and concentrated erosion.

5.2 Uncertainty, errors, and methodological issues in DEM differencing

It should be self-evident that future studies need to minimize the errors associated with DEM differencing if one is to accurately detect and quantify geomorphic changes, particularly in smaller streams. The challenges we ~~faced working with the~~ encountered in working with five different ALS datasets ~~used in this study provides a series of useful insights into~~ suggests a set of best practices for using repeat ALS data to document geomorphic change after wildfires or other disturbances. First, ALS data collection must happen as soon as possible following the disturbance, particularly after fires as these landscapes are extremely sensitive to runoff, erosion, and channel change from even relatively small rainstorms (e.g., Shakesby and Doerr, 2006; Moody et al., 2013). Second, high-resolution topography should be repeated at the temporal resolution needed to distinguish and understand the seasonal effects of different driving forces (e.g., summer thunderstorms versus snowmelt). Recent advances in the use of drones and drone-based structure-from-motion (SfM) photogrammetry rather than airplanes should greatly facilitate more frequent lidar data collection (e.g., Tulldahl and Larsson, 2014), and allow ~~researchers to be repeated~~ data to be collected at a sufficiently high temporal resolution to capture the effects of discrete storms and floods ~~in addition to the seasonal changes characteristic of our study area. Drone-based structure-from-motion (SfM) photogrammetry offers an increasingly popular alternative to lidar and can result in much higher resolution data over time and space~~ rather than the combined effects that were inherent in our datasets. Drones also can provide substantially much higher spatial resolution data (e.g., Smith et al., 2016).

Third, repeat high-resolution topographic data often requires translational rectification to better match the different datasets. In this study both vertical and horizontal translation was needed to more accurately match up the different the different ALS datasets, and thereby more accurately calculate elevation changes and associated volumes. Manual adjustments are laborious and non-repeatable, and our work was greatly facilitated by an automated approach to co-register the different point clouds Nuth and Kääb (2011). This approach, along with the availability of highly accurate RTK-GNSS field data (Brogan et al., 2019), reduced the vertical uncertainties of most of our ALS data to 10-15 cm. Fourth, ALS data should be collected at low altitudes with narrow flight pass widths, low scan angles, and good ground controls to improve the quality and density of the raw point clouds. The highest mean point density in our ALS datasets was 3.8 points m^{-2}. We therefore recommend a minimum point density of 4 points m^{-2}, as higher point densities would allow for a more detailed and accurate analysis.

~~Automated GIS tools~~ Fifth, automated GIS tools now allow faster and easier characterization of the channel, adjacent topography and specific geomorphic features; examples include FluvialCorridor (e.g., Roux et al., 2015), River Bathymetry Toolkit (e.g., McKean et al., 2009), TerEx (Stout and Belmont, 2014), V-BET (Gilbert et al., 2016), and the Valley Confinement Algorithm (Nagel et al., 2014). However, users must be aware of the limitations of these tools. FluvialCorridor provides objective valley bottom delineations that can be used over large spatial domains and facilitates longitudinal segmentation of the channel and valley bottom, but ~~there were some~~ we experienced problems in identifying valley margins when they ~~was delineated~~ were near very steep slopes. In some cases the delineated valley bottom included ~~the~~ this adjacent steep slope or rock outcrop~~, and the errors in estimating ground locations and elevations due to ALS interpolation error~~. In these locations ALS interpolation errors and horizontal displacement ~~error (Hodgson and Bresnahan, 2004) near these steep slopes can cause~~ errors (Hodgson and Bresnahan, 2004) can lead to errors in estimating ground locations and elevations, resulting in substantial errors in the DoD volume estimates (e.g., Heritage et al., 2009; Wheaton et al., 2010; Milan et al., 2011; Bangen et al., 2016). ~~The~~ These inaccuracies in identifying ~~the~~ valley margins also caused higher elevation points to be included within a given segment, ~~and these would bias the calculated~~ which will lead to inaccurate estimates of valley bottom slopes. ~~So our fifth cautionary point is that careful checking is needed of~~ Users of these automated tools need to carefully check the validity of any automated process, and we found it necessary to sometimes manually delineate the valley bottoms, especially when the valley bottoms were directly abutted by steep terrain.

Sixth, ~~techniques for computing elevation differences directly from point clouds are improving~~ we tried to directly compute elevation differences from the point clouds (e.g., Lague et al., 2013), but procedures to do so are still in their infancy (Passalacqua et al., 2015). In ~~this study we initially tried to compute~~ our case we ended up using the standard DoD approach to compute the volumes of erosion and deposition ~~volumes directly from the point clouds, but ultimately we used the standard DoD approach because there are lower uncertainties for raster-based methods when there are~~ because this resulted in lower uncertainties given our lower density point clouds (Hartzell et al., 2015). ~~Another advantage of~~ With raster-based differencing ~~is the~~ there also is a mature suite of tools to calculate spatially-varying uncertainties, ~~which improve~~ and this improves the accuracy of volume change estimates compared to assuming a uniform uncertainty (e.g., Wheaton et al., 2010; Milan et al., 2011).

~~A key problem in this study was the large error~~ Lastly, we had large errors due to the varying seasonal timing of the ALS datasets (i.e., leaf on versus leaf off). We ~~developed~~ therefore had to develop an algorithm to remove unrealistically large elevation changes due to changes in canopy cover, and ~~overall~~ removing about 2% of the valley bottom area this reduced the mean calculated total erosion, total deposition, and net volume differences by 46% (s.d. = 16%), 54% (s.d. = 15%), and 22% (s.d. = 33%), respectively. ~~However~~On the other hand, the use of this algorithm increased the net volume change in T3 by 11% in SG and 25% in HG as it reduced ~~the~~ total deposition more than ~~the~~ total erosion. Careful, manual checks of the DoDs and aerial imagery showed that this algorithm was still not able to always identify pixels with erroneous elevation changes due to changes in the vegetation heights between ALS datasets (e.g., Figure 2D). ~~So our seventh point is~~ Hence we strongly recommend that repeat ALS data ~~should~~ be collected at similar times of the year, preferably during leaf-off, to optimize the ~~detection of~~ accuracy of the bare earth DEMs and hence the accuracy and sensitivity for detecting elevation and volume changes. ~~Again this~~ Our experience again shows that visual checks of DoDs are essential to detect ~~a range of~~ various errors that otherwise ~~are~~ would be presumed to represent ~~a~~ real geomorphic change (e.g., Lane et al., 2004).

5.3 Controls on spatial and temporal patterns of geomorphic change

The linear regression results showed that post-fire volume changes for the different periods and watersheds were significantly correlated with ~~rainfall depths and intensities, burn~~ precipitation depth and maximum 30-minute intensities, percent area burned at moderate and/or high severity, and valley and basin morphology ~~. However, none of the metrics~~ (Figure 10. None of the independent variables had consistently strong coefficients of determination (~~R2~~r^2) with segment-scale volume changes over the different time periods and watersheds~~.~~, but the strongest relationships were generally with channel slope, contributing area, maximum 30-minute precipitation intensity, and percent area burned at moderate and/or high severity. Precipitation intensity and burn severity both make physical sense as these are two of the dominant controls on the amount of sediment that is likely to be generated after a wildfire (e.g., Benavides-Solorio and MacDonald, 2005; Abrahams et al., 2018), while channel slope is a key control on both erosion and deposition. Contributing area will be directly related with the volume of runoff for both snowmelt and widespread storms like in September 2013, and segments with larger contributing areas also will tend to have larger channels and valley bottoms where larger volumes of sediment can be either deposited or eroded. Surprisingly, the volumes of erosion, deposition, and net change were generally not correlated with valley width, and this could be partially due to the issues with accurately delineating the valley bottoms.

We hypothesized that stronger correlations might be present when the watershed data were stratified by valley bottom slope or drainage area, but this did not greatly improve the strength ~~or magnitude~~ of the correlations. ~~Alternatively, it~~ It has been suggested that better relationships between volume changes and morphometric characteristics could be attained by parsing the valley into more discrete geomorphic units (e.g., channel, floodplain, terrace) to reflect different dominant processes (e.g., Weber and Pasternack, 2017), but there was no easy way for us to ~~do this across~~ accurately identify these different geomorphic units throughout our study watersheds. ~~Nevertheless, the correlations still provide useful insights into the~~ The correlation results do help identify the key controls on the ~~volumetric changes~~direction and magnitude of volumetric changes for the different time periods. Not surprisingly, the largest amount of deposition occurred in the first period after burning, while the mesoscale flood caused by far the greatest erosion. ~~In particular, volume changes were consistently greater in segments with larger contributing areas, and where there were floodplain pockets, tributary junctions, and colluvial deposits. The largest volume changes were usually due to deposition in T1 and erosionin T2.~~ Correlations in ~~T3 and T4 generally were lower than in T1 and T2. This decrease in the strength of correlations is due in part to~~ the two periods after the mesoscale flood were lower due to both the lower magnitudes of erosion and deposition as the watersheds recovered from the fire, but also ~~due to~~ the reduced sensitivity to channel change following the removal of post-fire sediment and the channel coarsening caused by the mesoscale flood. Overall the results here and from our field data (Brogan et al., 2019) strongly indicate that ~~geomorphic changes~~ the magnitude of erosion in the channels and valley bottoms ~~of our two study watersheds~~ were largely controlled by sediment availability, and the closely-related studies show that post-fire sediment availability is largely dependent on the combination of burn severity and the intensity of the summer thunderstorms (Kampf et al., 2016; Schmeer et al., 2018).

~~This assertion is further~~ The importance of sediment availability is strongly supported by the ~~correlations between the~~ observation that the volumes eroded in T2 were often very similar to the segment-scale volumes deposited in ~~T1 and the erosion volumes in T2, even though the T1 depositional volumes captured almost none of the~~ T1, with the discrepancies stemming mostly from the locations where there were large amounts of ~~deposition that we observed in the~~ unrecorded deposition during first summer after burning (Figure 11; Brogan et al., 2017, 2019). ~~The importance of available sediment is also indicated by the scatterplots showing~~ There also was little net volume change in segments ~~where the slope was~~ with a slope much greater than about 0.2 $m\ m^{-1}$ (Figure 12). In these steep channels the bed is comprised primarily of large, generally immobile ~~sediment~~ clasts (e.g., Yager et al., 2012), and the steep slope means that there is very limited potential ~~to store~~ for storing the gravel and finer particles that ~~represent~~ comprise most of the post-fire sediment eroded by surface runoff~~after a fire. To estimate~~ . This means that efforts to predict potential geomorphic change ~~in mountain catchments it may be more important to quantify~~ may need to focus on quantifying where and how much sediment is available (e.g., Carling and Beven, 1989) rather than the spatial distribution of hydraulic and morphometric controls.

Areas of erosion and deposition are often highly correlated with the downstream gradient in stream power (e.g., Gartner et al., 2015; Yochum et al., 2017), but to our surprise none of our gradient metrics (i.e., ΔS, Δw_v, $\Delta \frac{S}{w_v}$) were strongly correlated to net volume change, total erosion, or total deposition. Most of the largest volume changes occurred in segments where these gradients were close to zero, resulting in low correlation coefficients. These results again suggest that for our montane watersheds the spatial and temporal differences in sediment supply can better predict the volumes of erosion, deposition, and net change than local changes in slope or valley width.

Overall our correlations generally were not improved if erosion or deposition were used as the dependent variable instead of net volume change, but in some cases there were sharp differences in the correlations according to the selected dependent variable. For example, contributing area explained 50% of the total erosion in SG during T2 as well as 32% of the ~~snowmelt~~ erosion in T1~~. In each case contributing area led to a consistent~~ , which included spring snowmelt but did not include a full thunderstorm season. In both of these cases a larger contributing area would lead to a more or less proportional increase in discharge~~along with the increase in sediment availability. Using deposition as the dependent variable generally did not improve correlations, with the primary exception being for T1 in HG as there was a stronger downstream trend in the initial volumes of post-fire deposition than in erosion or net change~~. ~~In this study our efforts to quantify the controls on post-fire geomorphic changes were hindered by missing the first summer of deposition, the inability to detect smaller changes in elevation, and the residual vegetation effects.~~

~~Our understanding of the relationships between the~~ The results from our two study watersheds show a clear commonality of controlling processes, but some substantial differences in the magnitude of post-fire sediment storage and net volume change. Our efforts to correlate the independent variables and volume changes ~~can be enhanced by more process-based research to couple estimated hillslope erosion rates to downstream volumetric changes. We found that valley morphometrics could explain some of the variations in post-fire deposition, erosion, and net volume change, and especially the erosion from the large mesoscale flood.~~ had only limited success, but the prediction of downstream deposition and erosion could potentially be improved by adding in spatially explicit hillslope erosion predictions. Spatially explicit erosion models (e.g., McGuire et al., 2016, 2017) could be used to predict the spatial distribution of post-fire sediment inputs, and ~~there is an urgent need to test the extent to which these varying sediment inputs are related to segment- and watershed-scale changes in sediment depositionand erosion. We might speculate that these predicted sediment inputs , which in this environment are most frequently caused by localized thunderstorms (e.g., Wagenbrenner and Robichaud, 2014; Kampf et al., 2016), may be more closely related to the observed volume changes than the valley and basin morphometric variables tested here. The observed correlations between volume changes, burn severity, and precipitation indicate that hillslope-scale erosion modeling could help improve our efforts to predict post-fire sediment storage and delivery as well as our understanding of~~ the ~~underlying processes. The goal would be a relatively complete~~ question is whether a better knowledge of sediment inputs could better help explain the variations in segment-scale deposition. More accurate predictions of sediment inputs and deposition would then help improve the spatially explicit predictions of erosion from the channels and valley bottoms. The ultimate goal is to develop the key components of a sediment budget (sensu Vericat et al., 2017) that ~~combines estimates of hillslope sediment delivery to~~ would link hillslope-scale predictions of sediment production and delivery into the channel network (e.g., Schmeer et al., 2018) with spatially explicit estimates of ~~volume changes over time in the downstream channels and valley bottoms.~~

~~The results from our two study watersheds show a clear commonality of controlling processes, but some substantial differences in the magnitude of post-fire sediment storage and net volume change. The~~ downstream deposition and erosion due to different types, magnitudes, and sequences of rainstorms and snowmelt. The next step is to estimate the magnitude of post-fire runoff and sediment effects on local residents and downstream water users~~depends on a suite of different factors, including the characteristics of the upstream burned area, the amount and intensity of precipitation, and the downstream watershed morphometry~~. After fires considerable funds are spent to reduce hillslope erosion risks (e.g., Robichaud et al., 2000), but there is a need to more rigorously evaluate the extent to which these hillslope risks are directly linked to the likelihood of a given downstream effect. Our research helps identify where burned area emergency rehabilitation teams might focus post-fire rehabilitation efforts. Ecosystem and infrastructure concerns within or very near ~~the burned area will~~ a burned area are more likely to require rehabilitation efforts immediately upstream. However, if the effects of greatest concern are much farther downstream, then post-fire treatments might best be focused on the tributary watersheds with relatively steep and narrow valleys that drain directly to the mainstem river and offer little potential for sediment storage. ~~If~~ Tributary watersheds with lower slopes and wider valley bottoms would have a lower priority for post-fire treatments given the greater potential for sediment storage in the channels and valley bottoms. However, if ash and suspended sediment are of primary concern, rehabilitation efforts should probably focus on rapidly increasing the amount of ground cover on the hillslopes as ~~these materials, once introduced to the stream system, will be readily carried~~ the ash and very fine sediments–once detached and being transported by overland flow–are very likely to be carried much further downstream. A more rigorous understanding of the controls on erosion and sediment storage, and the potential for longer-term storage of post-fire sediment, can help prioritize post-fire hillslope rehabilitation treatments and identify downstream locations with the greatest risk for post-fire sediment deposition.

6 Conclusions

Fires can induce tremendous amounts of overland flow and hillslope erosion, and these can cause profound erosion and deposition throughout the channel network. This study analyzed post-fire changes in the channels and valley bottoms in two 15 km^2 watersheds for three years after the 2012 High Park Fire. Field observations and a detailed analysis of channel and valley bottom changes from differencing five sequential airborne laser scanning datasets show the primary effect of the fire was deposition ~~following~~ resulting from summer thunderstorms with smaller amounts of ~~incision~~ channel erosion resulting from spring runoff. This sequence was interrupted by a very unusual and large sustained ~~flood~~ rainstorm in September 2013, 15 months after the fire~~, that~~. The sustained high flows from this storm eroded nearly all of the post-fire ~~deposition along with much of the~~ sediment deposits along with substantial amounts of the older, pre-fire valley bottom deposits. In the following two years there was much less ~~deposition~~ sediment deposition in the channels and valley bottoms as the hillslopes ~~recovered~~revegetated, and much less channel erosion as so much of the available sediment had been removed by the September 2013 mesoscale flood.

Precipitation depths and intensities, percent area burned at high and moderate severity, and valley and basin morphology were weakly to moderately correlated with segment-scale volumes of deposition, erosion, and net change. This suggests that it is possible to identify ~~areas~~ those portions of a watershed with a greater potential for ~~geomorphic change and hence a greater sensitivity. Our work shows that those~~ sediment storage. Our results also show that areas with more deposition ~~and sediment availability have the greatest~~ have more available sediment for erosion by subsequent high flows, and hence a greater potential for subsequent geomorphic change. These more sensitive locations include segments with lower slopes, tributary junctions, colluvial deposits and floodplain pockets, and wider valleys where there are more extensive and continuous floodplains.

Our experience in processing ALS datasets indicates the need to: 1) collect ALS data as soon as possible following a disturbance~~;~~, 2) with ~~a~~ sufficient frequency to capture the effects of different driving forces~~;~~, 3) at similar times of the year, preferably during leaf-off, to avoid vegetation artifacts~~;~~, 4) ~~establish~~ with good ground controls; 5) use an automated approach to co-register the point clouds; and 6) calculate spatially-varying uncertainties. ~~Drones~~ The use of drones and structure-from-motion ~~should~~ can greatly facilitate the collection of more frequent ~~, high-resolution~~ and higher spatial resolution elevation data.

Future research should be aimed at investigating post-fire sediment routing from hillslopes through channel networks, quantifying geomorphic changes at shorter temporal scales, and evaluating how geomorphic changes vary among specific geomorphic units (e.g., channel, ~~floodplain~~floodplains, pools, bars, etc.). Our ability to rigorously address these research needs is rapidly increasing as repeat high resolution topographic data become more readily available. Our results are an initial step towards more rigorously identifying downstream areas with higher sensitivity to geomorphic change, and thereby helping guide future post-fire mitigation efforts.

Data availability. Data associated with this manuscript can be accessed from the Colorado State University Digital Repository (Nelson and Brogan, 2019) (http://dx.doi.org/10.25675/10217/193080).

Author contributions. D.J.B. performed the analyses, collected field data, and wrote the manuscript. P.A.N. and L.H.M. assisted with the analysis and interpretation of data, writing, and editing of the paper.

Competing interests. No competing interests are present.

Acknowledgements. This work was supported financially by the National Science Foundation (EF-1250205, EF-1339928, and EAR-1419223), U.S. Department of Agriculture National Institute of Food and Agriculture Hatch project (1003276), the Arapaho-Roosevelt National Forest, and the USDA Forest Service National Stream and Aquatic Ecology Center. Airborne laser scanning was provided by the National Ecological Observatory Network, a project sponsored by the National Science Foundation. This material is based in part upon work supported by the National Science Foundation under Grant No. DBI-0752017. Constructive reviews from two anonymous reviewers helped to improve the manuscript.

References

Abbott, J. T.: Geology of Precambrian rocks and isotope geochemistry of shear zones in the Big Narrows area, northern Front Range, Colorado, US Geological Survey, Open-File Report OF-70-1, 1970.

Abbott, J. T.: Geologic map of the Big Narrows quadrangle, Larimer County, Colorado, US Geological Survey, Geologic Quadrangle Map GQ-1323, 1976.

Abrahams, E. R., Kaste, J. M., Ouimet, W., and Dethier, D. P.: Asymmetric hillslope erosion following wildfire in Fourmile Canyon, Colorado, Earth Surface Processes and Landforms, 43, 2009–2021, 2018.

Anderson, H. W.: Fire effects on water supply, floods, and sedimentation, in: Proceedings Tall Timbers Fire Ecology Conference, pp. 249–260, 1976.

Baker, V. and Costa, J.: Flood power, in: Catastrophic Flooding, edited by Baker, V. and Costa, J., pp. 1–21, Allen and Unwin, 1987.

Bangen, S., Hensleigh, J., McHugh, P., and Wheaton, J.: Error modeling of DEMs from topographic surveys of rivers using fuzzy inference systems, Water Resources Research, 52, 1176–1193, https://doi.org/10.1002/2015WR018299, 2016.

Benavides-Solorio, J. and MacDonald, L. H.: Post-fire runoff and erosion from simulated rainfall on small plots, Colorado Front Range, Hydrological Processes, 15, 2931–2952, https://doi.org/10.1002/hyp.383, 2001.

Benavides-Solorio, J. and MacDonald, L. H.: Measurement and prediction of post-fire erosion at the hillslope scale, Colorado Front Range, International Journal of Wildland Fire, 14, 457–474, https://doi.org/10.1071/WF05042, 2005.

Benda, L. and Dunne, T.: Stochastic forcing of sediment routing and storage in channel networks, Water Resources Research, 33, 2865–2880, https://doi.org/10.1029/97WR02387, 1997.

~~Benda, L., Miller, D., Bigelow, P., and Andras, K.: Effects of post-wildfire erosion on channel environments, Boise River, Idaho, Forest Ecology and Management, 178, 105–119, , 2003.~~

Bieger, K., Rathjens, H., Allen, P. M., and Arnold, J. G.: Development and evaluation of bankfull hydraulic geometry relationships for the physiographic regions of the United States, JAWRA Journal of the American Water Resources Association, 51, 842–858, 2015.

Braddock, W. A., Abbott, J. T., Connor, J. J., and Swann, G. A.: Geologic map of the Poudre Park quadrangle, Larimer County, Colorado, US Geological Survey, Geologic Quadrangle Map GQ-1620, 1988.

Brogan, D. J.: Spatial and temporal channel changes across the watershed scale following wildfire and floods, PhD dissertation, Department of Civil and Engineering. Colorado State University, Fort Collins, CO, 248 pp, 2018.

Brogan, D. J., Nelson, P. A., and MacDonald, L. H.: Reconstructing extreme post-wildfire floods: a comparison of convective and mesoscale events, Earth Surface Processes and Landforms, 42, 2505–2522, https://doi.org/10.1002/esp.4194, 2017.

Brogan, D. J., MacDonald, L. H., Nelson, P. A., and Morgan, J. A.: Geomorphic complexity and sensitivity ~~of~~ in channels to fire and floods in mountain catchments, Geomorphology, ~~in review.~~ 337, 53–68, https://doi.org/10.1016/j.geomorph.2019.03.031, 2019.

Brunsden, D. and Thornes, J.: Landscape sensitivity and change, Transactions of the Institute of British Geographers, pp. 463–484, https://doi.org/10.2307/622210, 1979.

Cammeraat, E. L.: Scale dependent thresholds in hydrological and erosion response of a semi-arid catchment in southeast Spain, Agriculture, Ecosystems & Environment, 104, 317–332, https://doi.org/10.1016/j.agee.2004.01.032, 2004.

Cannon, S. H., Kirkham, R. M., and Parise, M.: Wildfire-related debris-flow initiation processes, Storm King Mountain, Colorado, Geomorphology, 39, 171–188, https://doi.org/10.1016/S0169-555X(00)00108-2, 2001.

Carling, P. and Beven, K.: The Hydrology, Sedimentology and Geomorphological Implications of Floods: an Overview, in Floods: Hydrological, Sedimentological and Geomorphological Implications. John Wiley & Sons New York. 1989. p 1-9., 1989.

~~Coe, J. A., Kean, J. W., Godt, J. W., Baum, R. L., Jones, E. S., Gochis, D. J., and Anderson, G. S.: New insights into debris-flow hazards from an extraordinary event in the Colorado Front Range, GSA Today, 24, 4–10, , 2014.~~

Costa, J. E. and O'Connor, J. E.: Geomorphically effective floods, Natural and anthropogenic influences in fluvial geomorphology, pp. 45–56, https://doi.org/10.1029/GM089p0045, 1995.

Cotrufo, M. F., Boot, C. M., Kampf, S., Nelson, P. A., Brogan, D. J., Covino, T., Haddix, M. L., MacDonald, L. H., Rathburn, S., Ryan-Bukett, S., et al.: Redistribution of pyrogenic carbon from hillslopes to stream corridors following a large montane wildfire, Global Biogeochemical Cycles, 30, 1348–1355, https://doi.org/10.1002/2016GB005467, 2016.

Doehring, D. O.: The effect of fire on geomorphic processes in the San Gabriel Mountains, California, Rocky Mountain Geology, 7, 43–65, 1968.

Ebel, B. A., Moody, J. A., and Martin, D. A.: Hydrologic conditions controlling runoff generation immediately after wildfire, Water Resources Research, 48, https://doi.org/10.1029/2011WR011470, 2012.

Elliot, W. J.: WEPP internet interfaces for forest erosion prediction, Journal of the American Water Resources Association, 40, 299–309, https://doi.org/10.1111/J.1752-1688.2004.TB01030.X, 2004.

Elliot, W. J., Miller, M. E., and Enstice, N.: Targeting forest management through fire and erosion modelling, International Journal of Wildland Fire, 25, 876–887, https://doi.org/10.1071/WF15007, 2016.

Fryirs, K. A.: River sensitivity: A lost foundation concept in fluvial geomorphology, Earth Surface Processes and Landforms, 42, 55–70, https://doi.org/10.1002/esp.3940, 2017.

Fuller, I. C.: Geomorphic impacts of a 100-year flood: Kiwitea Stream, Manawatu catchment, New Zealand, Geomorphology, 98, 84–95, https://doi.org/10.1016/j.geomorph.2007.02.026, 2008.

Gabet, E. J. and Dunne, T.: Sediment detachment by rain power, Water Resources Research, 39, https://doi.org/10.1029/2001WR000656, 2003.

Gartner, J. D., Dade, W. B., Renshaw, C. E., Magilligan, F. J., and Buraas, E. M.: Gradients in stream power influence lateral and downstream sediment flux in floods, Geology, 43, 983–986, https://doi.org/10.1130/G36969.1, 2015.

Gilbert, J. T., Macfarlane, W. W., and Wheaton, J. M.: The Valley Bottom Extraction Tool (V-BET): A GIS tool for delineating valley bottoms across entire drainage networks, Computers & Geosciences, 97, 1–14, https://doi.org/10.1016/j.cageo.2016.07.014, 2016.

Goodrich, D., Canfield, H. E., Burns, I. S., Semmens, D., Miller, S., Hernandez, M., Levick, L., Guertin, D., and Kepner, W.: Rapid post-fire hydrologic watershed assessment using the AGWA GIS-based hydrologic modeling tool, in: Managing Watersheds for Human and Natural Impacts: Engineering, Ecological, and Economic Challenges, pp. 1–12, 2005.

Hamilton, E., Horton, J., Rowe, P., and Reimann, L.: Fire-flood sequences on the San Dimas Experimental Forest, Forest Service - U.S. Department of Agriculture, California Forest and Range Experiment Station, Technical Paper No. 6, 1954.

Hartzell, P. J., Gadomski, P. J., Glennie, C. L., Finnegan, D. C., and Deems, J. S.: Rigorous error propagation for terrestrial laser scanning with application to snow volume uncertainty, Journal of Glaciology, 61, 1147–1158, https://doi.org/10.3189/2015JoG15J031, 2015.

Henkle, J. E., Wohl, E., and Beckman, N.: Locations of channel heads in the semiarid Colorado Front Range, USA, Geomorphology, 129, 309–319, 2011.

Heritage, G. L., Milan, D. J., Large, A. R., and Fuller, I. C.: Influence of survey strategy and interpolation model on DEM quality, Geomorphology, 112, 334–344, https://doi.org/10.1016/j.geomorph.2009.06.024, 2009.

Hodgson, M. E. and Bresnahan, P.: Accuracy of airborne LiDAR-derived elevation, Photogrammetric Engineering & Remote Sensing, 70, 331–339, https://doi.org/10.14358/PERS.70.3.331, 2004.

HPF BAER Report: High Park Fire Burned Area Emergency Response (BAER) Report, Department of Transportation, Larimer County, Natural Resources Conservation Service, U.S. Forest Service, 25 pp, 2012.

Huffman, E. L., MacDonald, L. H., and Stednick, J. D.: Strength and persistence of fire-induced soil hydrophobicity under ponderosa and lodgepole pine, Colorado Front Range, Hydrological Processes, 15, 2877–2892, https://doi.org/10.1002/hyp.379, 2001.

Inbar, M., Tamir, M. i., and Wittenberg, L.: Runoff and erosion processes after a forest fire in Mount Carmel, a Mediterranean area, Geomorphology, 24, 17–33, https://doi.org/10.1016/S0169-555X(97)00098-6, 1998.

Isenburg, M.: LAStools - fast tools to catch reality, http://lastools.org, accessed: 2015-05-13, 2015.

Jin, S., Yang, L., Danielson, P., Homer, C., Fry, J., and Xian, G.: A comprehensive change detection method for updating the National Land Cover Database to circa 2011, Remote Sensing of Environment, 132, 159–175, https://doi.org/10.1016/j.rse.2013.01.012, 2013.

Kampf, S. K., Brogan, D. J., Schmeer, S., MacDonald, L. H., and Nelson, P. A.: How do geomorphic effects of rainfall vary with storm type and spatial scale in a post-fire landscape?, Geomorphology, 273, 39–51, https://doi.org/10.1016/j.geomorph.2016.08.001, 2016.

Kean, J. W., Staley, D. M., and Cannon, S. H.: In situ measurements of post-fire debris flows in southern California: Comparisons of the timing and magnitude of 24 debris-flow events with rainfall and soil moisture conditions, Journal of Geophysical Research: Earth Surface, 116, 2011.

Lague, D., Brodu, N., and Leroux, J.: Accurate 3D comparison of complex topography with terrestrial laser scanner: Application to the Rangitikei canyon (NZ), ISPRS Journal of Photogrammetry and Remote Sensing, 82, 10–26, https://doi.org/10.1016/j.isprsjprs.2013.04.009, 2013.

Lane, S. N., Reid, S. C., Westaway, R. M., and Hicks, D. M.: Remotely sensed topographic data for river channel research: the identification, explanation and management of error, in: Spatial Modelling of the Terrestrial Environment, edited by Kelly R, Barr S, D. N., pp. 113–136, John Wiley & Sons, Ltd: West Sussex, UK, 2004.

Larsen, I. J. and MacDonald, L. H.: Predicting postfire sediment yields at the hillslope scale: Testing RUSLE and Disturbed WEPP, Water Resources Research, 43, 2007.

Larsen, I. J., MacDonald, L. H., Brown, E., Rough, D., Welsh, M. J., Pietraszek, J. H., Libohova, Z., de Dios Benavides-Solorio, J., and Schaffrath, K.: Causes of post-fire runoff and erosion: water repellency, cover, or soil sealing?, Soil Science Society of America Journal, 73, 1393–1407, https://doi.org/10.2136/sssaj2007.0432, 2009.

Legleiter, C. J., Lawrence, R. L., Fonstad, M. A., Marcus, W. A., and Aspinall, R.: Fluvial response a decade after wildfire in the northern Yellowstone ecosystem: a spatially explicit analysis, Geomorphology, 54, 119–136, https://doi.org/10.1016/S0169-555X(02)00332-X, 2003.

Magilligan, F. J., Buraas, E., and Renshaw, C.: The efficacy of stream power and flow duration on geomorphic responses to catastrophic flooding, Geomorphology, 228, 175–188, https://doi.org/10.1016/j.geomorph.2014.08.016, 2015.

Mandlburger, G., Otepka, J., Karel, W., Wagner, W., and Pfeifer, N.: Orientation and processing of airborne laser scanning data (OPALS)–Concept and first results of a comprehensive ALS software, International archives of the photogrammetry, remote sensing and spatial information sciences, 38, 55–60, 2009.

McGuire, L. A., Kean, J. W., Staley, D. M., Rengers, F. K., and Wasklewicz, T. A.: Constraining the relative importance of raindrop-and flow-driven sediment transport mechanisms in postwildfire environments and implications for recovery time scales, Journal of Geophysical Research: Earth Surface, 121, 2211–2237, 2016.

McGuire, L. A., Rengers, F. K., Kean, J. W., and Staley, D. M.: Debris flow initiation by runoff in a recently burned basin: Is grain-by-grain sediment bulking or en masse failure to blame?, Geophysical Research Letters, 44, 7310–7319, 2017.

McKean, J., Nagel, D., Tonina, D., Bailey, P., Wright, C. W., Bohn, C., and Nayegandhi, A.: Remote sensing of channels and riparian zones with a narrow-beam aquatic-terrestrial LIDAR, Remote Sensing, 1, 1065–1096, https://doi.org/10.3390/rs1041065, 2009.

Meyer, G. A., Wells, S. G., Balling Jr, R. C., and Jull, A. T.: Response of alluvial systems to fire and climate change in Yellowstone National Park, Nature, 357, 147, https://doi.org/10.1038/357147a0, 1992.

Meyer, G. A., Wells, S. G., and Jull, A. J. T.: Fire and alluvial chronology in Yellowstone National Park: climatic and intrinsic controls on Holocene geomorphic processes, Geological Society of America Bulletin, 107, 1211–1230, https://doi.org/10.1130/0016-7606(1995)107<1211:FAACIY>2.3.CO;2, 1995.

Milan, D. J., Heritage, G. L., Large, A. R., and Fuller, I. C.: Filtering spatial error from DEMs: Implications for morphological change estimation, Geomorphology, 125, 160–171, https://doi.org/10.1016/j.geomorph.2010.09.012, 2011.

Miller, A. J.: Valley morphology and boundary conditions influencing spatial patterns of flood flow, Natural and anthropogenic influences in fluvial geomorphology, pp. 57–81, https://doi.org/10.1029/GM089p0057, 1995.

Miller, M. E., MacDonald, L. H., Robichaud, P. R., and Elliot, W. J.: Predicting post-fire hillslope erosion in forest lands of the western United States, International Journal of Wildland Fire, 20, 982–999, https://doi.org/10.1071/WF09142, 2011.

Montgomery, D. R. and Buffington, J. M.: Channel-reach morphology in mountain drainage basins, Geological Society of America Bulletin, 109, 596–611, https://doi.org/10.1130/0016-7606(1997)109<0596:CRMIMD>2.3.CO;2, 1997.

Moody, J. A.: Residence times and alluvial architecture of a sediment superslug in response to different flow regimes, Geomorphology, https://doi.org/10.1016/j.geomorph.2017.04.012, 2017.

Moody, J. A. and Kinner, D. A.: Spatial structures of stream and hillslope drainage networks following gully erosion after wildfire, Earth Surface Processes and Landforms, 31, 319–337, https://doi.org/10.1002/esp.1246, 2006.

Moody, J. A. and Martin, D. A.: Initial hydrologic and geomorphic response following a wildfire in the Colorado Front Range, Earth Surface Processes and Landforms, 26, 1049–1070, https://doi.org/10.1002/esp.253, 2001.

Moody, J. A. and Martin, D. A.: Wildfire impacts on reservoir sedimentation in the western United States, in: Proceedings of the Ninth International Symposium on River Sedimentation, pp. 1095–1102, Tsinghua University Press China, 2004.

Moody, J. A. and Martin, D. A.: Synthesis of sediment yields after wildland fire in different rainfall regimes in the western United States, International Journal of Wildland Fire, 18, 96–115, https://doi.org/10.1071/WF07162, 2009.

Moody, J. A., Shakesby, R. A., Robichaud, P. R., Cannon, S. H., and Martin, D. A.: Current research issues related to post-wildfire runoff and erosion processes, Earth-Science Reviews, 122, 10–37, 2013.

Morris, S. E. and Moses, T. A.: Forest fire and the natural soil erosion regime in the Colorado Front Range, Annals of the Association of American Geographers, 77, 245–254, https://doi.org/10.1111/j.1467-8306.1987.tb00156.x, 1987.

Nagel, D., Buffington, J., Parkes, S., Wenger, S., and Goode, J.: A Landscape Scale Valley Confinement Algorithm: Delineating Unconfined Valley Bottoms for Geomorphic, Aquatic, and Riparian Applications, US Dept of Agriculture, Forest Service, RMRS-GTR 321, Fort Collins, CO, p. 42, https://doi.org/10.2737/RMRS-GTR-321, 2014.

Nardi, L. and Rinaldi, M.: Spatio-temporal patterns of channel changes in response to a major flood event: the case of the Magra River (central–northern Italy), Earth Surface Processes and Landforms, 40, 326–339, https://doi.org/10.1002/esp.3636, 2015.

Nelson, P. A. and Brogan, D. J.: Dataset associated with “Spatial and temporal patterns of sediment storage and erosion following a wildfire and extreme flood”, https://doi.org/10.25675/10217/193080, 2019.

Nuth, C. and Kääb, A.: Co-registration and bias corrections of satellite elevation data sets for quantifying glacier thickness change, The Cryosphere, 5, 271, https://doi.org/10.5194/tc-5-271-2011, 2011.

Onda, Y., Dietrich, W. E., and Booker, F.: Evolution of overland flow after a severe forest fire, Point Reyes, California, Catena, 72, 13–20, https://doi.org/10.1016/j.catena.2007.02.003, 2008.

Orem, C. A. and Pelletier, J. D.: Quantifying the time scale of elevated geomorphic response following wildfires using multi-temporal LiDAR data: An example from the Las Conchas fire, Jemez Mountains, New Mexico, Geomorphology, 232, 224–238, 2015.

Passalacqua, P., Belmont, P., Staley, D. M., Simley, J. D., Arrowsmith, J. R., Bode, C. A., Crosby, C., DeLong, S. B., Glenn, N. F., Kelly, S. A., et al.: Analyzing high resolution topography for advancing the understanding of mass and energy transfer through landscapes: A review, Earth-Science Reviews, 148, 174–193, https://doi.org/10.1016/j.earscirev.2015.05.012, 2015.

Pelletier, J. D. and Orem, C. A.: How do sediment yields from post-wildfire debris-laden flows depend on terrain slope, soil burn severity class, and drainage basin area? Insights from airborne-LiDAR change detection, Earth Surface Processes and Landforms, 39, 1822–1832, https://doi.org/10.1002/esp.3570, 2014.

~~Pettit, N. E. and Naiman, R. J.: Fire in the riparian zone: characteristics and ecological consequences, Ecosystems, 10, 673–687, , 2007.~~

Phillips, J. D. and Van Dyke, C.: Principles of geomorphic disturbance and recovery in response to storms, Earth Surface Processes and Landforms, https://doi.org/10.1002/esp.3912, 2016.

Prosser, I. P. and Williams, L.: The effect of wildfire on runoff and erosion in native Eucalyptus forest, Hydrological processes, 12, 251–265, https://doi.org/10.1002/(SICI)1099-1085(199802)12:2<251::AID-HYP574>3.0.CO;2-4, 1998.

Rathburn, S. L., Shahverdian, S. M., and Ryan, S. E.: Post-disturbance sediment recovery: Implications for watershed resilience, Geomorphology, 305, 61–75, https://doi.org/10.1016/j.geomorph.2017.08.039, 2017.

Renard, K. G., Foster, G. R., Weesies, G. A., McCool, D. K., and Yoder, D. C.: Predicting soil erosion by water: a guide to conservation planning with the Revised Universal Soil Loss Equation (RUSLE), US Government Printing Office Washington, DC, 1997.

Reneau, S. L., Katzman, D., Kuyumjian, G. A., Lavine, A., and Malmon, D. V.: Sediment delivery after a wildfire, Geology, 35, 151–154, https://doi.org/10.1130/G23288A.1, 2007.

Rengers, F., McGuire, L., Kean, J. W., Staley, D. M., and Hobley, D.: Model simulations of flood and debris flow timing in steep catchments after wildfire, Water Resources Research, 52, 6041–6061, 2016a.

Rengers, F., Tucker, G., Moody, J., and Ebel, B.: Illuminating wildfire erosion and deposition patterns with repeat terrestrial lidar, Journal of Geophysical Research: Earth Surface, 121, 588–608, https://doi.org/10.1002/2015JF003600, ~~2016.~~ 2016b.

Rhoades, C. C., Entwistle, D., and Butler, D.: The influence of wildfire extent and severity on streamwater chemistry, sediment and temperature following the Hayman Fire, Colorado, International Journal of Wildland Fire, 20, 430–442, https://doi.org/10.1071/WF09086, 2011.

Rinaldi, M., Surian, N., Comiti, F., and Bussettini, M.: A method for the assessment and analysis of the hydromorphological condition of Italian streams: the Morphological Quality Index (MQI), Geomorphology, 180, 96–108, https://doi.org/10.1016/j.geomorph.2012.09.009, 2013.

Robichaud, P. R., Beyers, J. L., and Neary, D. G.: Evaluating the effectiveness of postfire rehabilitation treatments, USDA Forest Service, RMRS-GTR-63, Fort Collins, CO., 2000.

Robichaud, P. R., Elliot, W. J., Pierson, F. B., Hall, D. E., and Moffet, C. A.: Predicting postfire erosion and mitigation effectiveness with a web-based probabilistic erosion model, Catena, 71, 229–241, https://doi.org/10.1016/j.catena.2007.03.003, 2007.

Roering, J. J. and Gerber, M.: Fire and the evolution of steep, soil-mantled landscapes, Geology, 33, 349–352, https://doi.org/10.1130/G21260.1, 2005.

Roux, C., Alber, A., Bertrand, M., Vaudor, L., and Piégay, H.: "FluvialCorridor": A new ArcGIS toolbox package for multiscale riverscape exploration, Geomorphology, 242, 29–37, https://doi.org/10.1016/j.geomorph.2014.04.018, 2015.

Santi, P. M., Higgins, J. D., Cannon, S. H., Gartner, J. E., et al.: Sources of debris flow material in burned areas, Geomorphology, 96, 310–321, https://doi.org/10.1016/j.geomorph.2007.02.022, 2008.

Schmeer, S. R., Kampf, S. K., MacDonald, L. H., Hewitt, J., and Wilson, C.: Empirical models of annual post-fire erosion on mulched and unmulched hillslopes, CATENA, 163, 276–287, https://doi.org/10.1016/j.catena.2017.12.029, 2018.

Schumm, S. A.: Geomorphic thresholds and complex response of drainage systems, Fluvial geomorphology, 6, 69–85, 1973.

Shakesby, R. A. and Doerr, S. H.: Wildfire as a hydrological and geomorphological agent, Earth-Science Reviews, 74, 269–307, 2006.

Smith, M., Carrivick, J., and Quincey, D.: Structure from motion photogrammetry in physical geography, Progress in Physical Geography, 40, 247–275, https://doi.org/10.1177/0309133315615805, 2016.

Soil Survey Staff: Natural Resources Conservation Service, United States Department of Agriculture. Web Soil Survey, https://websoilsurvey.sc.egov.usda.gov/, Accessed: 2018-01-25, 2018.

Stoffel, M., Wyżga, B., and Marston, R. A.: Floods in mountain environments: A synthesis, Geomorphology, 272, 1–9, https://doi.org/10.1016/j.geomorph.2016.07.008, 2016.

Stone, B.: Mapping burn severity, pine beetle infestation, and their interaction at the High Park Fire, Master's thesis, Graduate Degree Program in Ecology. Colorado State University, Fort Collins, CO, 90 pp, 2015.

Stoof, C. R., Vervoort, R., Iwema, J., Van den Elsen, E., Ferreira, A., and Ritsema, C.: Hydrological response of a small catchment burned by experimental fire, Hydrology and Earth System Sciences, 16, 267, https://doi.org/10.5194/hess-16-267-2012, 2012.

Stout, J. C. and Belmont, P.: TerEx Toolbox for semi-automated selection of fluvial terrace and floodplain features from lidar, Earth Surface Processes and Landforms, 39, 569–580, https://doi.org/10.1002/esp.3464, 2014.

Surian, N., Righini, M., Lucía, A., Nardi, L., Amponsah, W., Benvenuti, M., Borga, M., Cavalli, M., Comiti, F., Marchi, L., et al.: Channel response to extreme floods: insights on controlling factors from six mountain rivers in northern Apennines, Italy, Geomorphology, 272, 78–91, https://doi.org/10.1016/j.geomorph.2016.02.002, 2016.

Swanson, F. J.: Fire and geomorphic processes, in: Fire Regime and Ecosystem Properties, edited by Mooney, H., Bonnicksen, T., Christensen, N., Lotan, J., and Reiners, W., pp. 401–444, United States Department of Agriculture Forest Service General Technical Report WO-26, 1981.

Thomas, M. F.: Landscape sensitivity in time and space – an introduction, Catena, 42, 83–98, https://doi.org/10.1016/S0341-8162(00)00133-8, 2001.

Thompson, C. and Croke, J.: Geomorphic effects, flood power, and channel competence of a catastrophic flood in confined and unconfined reaches of the upper Lockyer valley, southeast Queensland, Australia, Geomorphology, 197, 156–169, https://doi.org/10.1016/j.geomorph.2013.05.006, 2013.

Tulldahl, H. M. and Larsson, H.: Lidar on small UAV for 3D mapping, in: Electro-Optical Remote Sensing, Photonic Technologies, and Applications VIII; and Military Applications in Hyperspectral Imaging and High Spatial Resolution Sensing II, International Society for Optics and Photonics, Amsterdam, Netherlands, https://doi.org/10.1117/12.2068448, 2014.

Vericat, D., Wheaton, J. M., and Brasington, J.: Revisiting the Morphological Approach: Opportunities and Challenges with Repeat High-Resolution Topography, in: Gravel-Bed Rivers: Process and Disasters, pp. 121–155, John Wiley & Sons, 2017.

Wagenbrenner, J., MacDonald, L., and Rough, D.: Effectiveness of three post-fire rehabilitation treatments in the Colorado Front Range, Hydrological Processes, 20, 2989–3006, https://doi.org/10.1002/hyp.6146, 2006.

Wagenbrenner, J. W. and Robichaud, P. R.: Post-fire bedload sediment delivery across spatial scales in the interior western United States, Earth Surface Processes and Landforms, 39, 865–876, https://doi.org/10.1002/esp.3488, 2014.

Weber, M. D. and Pasternack, G. B.: Valley-scale morphology drives differences in fluvial sediment budgets and incision rates during contrasting flow regimes, Geomorphology, 288, 39–51, https://doi.org/10.1016/j.geomorph.2017.03.018, 2017.

Wheaton, J. M., Brasington, J., Darby, S. E., and Sear, D. A.: Accounting for uncertainty in DEMs from repeat topographic surveys: improved sediment budgets, Earth Surface Processes and Landforms, 35, 136–156, https://doi.org/10.1002/esp.1886, 2010.

Wicherski, W., Dethier, D. P., and Ouimet, W. B.: Erosion and channel changes due to extreme flooding in the Fourmile Creek catchment, Colorado, Geomorphology, https://doi.org/10.1016/j.geomorph.2017.03.030, 2017.

Wilson, C., Kampf, S. K., Wagenbrenner, J. W., and MacDonald, L. H.: Rainfall thresholds for post-fire runoff and sediment delivery from plot to watershed scales, Forest Ecology and Management, 430, 346–356, https://doi.org/10.1016/j.foreco.2018.08.025, 2018.

Wohl, E.: Migration of channel heads following wildfire in the Colorado Front Range, USA, Earth Surface Processes and Landforms, 38, 1049–1053, https://doi.org/10.1002/esp.3429, 2013.

Wohl, E. and Scott, D. N.: Transience of channel head locations following disturbance, Earth Surface Processes and Landforms, 42, https://doi.org/10.1002/esp.4124, 2017.

Wolman, M. G. and Eiler, J. P.: Reconnaissance study of erosion and deposition produced by the flood of August 1955 in Connecticut, EOS, Transactions American Geophysical Union, 39, 1–14, https://doi.org/10.1029/TR039i001p00001, 1958.

Wright, D. B., Smith, J. A., Villarini, G., and Baeck, M. L.: Long-term high-resolution radar rainfall fields for urban hydrology, JAWRA Journal of the American Water Resources Association, 50, 713–734, https://doi.org/10.1111/jawr.12139, 2014.

Writer, J. H., Hohner, A., Oropeza, J., Schmidt, A., Cawley, K. M., Rosario-Ortiz, F. L., et al.: Water treatment implications after the high Park wildfire, Colorado, J. Am. Water Works Assoc, 106, E189–E199, https://doi.org/10.5942/jawwa.2014.106.0055, 2014.

Yager, E. M., Dietrich, W., Kirchner, J. W., and McArdell, B.: Patch dynamics and stability in steep, rough streams, Journal of Geophysical Research: Earth Surface, 117, https://doi.org/10.1029/2011JF002253, 2012.

Yochum, S. E., Sholtes, J. S., Scott, J. A., and Bledsoe, B. P.: Stream power framework for predicting geomorphic change: The 2013 Colorado Front Range flood, Geomorphology, https://doi.org/10.1016/j.geomorph.2017.03.004, 2017.

Table 1. General watershed metrics for Skin Gulch and Hill Gulch.

Metric	Skin Gulch	Hill Gulch
Contributing area (km^2)	15.3	14.2
Elevation range (m)	1842-2683	1723-2397
Relief (m)	841	674
Mean slope (%)	23	24
Total stream length (km)	39	33
Drainage density ($km\ km^{-2}$)	2.5	2.3
Elongation ratio	0.53	0.44

Table 2. Mean total precipitation and mean maximum 30-min intensities (MI_{30}) for Skin Gulch and Hill Gulch for each time period. Ranges are in parentheses, and the values are derived from the gage-corrected radar data.

Time Period	Months	Skin Gulch		Hill Gulch	
		Total precipitation (mm)	MI_{30} (mm h^{-1})	Total precipitation (mm)	MI_{30} (mm h^{-1})
T1	8	174 (156–234)	24 (11–85)	185 (175-205)	17 (13–32)
T2	3	366 (276–439)	49 (32–73)	327 (302–439)	49 (36–106)
T3	11	527 (441–634)	38 (23–63)	488 (443–559)	41 (21–71)
T4	9	340 (259–403)	30 (17–39)	397 (362–446)	38 (26–58)

Table 3. Point density and average mean absolute error (MAE) for each ALS dataset for Skin Gulch and Hill Gulch, respectively. MAE was determined by the elevation difference between total station and RTK-GNSS survey points and interpolated ALS points.

ALS dataset	Skin Gulch		Hill Gulch	
	Point density (pts/m^2)	MAE (cm)	Point density (pts/m^2)	MAE (cm)
201210	1.16	12	1.18	23
201307	2.00	11	2.21	15
201310	3.01	11	2.78	9
201409	3.27	12	3.82	10
201506	3.67	13	2.21	13

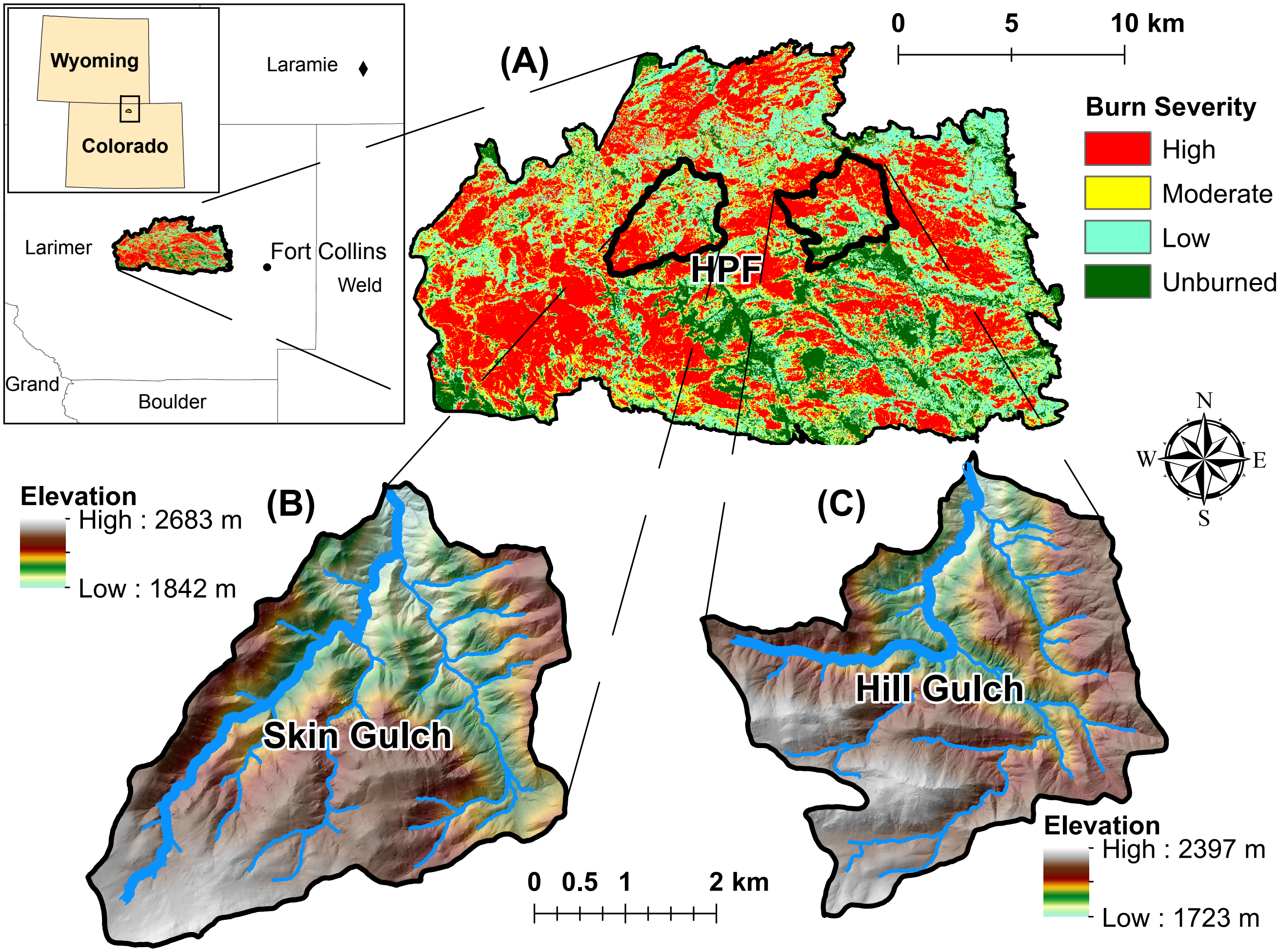

Figure 1. Location and burn severity of the (A) High Park Fire (HPF) in the Colorado Front Range of the western U.S., and elevations of (B) Skin Gulch and (C) Hill Gulch. ~~The black diamond to~~ Inset map shows identifies the ~~east~~ city of ~~Laramie in (A)~~ Fort Collins and the surrounding counties, and the black diamond is the location of the KCYS Doppler radar station in Cheyenne, ~~WY~~Wyoming. The thick blue lines in each watershed represent the reach used to present longitudinal results in Figures 8 and 9.

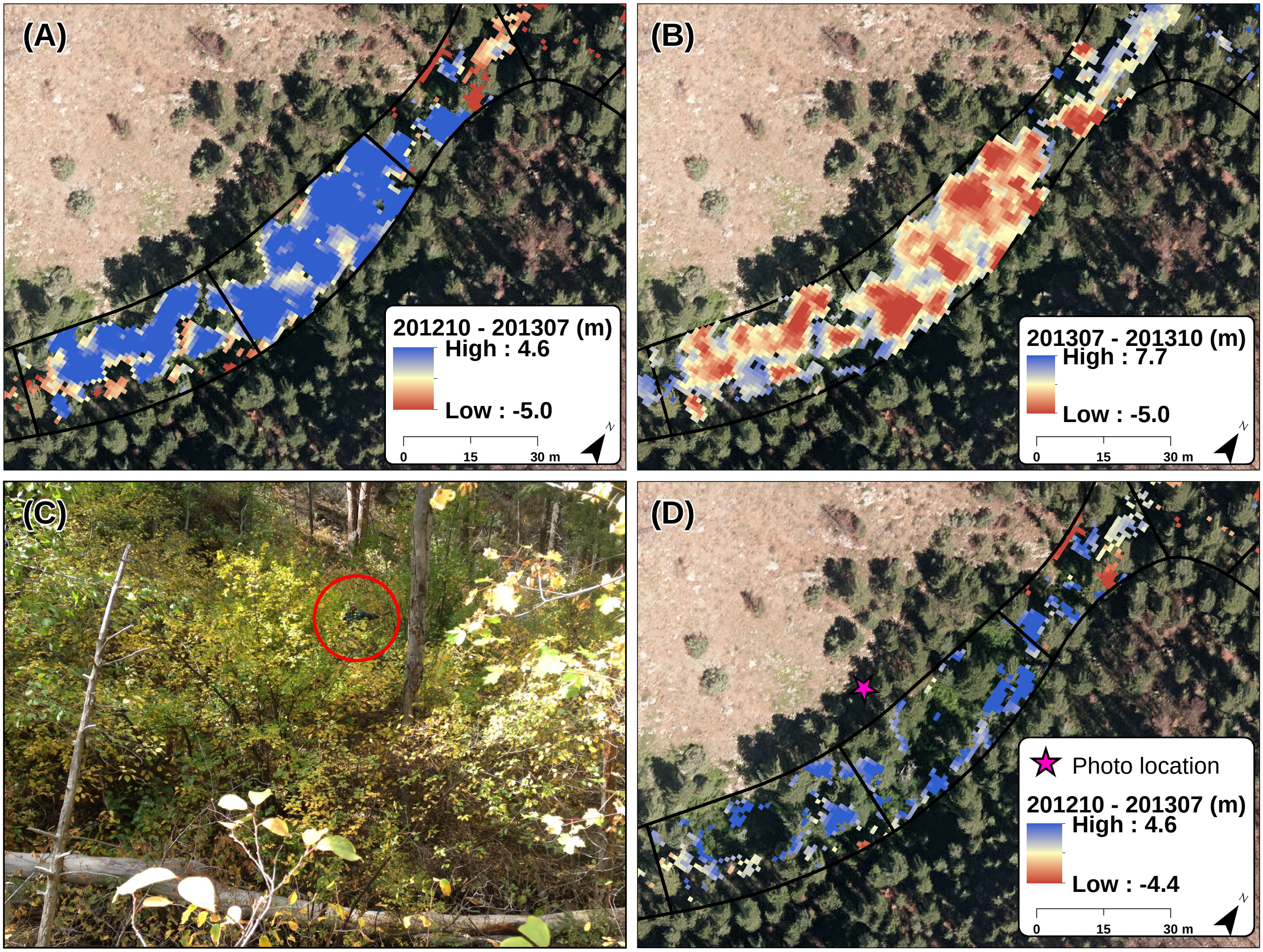

Figure 2. Seasonal changes in vegetation led to spurious deposition during fall to summer DoDs (A), and ~~(B)~~ spurious erosion in the summer to fall DoDs (B). The valley bottom in (A) and (B) includes several woody deciduous species along with some ponderosa pine (C). (D) shows the remaining change after using our raster-based algorithm to reduce the errors due to leaf out and leaf drop. Red circle in (C) identifies the upper half of a person standing in the understory, and the pink star in (D) represents the approximate location of the photo in (C).

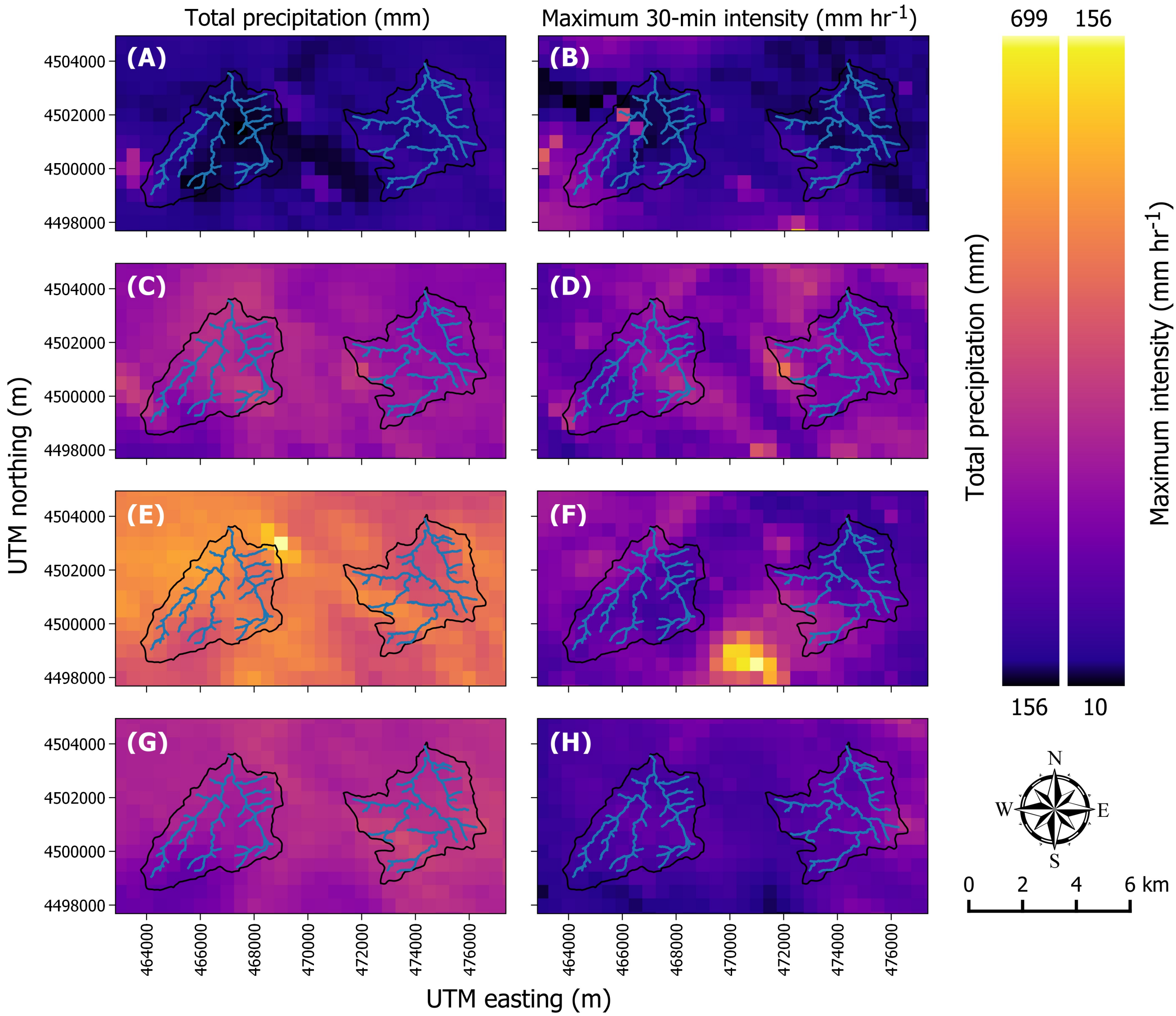

Figure 3. Total ~~rainfall~~ precipitation (mm) and maximum 30-minute intensity (mm hr^{-1}) for each of the four time periods ~~between each successive DoD~~ for: (A, B) T1 (201210 to 201307); (C, D) T2 (201307 to 201310); (E, F) T3 (201310 to 201409); and (G, H) T4 (201409 to ~~201506.~~ 201506). Within each panel Skin Gulch is the watershed on the left and Hill Gulch is to the right.

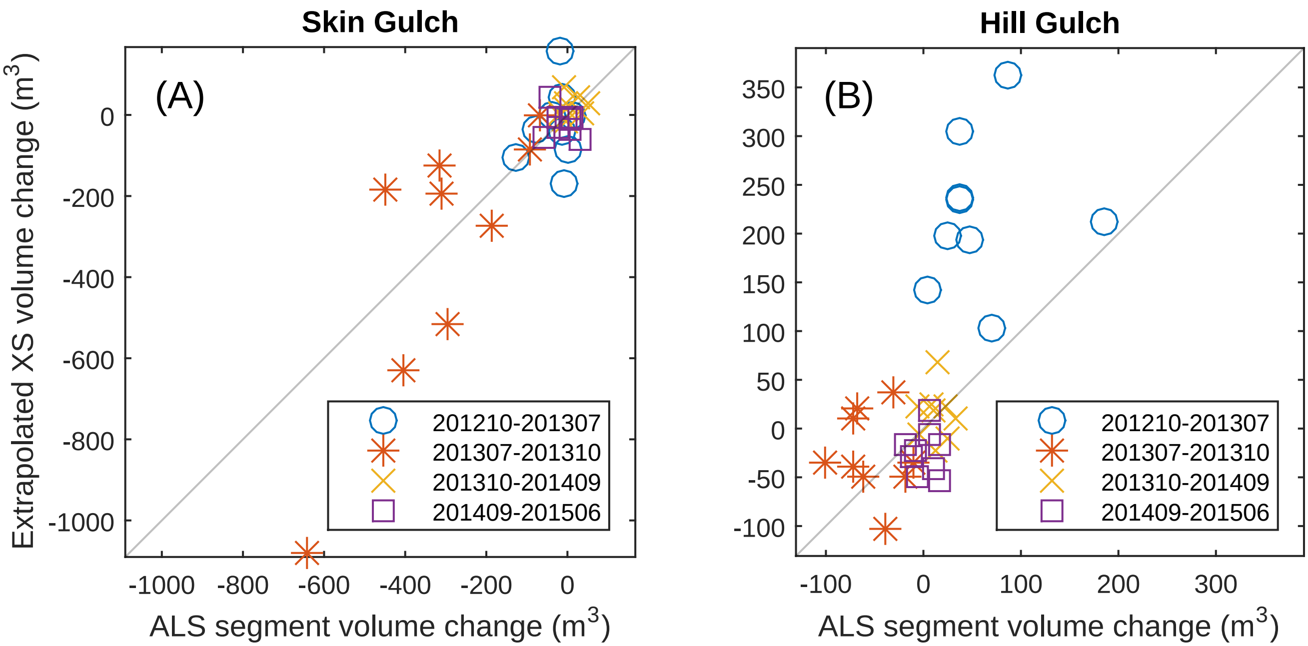

Figure 4. ~~Comparison~~ Plots of the extrapolated cross section (XS) volume ~~change and~~ changes versus the corresponding ALS segment volume ~~change~~ changes for (A) Skin Gulch and (B) Hill Gulch. Diagonal lines are the 1:1 relationship, and the different symbols in each plot represent the different time periods.

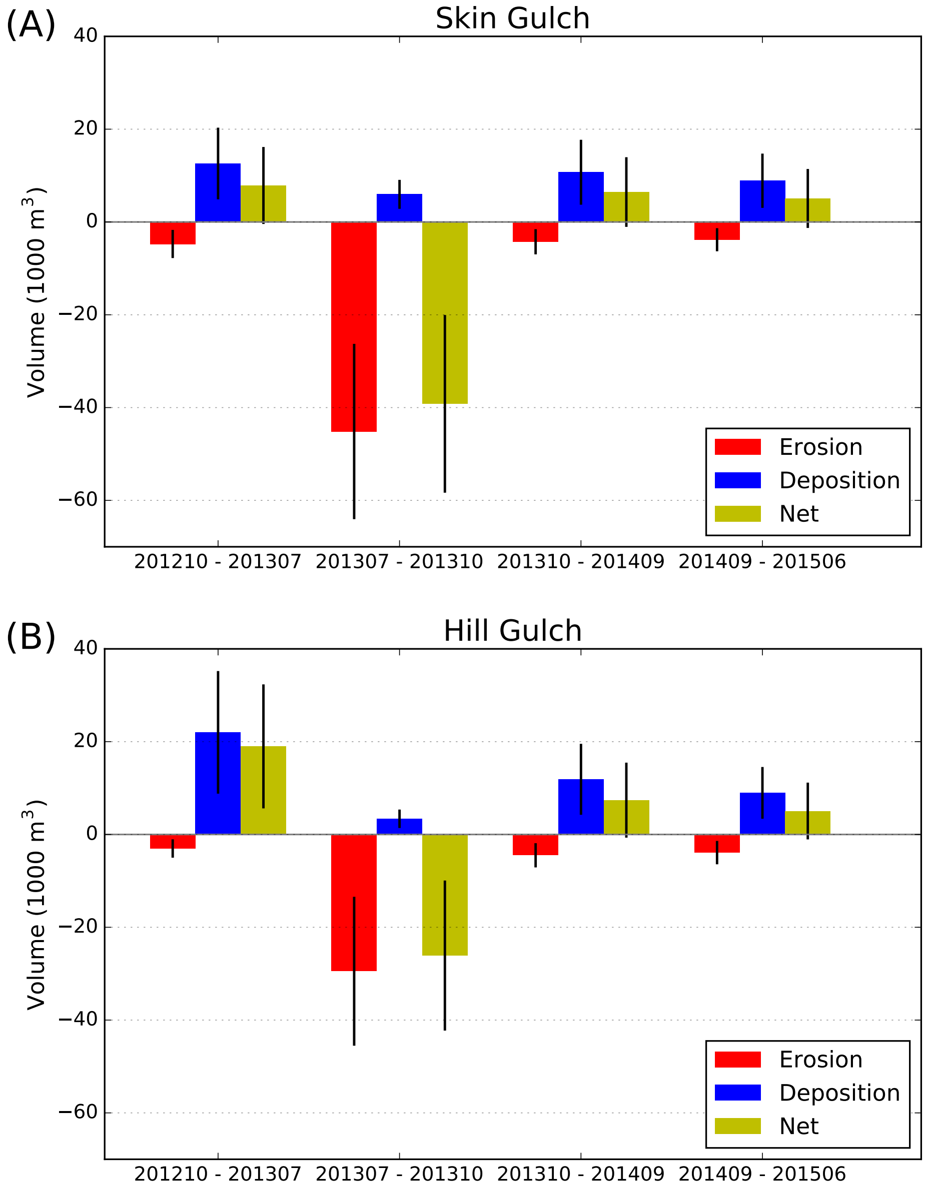

Figure 5. Total valley erosion, deposition, and net volume change for each time period for (A) Skin Gulch, and (B) Hill Gulch. Black vertical bars indicate the uncertainty ~~in the~~ for each volume ~~estimates~~estimate.

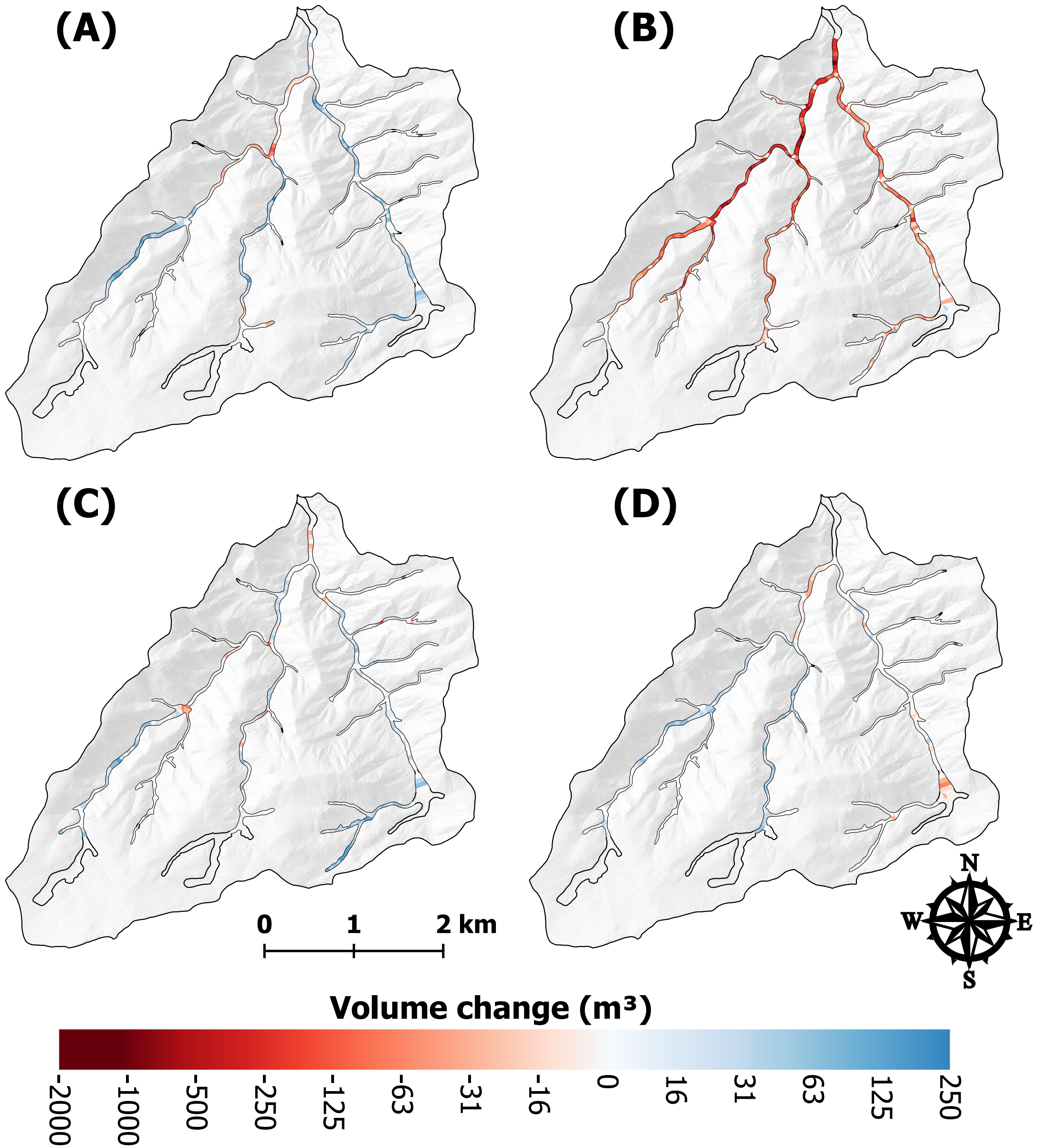

Figure 6. Net volume differences for each valley bottom segment in Skin Gulch for (A) ~~201210–201307~~T1 (201210-201307), (B) ~~201307–201310~~T2 (201307-201310), (C) ~~201310–201409~~T3 (201310-201409), and (D) ~~201409–201506~~T4 (201409-201506. Calculated volumes are not reported for the transparent segments in the headwaters and segments furthest downstream (outlined by heavier black lines) due to unrealistically wide valley widths, repeat excavations, or the ground surface could not be reliably determined.

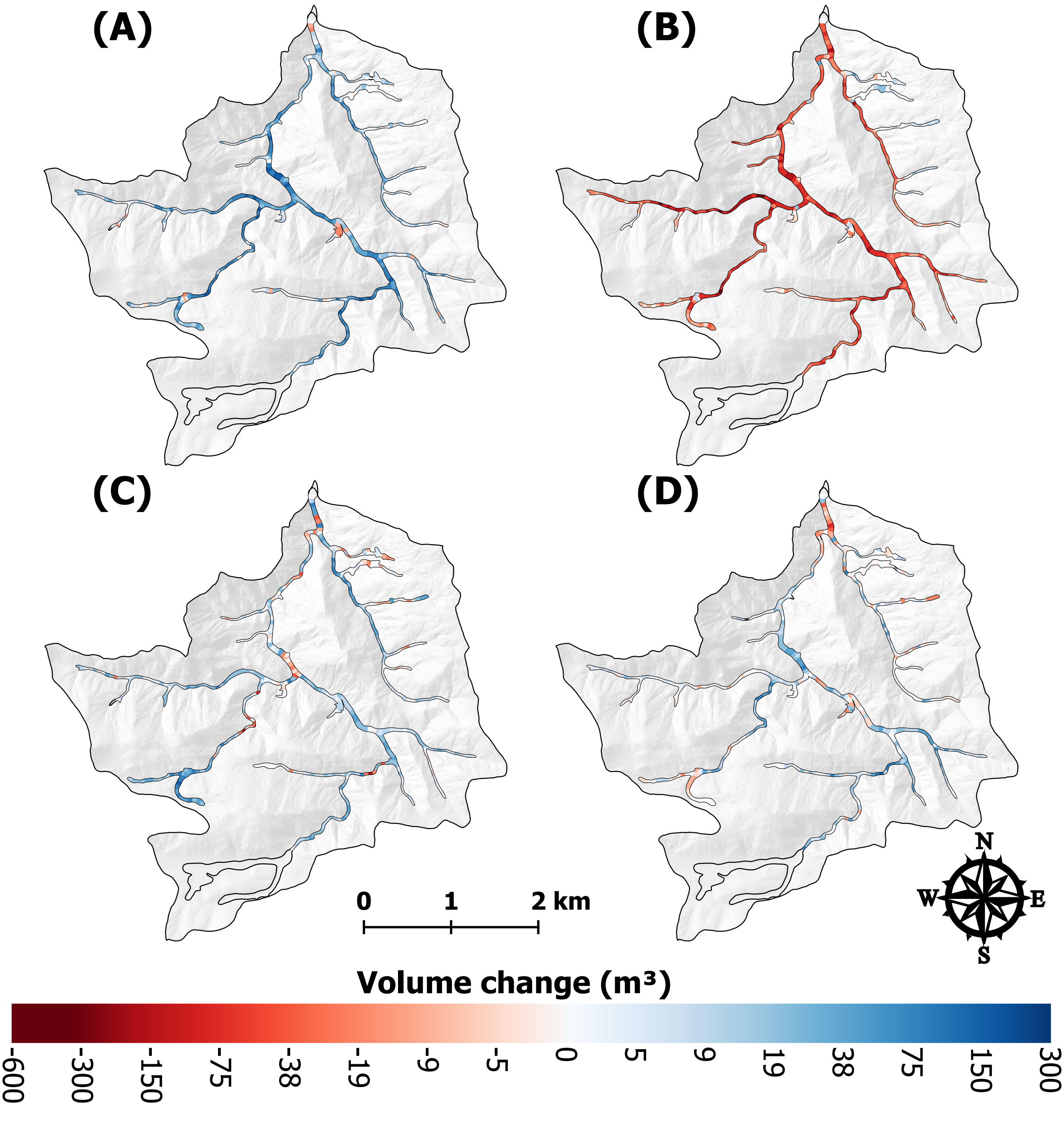

Figure 7. Net volume differences for each valley bottom segment in Hill Gulch for (A) ~~201210–201307~~T1 (201210-201307), (B) ~~201307–201310~~T2 (201307-201310), (C) ~~201310–201409~~T3 (201310-201409), and (D) ~~201409–201506~~T4 (201409-201506). Calculated volumes are not reported for the transparent segments in the headwaters and segments furthest downstream (outlined by heavier black lines) due to unrealistically wide valley widths, repeat excavations, or the ground surface could not be reliably determined.

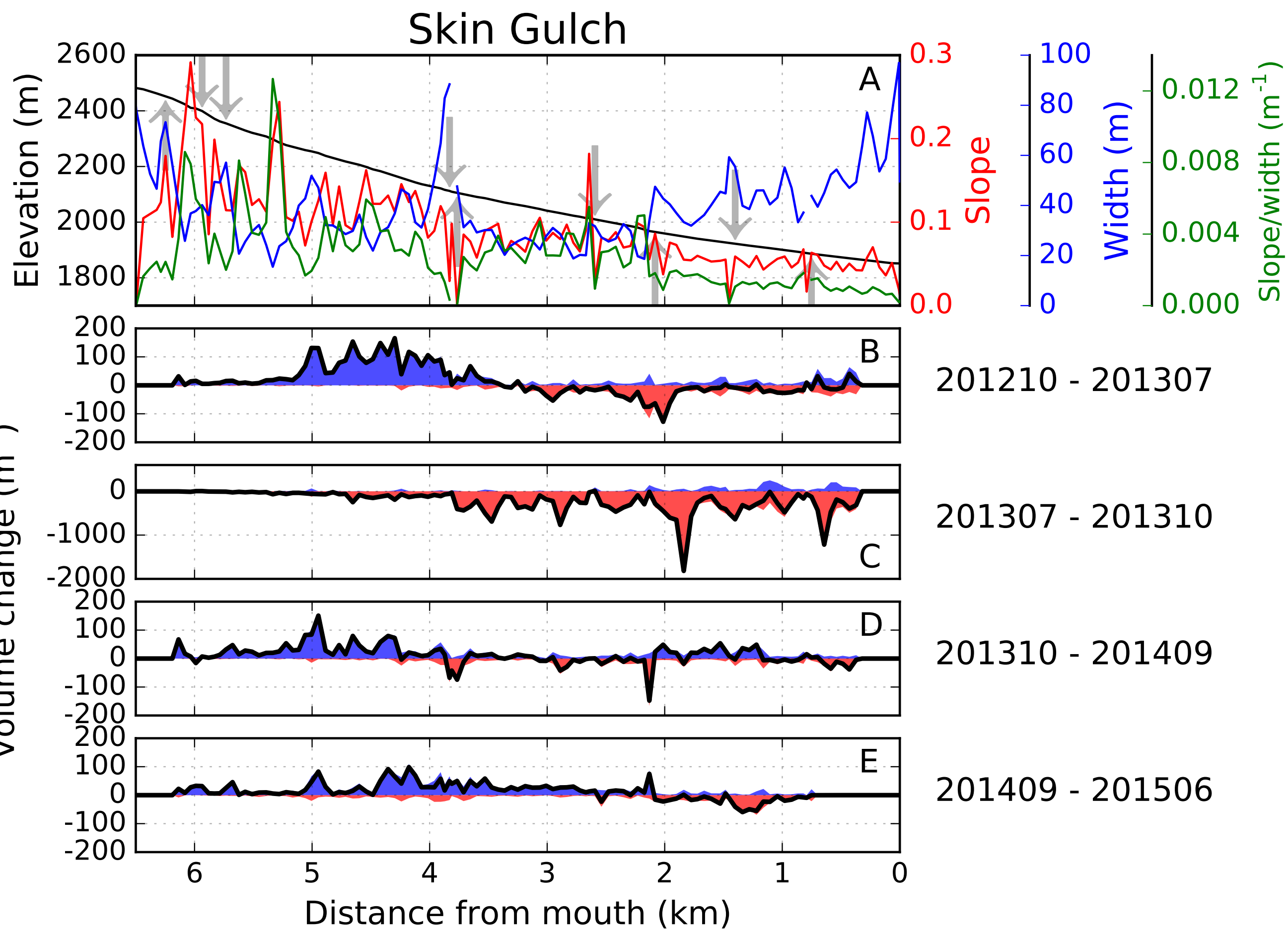

Figure 8. Longitudinal distributions in Skin Gulch of (A) elevation, channel slope, valley width and slope/width, and the corresponding ~~change~~ longitudinal changes in ~~volume~~ volumes for (B) ~~201210–201307~~T1 (201210-201307), (C) ~~201307–201310~~T2 (201307-201310), (D) ~~201310–201409~~T3 (201310-201409), and (E) ~~201409–201506~~T4 (201409-201506). Up and down arrows in (A) represent tributaries that enter the main channel from the right and left, respectively. Blue and red areas in (B)–(E) are deposition and erosion, respectively, and the black line is net volume change. Removal of excess sediment and restoration activities means that the data for the lowest 400 m were excluded for all time periods, and for the ~~lower~~ lowest 700 m in (E). See Figure 1 for the location of the reaches being represented, and the data in (A) were taken from the 201310 lidar dataset.

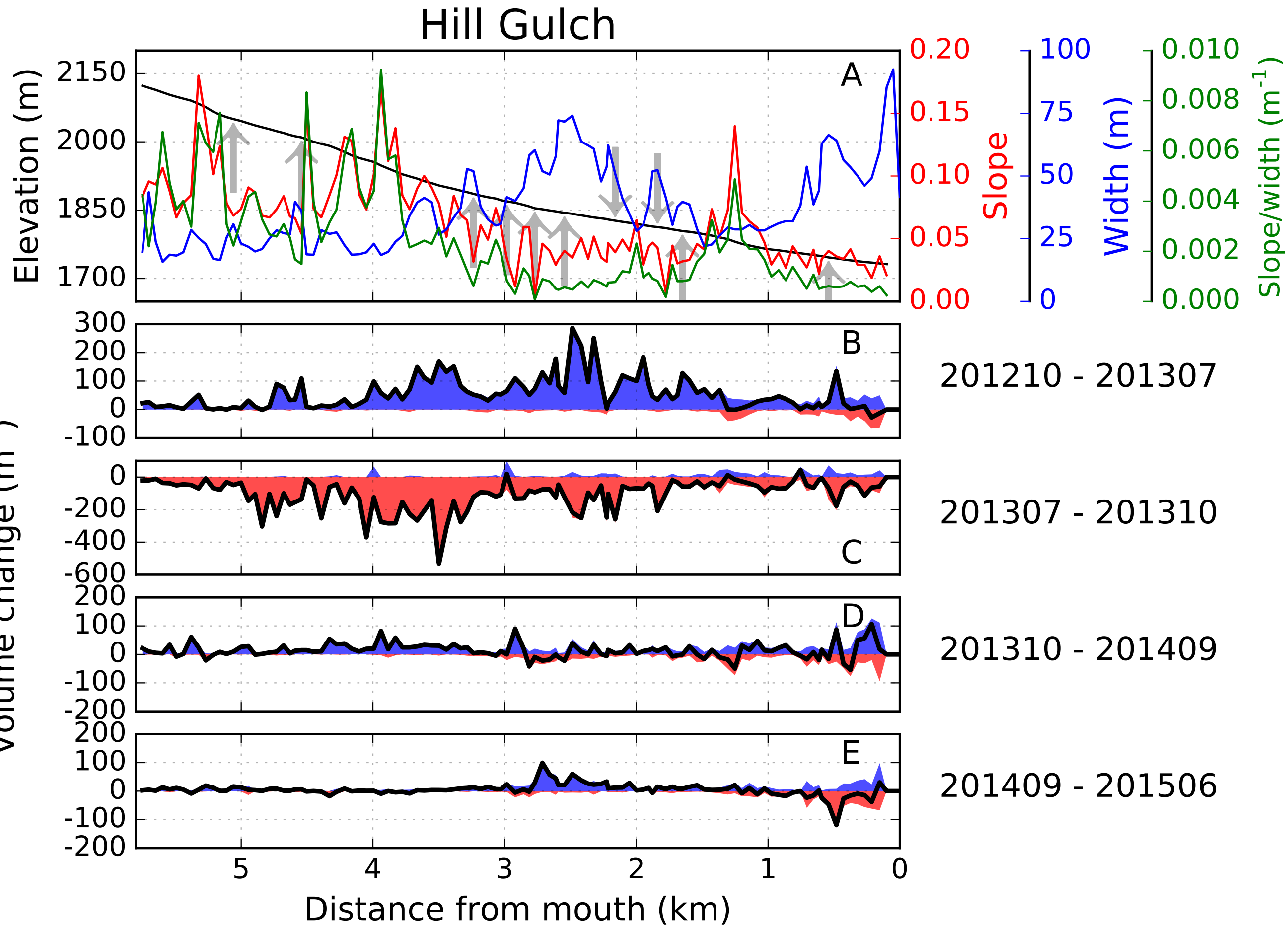

Figure 9. Longitudinal distributions in Hill Gulch of (A) elevation, channel slope, valley width and flood power, and the corresponding ~~change~~ longitudinal changes in volume for (B) ~~201210–201307~~T1 (201210-201307), (C) ~~201307–201310~~T2 (201307-201310), (D) ~~201310–201409~~T3 (201310-201409), and (E) ~~201409–201506~~T4 (201409-201506). Up and down arrows in (A) represent tributaries that enter the main channel from the right and left, respectively. Blue and red areas in (B)~~–~~-(E) are deposition and erosion, respectively, and the black line is net volume change. See Figure 1 for the location of the reaches being represented, and the data in (A) were taken from the 201310 lidar dataset.

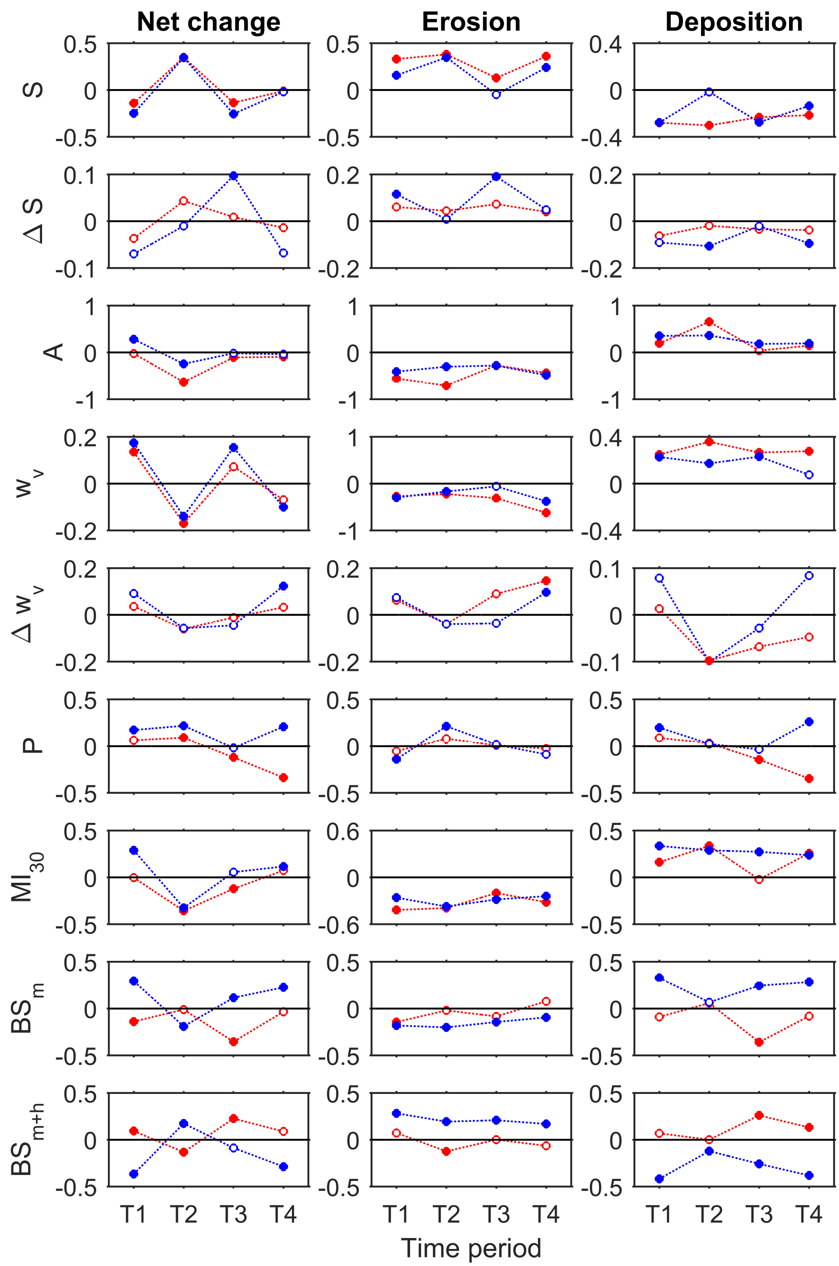

Figure 10. ~~Correlation~~ Pearson correlation coefficients for Skin Gulch (dotted red ~~dashed~~ lines) and Hill Gulch (dotted blue ~~dashed~~ lines) for each time period between the independent metrics and the dependent variables of net volume change, total erosion, and total deposition, respectively. ~~Time~~ T1 to T4 are for the time periods (T#) ~~are for~~ of 201210–201307, 201307–201310, 201310–201409, and 201409–201506, respectively. Independent variables include channel slope (S), change in channel slope ΔS, contributing area (A), valley width (w_{v}), change in valley width (Δw_{v})~~, total rainfall~~total precipitation(P), maximum 30-minute intensity (MI_{30}), percent burned at moderate severity (BS_{m}), and percent burned at moderate-to-high severity ($BS_{\mathrm{m+h}}$). Filled circles indicate correlations that are significant at p-value ≤ 0.05. Note that the vertical axes vary according to the strength of the correlations.

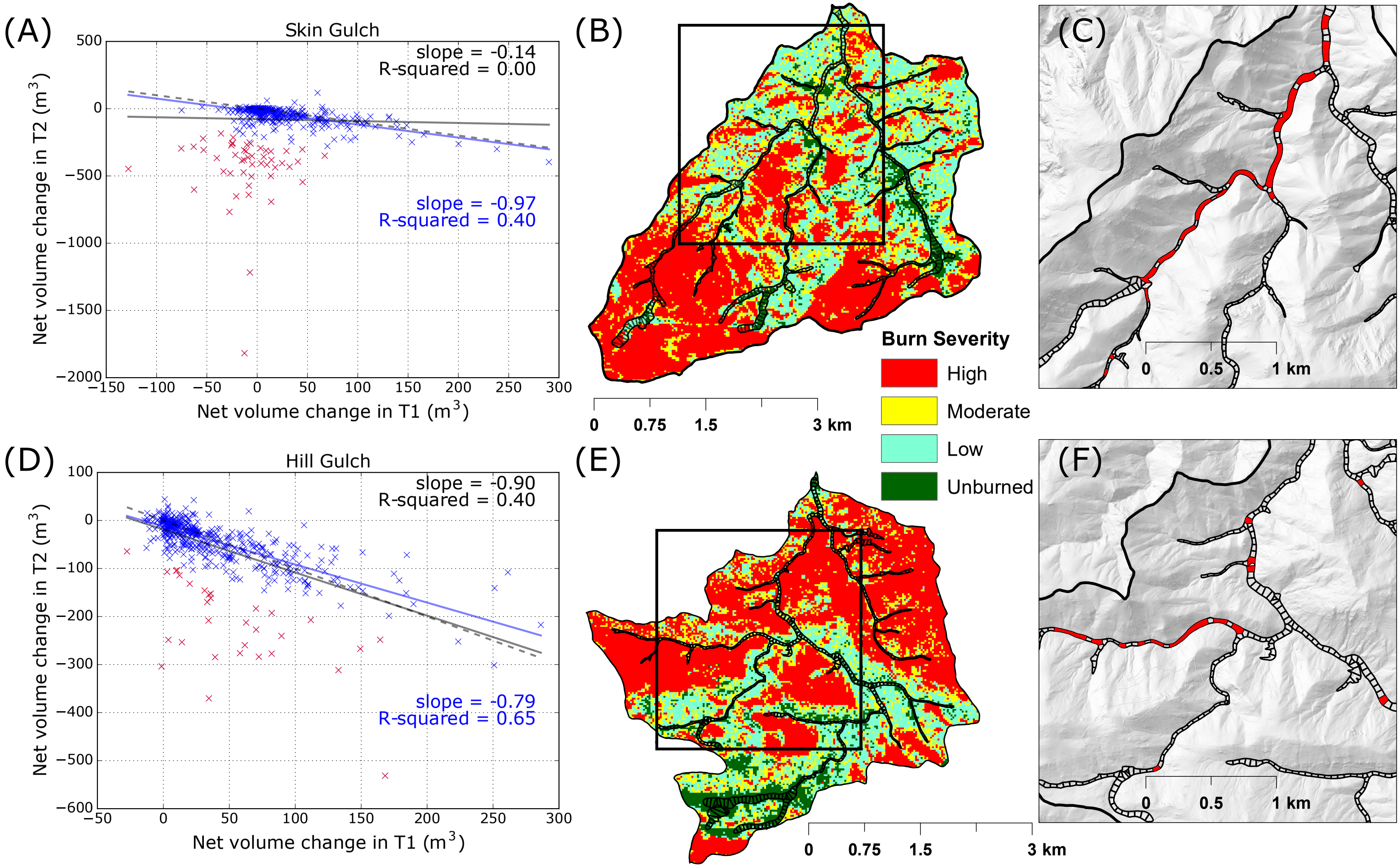

Figure 11. Regression of the net volume change for each 50-m segment for T2 (the period including the large erosional mesoscale flood ~~;~~ of 201307–201310) against the net volume change for T1 (the depositional period of 201210–201307) for (A) Skin Gulch and (D) Hill Gulch. The red x's in (A) and (D) are the segments with much more erosion in T2 than deposition in T1, causing them to deviate substantially from the dashed -1:1 line. The regression line and statistics for all of the data are shown in black, while the regression line and statistics in blue are for the truncated data after removing the red data points. (B) and (E) are burn severity maps of Skin Gulch and Hill Gulch, respectively, and the black boxes show the valley bottom segments in (C) and (F). The red segments in (C) and (F) are the red data points in (A) and (D).

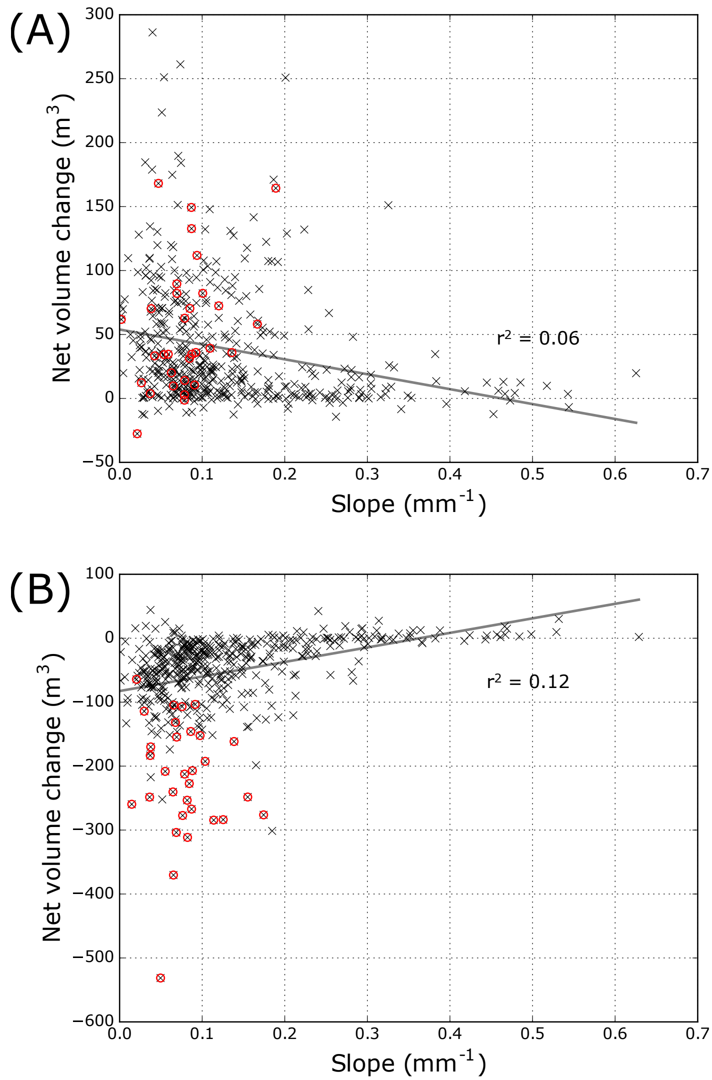

Figure 12. Scatterplot during of Hill Gulch for net volume change versus slope for (A) T1 and (B) T2. Red circles correspond to the segments highlighted in Figure 11.

Table A1. Pearson correlation coefficients (r) for the independent variables used in our statistical analysis in Skin Gulch. Independent variables include channel slope (S), ΔS, contributing area (A), valley width (w_v), change in valley width (Δw_v), slope-width ratio ($\frac{S}{w_v}$), change in slope-width ratio ($\Delta \frac{S}{w_v}$), channel width (w_c), confinement ratio (C_r), total precipitation (P), maximum 30-minute intensity (MI_{30}), percent burned at moderate severity (BS_m), percent burned at high severity (BS_h), and percent burned at moderate-to-high severity ($BS_\mathrm{m+h}$).

r	S	ΔS	A	w_v	Δw_v	$\frac{S}{w_v}$	$\Delta \frac{S}{w_v}$	w_c	C_r	P	MI_{30}	BS_m	BS_h	$BS_\mathrm{m+h}$
S	-	-	-	-	-	-	-	-	-	-	-	-	-	-
ΔS	0.33	-	-	-	-	-	-	-	-	-	-	-	-	-
A	-0.54	0.03	-	-	-	-	-	-	-	-	-	-	-	-
w_v	-0.48	-0.08	0.37	-	-	-	-	-	-	-	-	-	-	-
Δw_v	0.00	-0.16	-0.02	0.41	-	-	-	-	-	-	-	-	-	-
$\frac{S}{w_v}$	0.88	0.27	-0.48	-0.62	-0.17	-	-	-	-	-	-	-	-	-
$\Delta \frac{S}{w_v}$	0.15	0.68	0.05	-0.20	-0.52	0.32	-	-	-	-	-	-	-	-
w_c	-0.65	0.02	0.94	0.42	-0.04	-0.59	0.06	-	-	-	-	-	-	-
C_r	0.21	-0.08	-0.44	0.41	0.46	-0.03	-0.31	-0.54	-	-	-	-	-	-
P	0.00	-0.05	0.04	0.06	0.04	0.02	-0.06	0.00	0.08	-	-	-	-	-
MI_{30}	-0.40	0.04	0.59	0.30	-0.04	-0.38	0.03	0.64	-0.28	0.32	-	-	-	-
BS_m	0.16	-0.07	0.05	-0.14	0.07	0.24	-0.10	0.01	-0.11	0.17	0.00	-	-	-
BS_h	-0.16	0.07	0.02	0.13	-0.10	-0.23	0.10	0.08	0.02	-0.08	0.14	-0.84	-	-
$BS_\mathrm{m+h}$	-0.15	0.06	0.05	0.12	-0.10	-0.21	0.09	0.10	-0.01	-0.04	0.17	-0.74	0.99	-

Table A2. Pearson correlation coefficients (r) for the independent variables used in our statistical analysis in Skin Gulch. Independent variables include channel slope (S), ΔS, contributing area (A), valley width (w_{v}), change in valley width (Δw_{v}), slope-width ratio ($\frac{S}{w_v}$), change in slope-width ratio ($\Delta \frac{S}{w_v}$), channel width (w_{c}), confinement ratio (C_{r}), total precipitation (P), maximum 30-minute intensity (MI_{30}), percent burned at moderate severity (BS_{m}), percent burned at high severity (BS_{h}), and percent burned at moderate-to-high severity ($BS_{\mathrm{m+h}}$).

r	S	ΔS	A	w_{v}	Δw_{v}	$\frac{S}{w_v}$	$\Delta \frac{S}{w_v}$	w_{c}	C_{r}	P	MI_{30}	BS_{m}	BS_{h}	$BS_{\mathrm{m+h}}$
S	-	-	-	-	-	-	-	-	-	-	-	-	-	-
ΔS	0.31	-	-	-	-	-	-	-	-	-	-	-	-	-
A	-0.45	0.01	-	-	-	-	-	-	-	-	-	-	-	-
w_{v}	-0.33	-0.12	0.47	-	-	-	-	-	-	-	-	-	-	-
Δw_{v}	-0.05	-0.21	0.03	0.45	-	-	-	-	-	-	-	-	-	-
$\frac{S}{w_v}$	0.88	0.35	-0.43	-0.55	-0.18	-	-	-	-	-	-	-	-	-
$\Delta \frac{S}{w_v}$	0.18	0.80	0.03	-0.20	-0.44	0.36	-	-	-	-	-	-	-	-
w_{c}	-0.54	0.01	0.96	0.47	0.02	-0.51	0.03	-	-	-	-	-	-	-
C_{r}	0.34	-0.12	-0.41	0.37	0.33	0.06	-0.24	-0.53	-	-	-	-	-	-
P	0.03	0.02	-0.10	-0.01	-0.03	0.02	0.03	-0.10	0.08	-	-	-	-	-
MI_{30}	-0.41	0.02	0.52	0.29	0.01	-0.39	0.03	0.55	-0.26	0.33	-	-	-	-
BS_{m}	-0.42	0.00	0.17	0.16	0.03	-0.37	0.02	0.22	-0.12	0.18	0.43	-	-	-
BS_{h}	0.42	-0.04	-0.27	-0.25	0.00	0.39	-0.05	-0.35	0.16	-0.27	-0.50	-0.82	-	-
$BS_{\mathrm{m+h}}$	0.39	-0.05	-0.28	-0.26	0.01	0.37	-0.05	-0.36	0.17	-0.28	-0.49	-0.73	0.99	-

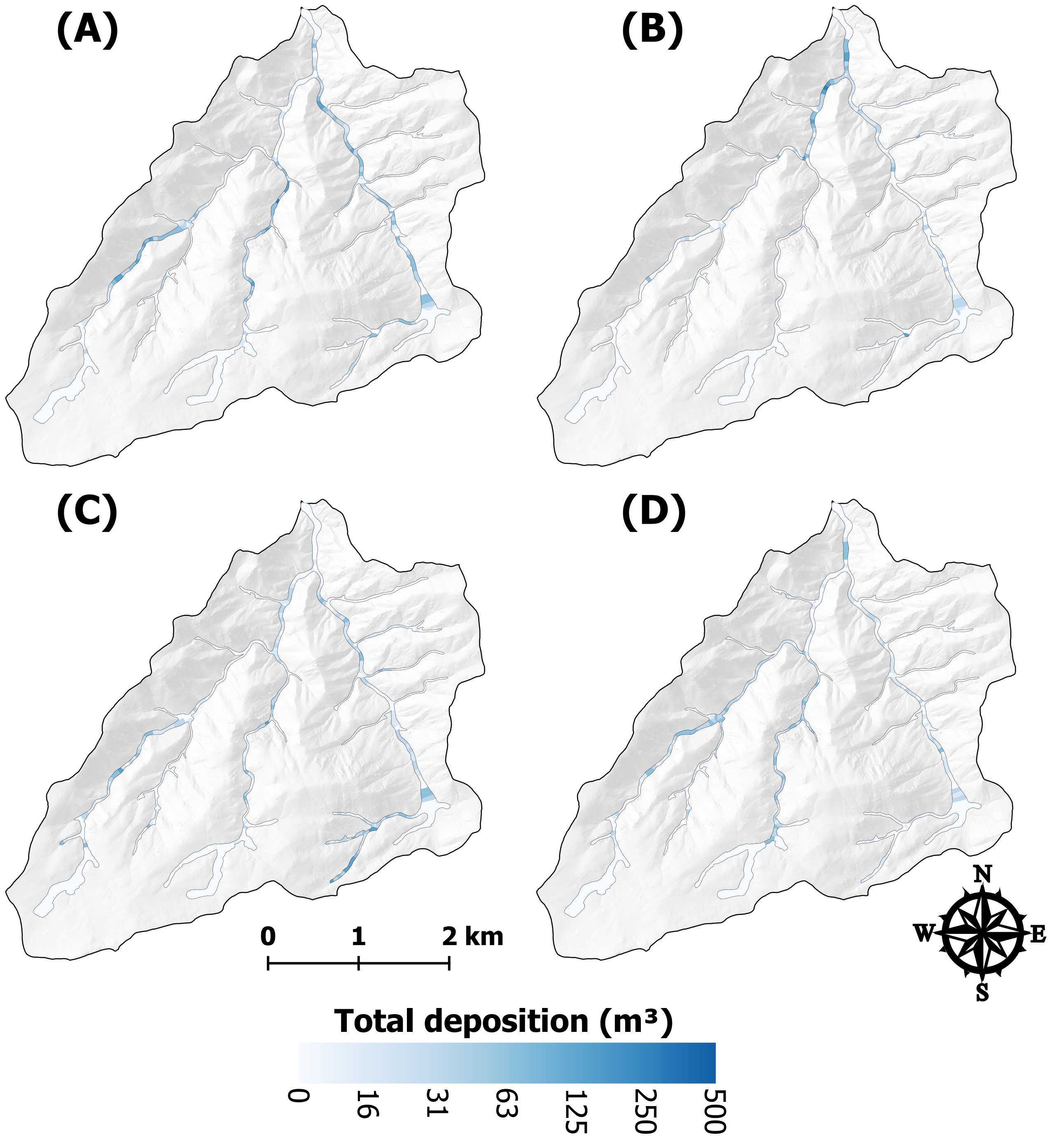

Figure A1. Total deposition for each valley bottom segment in Skin Gulch for (A) ~~201210–201307~~201210-201307, (B) ~~201307–201310~~201307-201310, (C) ~~201310–201409~~201310-201409, and (D) ~~201409–201506~~201409-201506. Calculated volumes are not reported for the transparent segments due to unrealistically wide valley widths, repeat excavations, or the ground surface could not be reliably determined.

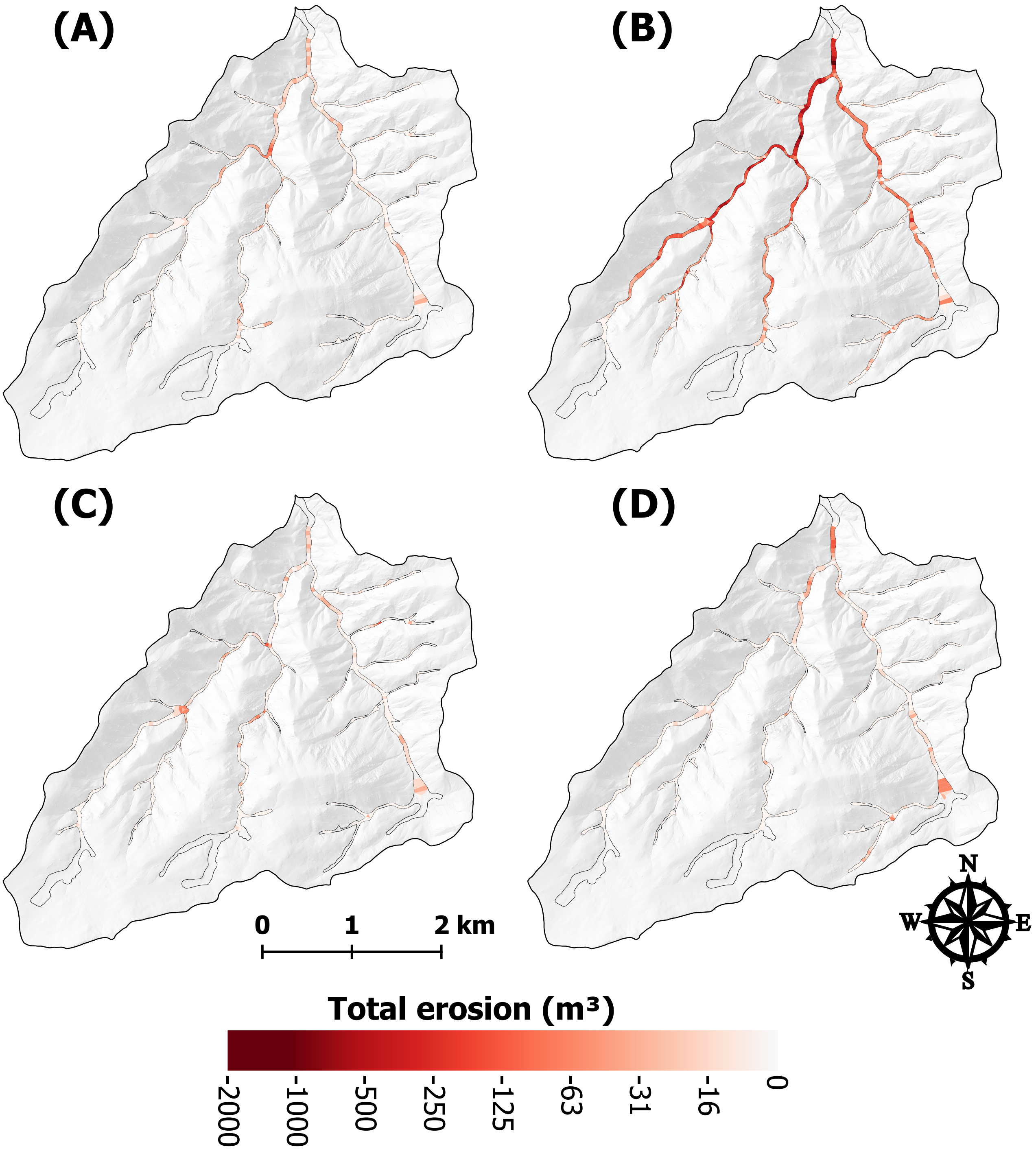

Figure A2. Total erosion for each valley bottom segment in Skin Gulch for (A) ~~201210–201307~~201210-201307, (B) ~~201307–201310~~201307-201310, (C) ~~201310–201409~~201310-201409, and (D) ~~201409–201506~~201409-201506. Calculated volumes are not reported for the transparent segments due to unrealistically wide valley widths, repeat excavations, or the ground surface could not be reliably determined.

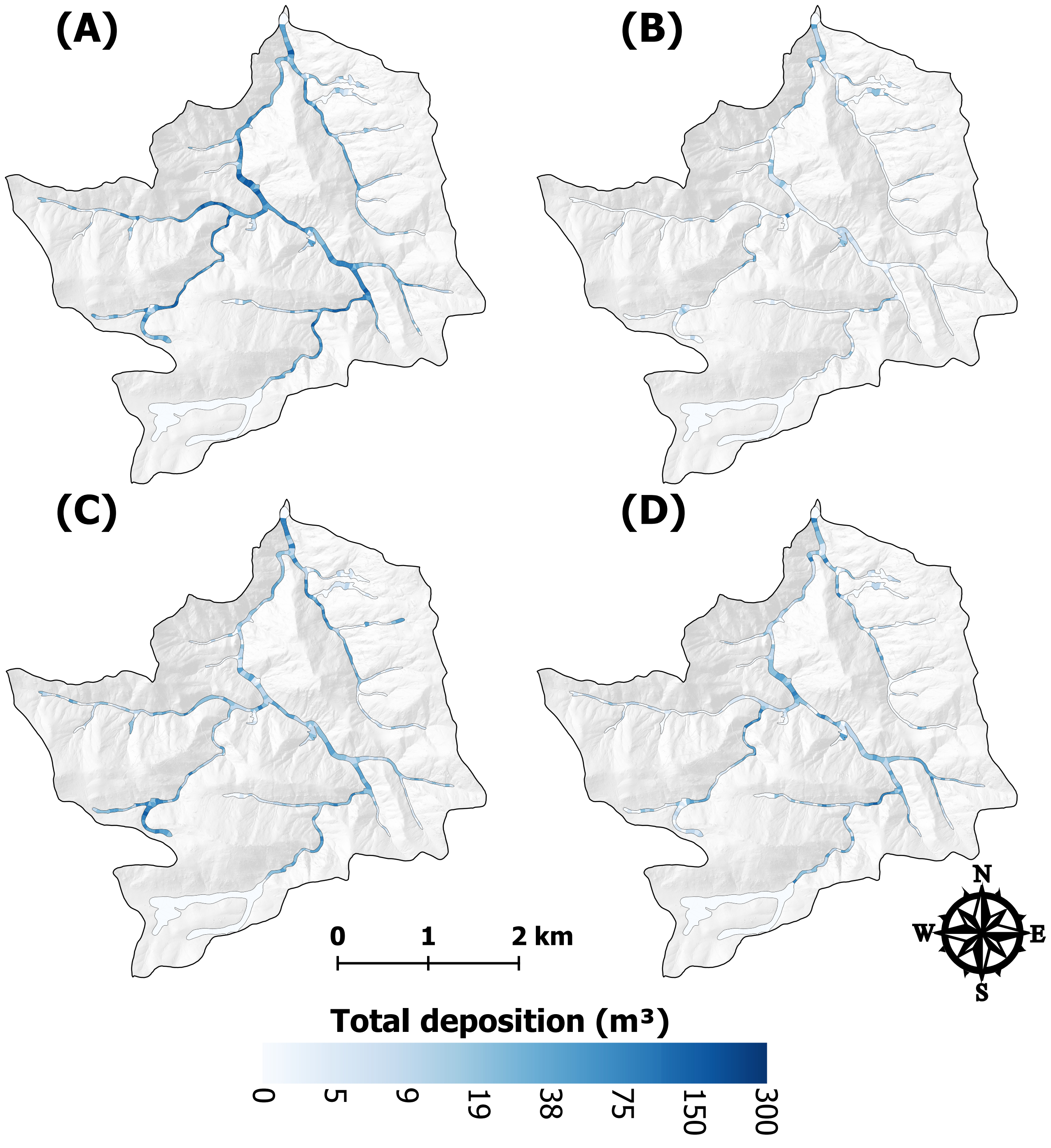

Figure A3. Total deposition for each valley bottom segment in Hill Gulch for (A) ~~201210–201307~~201210-201307, (B) ~~201307–201310~~201307-201310, (C) ~~201310–201409~~201310-201409, and (D) ~~201409–201506~~201409-201506. Calculated volumes are not reported for the transparent segments due to unrealistically wide valley widths, repeat excavations, or the ground surface could not be reliably determined.

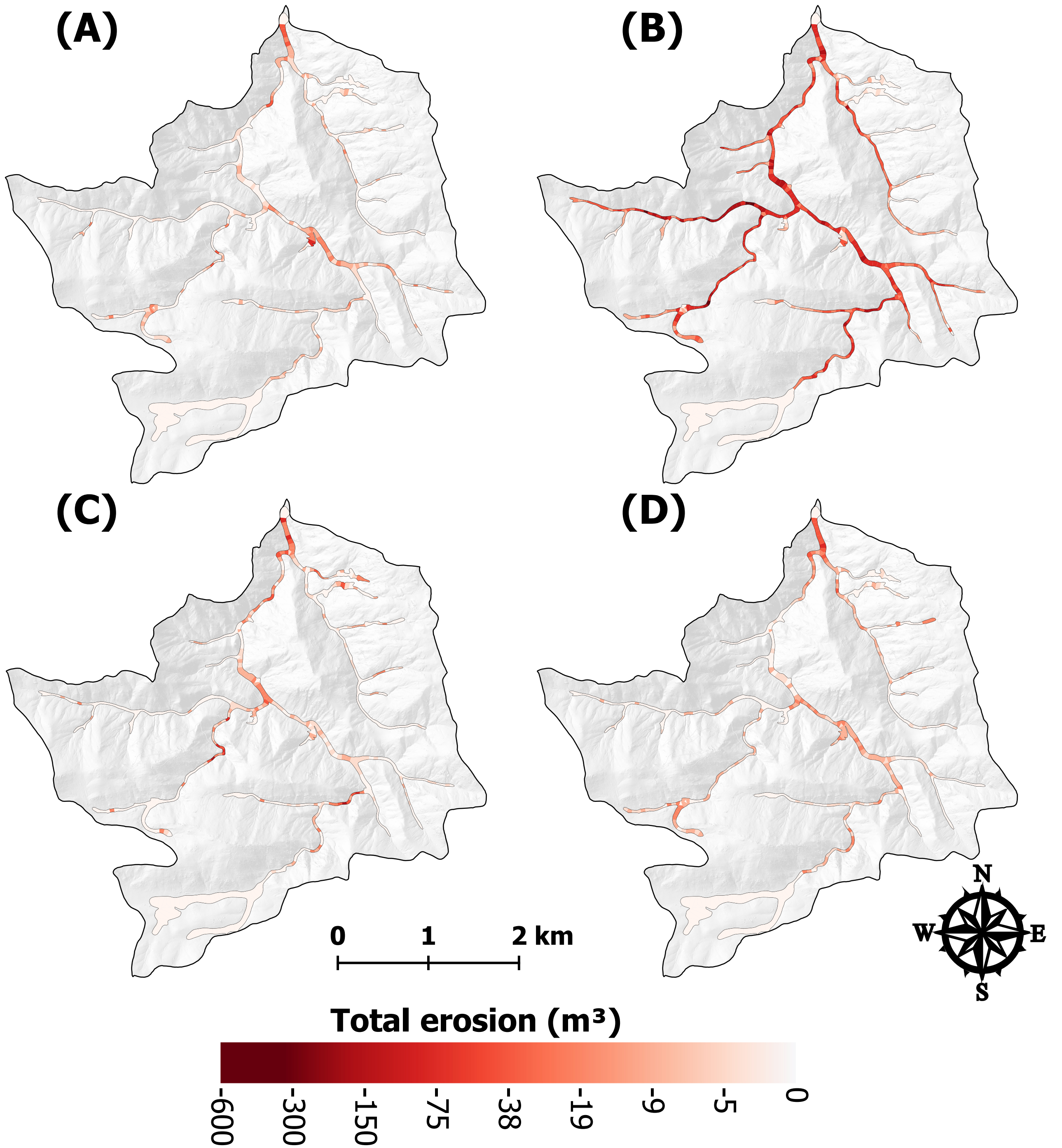

Figure A4. Total erosion for each valley bottom segment in Hill Gulch for (A) ~~201210–201307~~201210-201307, (B) ~~201307–201310~~201307-201310, (C) ~~201310–201409~~201310-201409, and (D) ~~201409–201506~~201409-201506. Calculated volumes are not reported for the transparent segments due to unrealistically wide valley widths, repeat excavations, or the ground surface could not be reliably determined.